Univerzita Karlova

1. lékařská fakulta

Studijní program: Biologie a patologie buňky (P1516)

Studijní obor: Biologie a patologie buňky (1501V000)

MSc. Dijana, Lađinović

Epigenetika v genové regulaci a struktuře chromatinu

Epigenetics in gene regulation and chromatin structure

Disertační práce

Vedoucí závěrečné práce/Školitel:

Ing. Tomáš Vacík, PhD

Praha, 2019

Prohlášení o samostatném zapracováni disertačni práce

Prohlašuji, že jsem závěrečnou práci zpracovala samostatně a že jsem řádně uvedla a citovala všechny použité prameny a literaturu. Současně prohlašuji, že práce nebyla využita k získání jiného nebo stejného titulu.

Souhlasím s trvalým uložením elektronické verze mé práce v databázi systému meziuniverzitního projektu Theses.cz za účelem soustavné kontroly podobnosti kvalifikačních prací.

V Praze, 07.10.2019 MSc. Dijana Lađinović

Identifikační záznam

LAĐINOVIĆ, Dijana. Epigenetika v genové regulaci a struktuře chromatinu [Epigenetics in gene regulation and chromatin structure]. Praha, 2019. 70s., 0 příl. Disertační práce (Ph.D). Univerzita Karlova v Praze, 1. lékařská fakulta, Ústav biologie a lékařské genetiky. Vedoucí práce Vacík, Tomáš.

Acknowledgements

I would first like to thank my supervisor, Ing. Tomáš Vacík, PhD. Thank you for being exceptional mentor and critical reviewer. Without your expertise and unselfish knowledge share, this whole project wouldn't be possible.

All the members of Dr. Vacík Lab (current and past), thank you for your cooperation and help throughout my PhD studies.

I would like to acknowledge prof. RNDr. Ivan Raška, DrSc. for constant support during my whole PhD studies. Thank you for your excellent cooperation and for all of the opportunities I was given to conduct my research.

In addition, I would like to thank all my friends, especially Jelena, Sravya, Patrick and Ines, for always being there for me. Thank you for listening, supporting and motivating me in every step of my life in Prague. Fernando, thank you for believing in me, pushing me and motivating me to be better. Your great support, especially during writing this thesis, was irreplaceable.

Finally, nothing of this would be possible without unlimited love and support from my family. Sandra, thank you for being amazing sister. Mom and Dad, thank you for trying to understand me and motivating me to go further.

Table of Contents

1. Souhrn

Metylace histonů hraje důležitou roli téměř ve všech buněčných procesech a udržování její správné hladiny zajišťují histon metyltransferázy a histon demetylázy. Nesprávná regulace hladiny metylace histonů je spojena s narušením regulace genové exprese a následně také s různými vývojovými defekty a nemocemi. V této práci jsme se zaměřili na lyzin demetylázy KDM2A a KDM2B a na jejich KDM2A-SF a KDM2B-SF izoformy postrádající demetylační aktivitu. Lyzin demetylázy KDM2A a KDM2B byly studovány převážně pro svojí demetylační funkci, kterou vykonávají na promotorech obsahujících CpG ostrovy. Jejich alternativní izoformy KDM2A-SF a KDM2B-SF však nebyly doposud detailněji studovány. Hlavním úkolem této práce bylo proto podrobně charakterizovat KDM2A-SF a zaměřit se také na roli, kterou by KDM2A-SF a KDM2B-SF mohli potenciálně hrát v kanonické Wnt signalizaci. Zjistili jsme, že *KDM2A-SF* mRNA vzniká působením alternativního intronového promotoru a není tak produktem alternativního sestřihu. Ukázali jsme, že KDM2A-SF startovní kodón leží v exonu, který odpovídá *KDM2A* exonu 14 a určili jsme tak přesnou aminokyselinovou sekvenci KDM2A-SF proteinu. Pomocí knockdown experimentů specifických pro jednotlivé KDM2A izoformy jsme dale ukázali, že KDM2A-SF narozdíl od KDM2A-LF vytváří v jádře distiktní struktury na pericentromerickém heterochromatin a to v závislosi na proteinu HP1α. Tyto transkripčně umlčené pericentromerické oblasti vykazují vysoké hladiny H3K36me2. Jelikož H3K36me2 je substrátem demetylázové activity KDM2A, došli jsme k závěru, že tyto oblasti jsou vázány KDM2A-SF izoformou. Dále jsme ukázali, že KDM2A-SF a KDM2B-SF potlačují kanonickou Wnt signalizaci navzdory tomu, že jim chybí demetylázová doména. Tato práce zdůrazňuje důležitost rozlišovaní mezi různými proteinovými izoformami a jejich rozdílnými funkcemi, které mohou v některých případech být i antagonistické.

2. Abstract

Histone methylation plays an important role in almost all cellular processes and its homeostasis is maintained by histone methyltransferases and histone demethylases. Misregulation of histone methylation levels is associated with gene expression misregulation and consequently also with various developmental defects and diseases. In this thesis we focus on the lysine demethylases KDM2A and KDM2B and on their demethylation deficient isoforms KDM2A-SF and KDM2B-SF. The lysine specific demethylases KDM2A and KDM2B have been predominantly studied for their demethylation function on CpG island-rich gene promoters. However, KDM2A-SF and KDM2B-SF have not been studied in detail. Therefore, the main goal of this thesis was to characterize KDM2A-SF more in detail and to focus on the role that KDM2A/B-SF might potentially play in canonical Wnt signaling pathway. We found that the *KDM2A-SF* mRNA arises through the action of an alternative intronic promoter and not by alternative splicing. We showed that the KDM2A-SF start codon is located in the exon that corresponds to KDM2A exon 14 and we thus determined the exact amino acid sequence of the KDM2A-SF protein. Furthermore, using an isoform specific knockdown assay we showed that KDM2A-SF, unlike KDM2A-LF, forms distinct nuclear foci on pericentromeric heterochromatin dependingly on the heterochromatin protein HP1α. These transcriptionally silent pericentromeric regions exhibit high levels of H3K36me2. Since H3K36me2 is the substrate of the KDM2A demethylase activity, we concluded that these regions are occupied by the demethylase deficient KDM2A-SF isoform. Further, we demonstrated that KDM2A-SF and KDM2B-SF repress canonical Wnt signaling despite lacking the demethylase domain. This thesis highlights the importance of distinguishing between different protein isoforms and their different functions, which can be sometimes even antagonistic.

3. Introduction

3.1. Chromosome structure

Chromatin is built up from DNA that together with histones forms chromosomes (Alberts et al. 2002). The first level of packing DNA into chromosomes is a nucleosome. A nucleosome is built of 147 base pairs (bp) of DNA wrapped around 8 histone proteins (Coleman 2018; Annunziato 2008). Histones are small positively charged proteins that tightly interact with the negatively charged phosphate groups of DNA. According to their electrophoretic mobility, histone proteins are divided into five types: H1, H2A, H2B, H3, and H4 (Castelnovo and Grauwin 2007). Histone H2A has two variants: H2AX with function in DNA repair and H2AZ associated with gene regulation and suppression of antisense RNA (Redon et al. 2002). The core histones have a conserved domain of 3 alfa helixes separated by loops that enables interactions between core histones (Mariño-Ramírez et al. 2005). Forming of the nucleosomal core is done in a specific order. First, the H3-H4 heterodimer is made, followed by the H3-H4 tetramer. DNA binding to the H3-H4 tetramer is followed by forming the H2A-H2B dimers and tetramers and their binding to the complex (Leuba and Brewer 2009). The core histones have long N-terminal ends (tails) protruding out of the nucleosome. The H3-H4 tetramer interacts with the central 60 bp, H3 interacts with 13 bp on each end of the core and the H2A-H2B dimers interact with 30 bp on both sides from the central 60 bp (White et al. 2001). The histone tails stabilize folding DNA around octamers. Histone H1 is a linking histone and it is twice less abundant. H1 is bound to DNA on the inside of the histone solenoid and each nucleosome associated with one H1 molecule is called chromatosome (Kornberg 1977; Rivenbark 2010). Nucleosomes form the 30 nm fiber and their tight coiling and interactions with other non-histone (scaffold) proteins and long noncoding RNAs (lncRNAs) forms higher order structures such as the 300nm and 700nm fiber (Poonperm et al. 2015; Hall and Lawrence 2016) (Figure 1). These fibers represent the structure of the interphase chromosome.

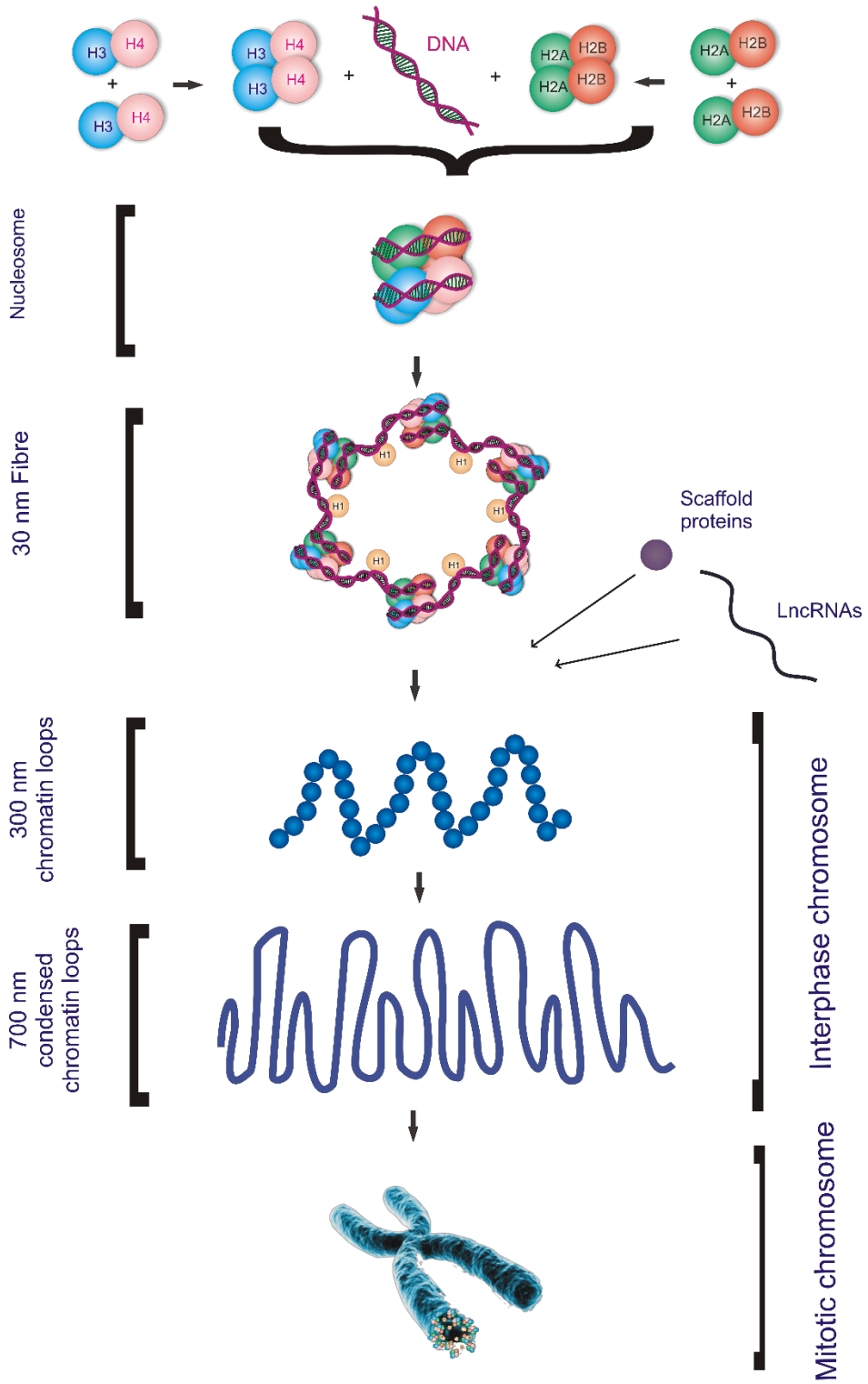

Figure 1. Chromosome structure – Nucleosome is formed by histone-DNA interactions and it represents the lowest level of chromosome organization. Nucleosomes connect to one another creating the 30nm fiber. Further binding of scaffold proteins and

lncRNAs enables weaving into the higher order structures, the 300-700nm fibers that represent the structure of the interphase chromosome. During the cell division chromosomes are condensing into the metaphase chromosome structure. (Felsenfeld and Groudine 2003; Poonperm et al. 2015; Hall and Lawrence 2016).

Before a mitotic division, the chromosome structure is altered by the complex called condensin which enables chromosome condensation into the characteristic four arm structure (Hirano 2012) (Figure 1). In this condensed state chromosomes consist of two chromatids that are connected together by a centromere. The centromere is the place through which chromosomes attach to the microtubules of the mitotic spindle during cell division using a special structure called kinetochore (O'Connor 2008). During the S phase of the mitotic cell cycle the centromere duplicates and the chromatid pairs separate becoming separate chromosomes. The centromere region mostly consists of highly repetitive short DNA sequences which makes them one of the fragile sites of chromosomes. Another characteristic of the centromere is that its nucleosomes contain a histone H3 variant called CENP-A (O'Connor 2008, Westhorpe and Straight 2014). These CENP-A containing nucleosomes are required for the formation of the kinetochore. The kinetochore is a protein complex that establishes the connection between the spindle microtubules and chromosomes and regulates chromosome segregation during mitosis and meiosis (Cleveland et al. 2003; O'Connor 2008).

The centromeric H3 histones are enriched in various posttranslational modifications such as dimethylation on lysines 4, 9, and 36. It has been shown that the H3K4me2 modification is specific for the centromeric region and that it promotes assembly of CENP-A into chromatin (Westhorpe and Straight 2014). CENP-A also undergoes specific posttranslational modifications that control the chromatin function. Disruption of the CENP-A phosphorylation at Ser7 leads to defects in chromosome segregation and cytokinesis. Furthermore, dephosphorylation of CENP-A at Ser16 and Ser18 also leads to chromosome missegregation. CENP-A is also subject to methylation

and it is trimethylated on the alpha-amino group. This trimethylation is required for recruitment of other constitutive centromere associated proteins, CENP-T and CENP-I. Within the histone fold domain, CENP-A undergoes methylation, acetylation, as well as ubiquitination on Lysine 124 in the α3 helix and these modifications are essential for CENP-A deposition, centromere formation and chromosome segregation (Srivastava et al. 2018).

The centromere divides a chromosome into two sections – arms. The longer arms are marked as "q-arms", while the shorter arms are marked as "p – arms" (Figure 2). Depending on the centromere location chromosomes are categorized as follows:

1. Metacentric – the centromere is in the middle of the chromosome, p arms and q arms are of similar length (human chromosomes 1, 3, 16, 19, 20);
2. Submetacentric – the centromere is not in the center of the chromosome, p arms are shorter then q arms (human chromosomes 2, 4 – 12, 17, 18, X);
3. Acrocentric – the centromere is closer to one side of the chromosome, p arms are much shorter then q arms (human chromosomes 13 – 15, 21, 22, Y);
4. Telocentric – the centromere is located at the end of the chromosome; the p arms do not exist (this type of chromosome is not found in the human karyotype) (O'Connor 2008).

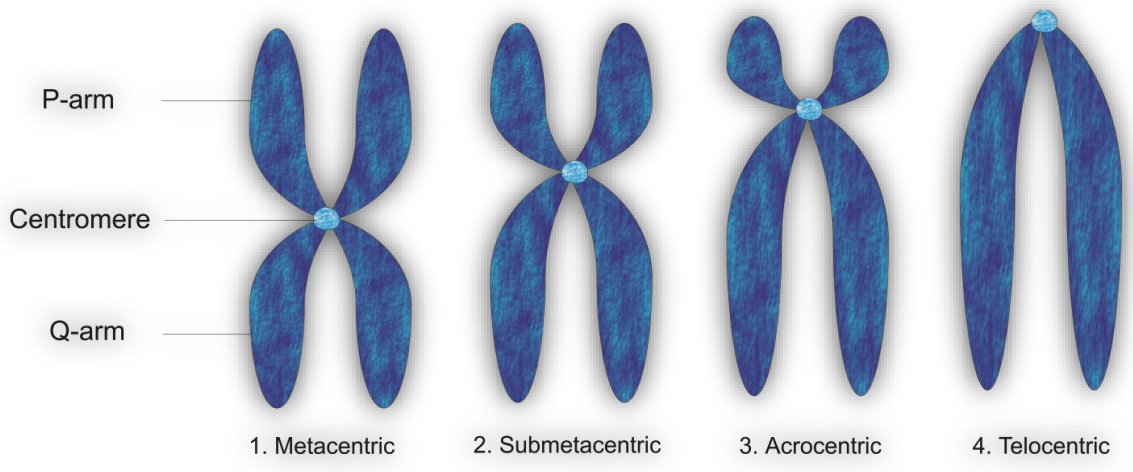

Figure 2. Chromosome classification according to the centromere position.

The region next to the centromere is called pericentromeric heterochromatin. Pericentromeric heterochromatin consists of tandem repeats of major and minor satellites. Another characteristic of pericentromeric heterochromatin is the presence of high levels of di- and tri-methylation on lysine residues 9 and 27 of histone H3 (H3K9me2, H3K9me3, H3K27me2, and H3K27me3) which are required for initial transcriptional silencing of pericentromeric heterochromatin (Hall et al. 2012; Jachowicz et al. 2013). These histone modifications are typically associated with transcriptional silencing. Polycomb group (PcG) proteins have been shown to tightly associate with the pericentromeric heterochromatin regions on different chromosomes even throughout mitosis. The PcG complex is thus potentially inherited through successive cell divisions (Saurin et al. 1998). Polycomb Repressive Complex 1 (PRC1) is also recruited by the KDM2B demethylase to CpG islands and it maintains gene silencing on pericentromeric heterochromatin (Farcas et al. 2012; Wong et al. 2016). Pericentromeric heterochromatin plays a role in the correct chromosomal segregation and facilitates the attachment of sister kinetochores to microtubules from the opposite spindle poles. During the cell division, mitosis and meiosis, pericentromeric heterochromatin is involved in establishing the proper orientation of the sister chromatids before anaphase is initiated. Through this function pericentromeric heterochromatin prevents chromosomes from mis-segregation, which leads to aneuploidy and chromosome instability (Tanaka et al. 2013).

Telomeres are the regions located at the end of chromosomes and their main function is to prevent chromosome ends from nucleolytic degradation, unnecessary recombination, interchromosomal fusion, as well as from being recognized as DNA double strand breaks (Lu et al. 2013). Due to the inability of DNA polymerases to replicate linear genomes fully, telomere length is shortening by age. The loss of terminal DNA leads to oncogenic transformation of somatic cells, senescence, or apoptosis that affects the health and lifespan of an individual (Shammas 2011). In germ lines and stem cells shortening of telomeres is prevented by the action of the telomerase enzymes that add new telomeric repeats to the G rich ends (Galati et al. 2013). Telomeric regions are composed of short DNA repeats and they are subject to different posttranslational

modifications. These epigenetic modifications include methylation of lysines 4, 9 and 79 on histone H3 (H3K4, H3K9, H3K79), and of lysine 20 on histone H4 (H4K20). Together with acetylation of lysine 27 on histone H3 (K3K27) and deacetylation of lysines 9 and 56 on histone H3 (H3K9ac, H3K55ac) they have a role in chromatin compaction. Phosphorylation of telomeric H2AX as well as ubiquitination of telomeric H2A and H2AX play a role in double damage repair signaling (Galati et al. 2013; Cubiles et al. 2018).

Unlike mitotic chromosomes, interphase chromosomes are decondensed and distributed all over the nucleus (Ris and Mirsky 1949) (Figure 1). In 1928, Emil Heitz described condensed and decondensed chromatin according to their interphase staining. The nuclear material that was highly condensed and strongly stained was named as heterochromatin, while the less condensed regions with lighter staining were named euchromatin (Alberts et al. 2002).

Heterochromatin represents such genomic regions as centromeres and telomeres which are transcriptionally inactive DNA structures. Another example of heterochromatin is inactivated X-chromosome in a female – Barr body (Sharakhov and Sharakhova 2015). Condensation of heterochromatin is established by various epigenetic modifications such as hypoacetylation and hypermethylation (e.g. H4K20me1/3, H3K9me2/3, H3K27me2/3) (Trojer and Reinberg 2007). It is believed that aside from gene regulation, heterochromatin plays a role in the chromosome integrity (Janssen et al. 2018). In addition to the histone modifying enzymes such as histone deacetylases, histone methyltransferases and histone ubiquitin ligases, chromatin condensation can be also affected by ATP-dependent chromatin remodeling factors and DNA methyltransferases (Trojer and Reinberg 2007).

Heterochromatin can be detected in two different states: constitutive and facultative heterochromatin. Constitutive heterochromatin is characterized by tandem repeats or satellite sequences, with relatively high levels of H3K9me3 and HP1α/β. It represents permanently transcriptionally silenced regions such as the centromeres and telomeres (Nielsen et al. 2001; Alberts et al. 2002). Facultative heterochromatin also

represents transcriptionally silent regions, but it retains the potential to switch between heterochromatin and euchromatin. These genomic regions can be expressed through the specific developmental and/or cell cycle states (temporal regulation), localization dependent due to exogenous signals (spatial regulation) and heritable parental monoallelic gene expression. As opposed to constitutive heterochromatin, facultative heterochromatin is not rich in tandem repeat sequences (Trojer and Reinberg 2007).

Euchromatin is more relaxed decondensed chromatin distributed all over the nucleus (Alberts et al. 2002). Euchromatin is also known as “beads on a string” because of its open decondensed structure of nucleosomes and linker DNA. This “beads on a string” conformation makes the chromatin accessible to RNA and DNA polymerases, transcription factors and other factors that are necessary for replication and transcription. Euchromatin is also rich in certain histone modifications such as lysine acetylation and methylation. Euchromatin modifications are represented mostly by hyperacetylation of lysine residues at positions 5, 8, 12, and 16 of H4 and 9, 14, 18, and 23 of H3, and methylation H3K4me2/3 and H3K36me3 that are marks of transcriptionally active regions (Jasencakova et al. 2000; Trojer and Reinberg 2007). Euchromatin contains most of the transcriptionally active genes and undergoes cyclical changes of transcriptional activation and repression during the cell cycle (Ma et al. 2015).

3.2. Epigenetics

As mentioned in the previous chapter chromatin is subject to various modifications called epigenetic modifications. Term epigenetics was proposed for the first time by developmental biologist and geneticist Conrad H. Waddington in 1939. Originally term epigenetics was used to describe the influence of genetic processes on early embryonic development (Waddington 1939). In 1975, a British molecular biologist, Robin Holliday, defined epigenetics as the study about mechanisms that control gene activity during development of complex organisms in the spatiotemporal manner (Holliday and Pugh 1975; Holliday 1994). Later, Artur Riggs defined epigenetics as the study of mitotic

and meiotic heritable changes that are not caused by changes in the DNA sequence (Riggs and Porter 1996).

Epigenetics is the field of genetics that studies phenotypic traits that are not defined by the DNA sequence, but by DNA methylation, various histone modifications and through non-coding RNAs (Razin and Kantor 2005; Butler et al. 2016; Alaskhar Alhamwe et al. 2018). These epigenetic changes can last through the whole cell division or they can last through several generations (Holliday 1994; Barros and Offenbacher 2009; Heard and Martienssen 2014; Burggren 2016; Lester et al. 2016). Epigenetic changes can be heritable, a phenomenon called trans-generational epigenetic inheritance (Heard and Martienssen 2014). If an epigenetic change occurs in germs cells, sperm or in oocyte that are involved in fertilization, this epigenetic modification can be transferred to all future generations (Skvortsova et al. 2018; Lacal and Ventura 2018). Transgenerational epigenetic inheritance occurs as a response to environmental or metabolic factors such as trauma, diet, obesity, diabetes, undernourishment, endocrine disruptors, and lifestyle (Bernhard 2018).

Epigenetics affects almost all biological processes ranging from embryogenesis to aging (Sharma et al. 2010; Skinner 2011; Calvanese and Fraga 2012; Moosavi and Motevalizadeh Ardekani 2016; Ashapkin et al. 2017). Cell differentiation is one example of such processes and epigenetics enables the cell to express just the genes that are necessary for its differentiation. During morphogenesis, cells are going through different stages in order to create differentiated cells. Totipotent cells, embryonic cells made immediately after fertilization that can transform into all types of body cells including extraembryonic or placental cells, transform into different pluripotent cell lines. Pluripotent cells can transform into all types of body cells of the embryo. Later these pluripotent cells give rise to completely differentiated cells, and the zygote, as one fertilized oocyte, continues to divide to create daughter cells (Wu and Sun 2006; Atlasi and Stunnenberg 2017). Also, epigenetic alterations have an important role in the cellular transformation to cancer (Sharma et al. 2010). Furthermore, epigenetic changes are responsible for everyday homeostasis of the cell by activating and repressing certain

genes. If homeostasis of the cell is disrupted by a higher or lower expression of some genes, it can cause various developmental defects, diseases or even cancer (Beerman and Rossi 2015; Abdelsamed et al. 2018). Epigenetic modifications can affect also other biological processes such as transcription of genes, DNA damage repair, as well as alternative splicing (Gibney and Nolan 2010; Mao and Wyrick 2016; Xu et al. 2018).

3.2.1. Epigenetics in transcriptional regulation

Regulation of gene expression is one of the most fundamental processes in living organisms and epigenetic modifications are crucial in this process, as well as in the regulation of various genomic functions and genome integrity (Jaenisch and Bird 2003; Reik 2007; Gibney and Nolan 2010). Epigenetic mechanisms regulate accessibility of transcriptional factors and of RNA polymerases to chromosomal regions and by doing so they control gene transcription. DNA methylation, histone modifications and non-coding RNA transcripts are recognized as important epigenetic mechanisms that have an impact on transcriptional regulation (Gibney and Nolan 2010; Turner 2002; Smith and Meissner 2013; Peschansky and Wahlestedt 2014). These mechanisms control packing of DNA into chromosomes and how tightly the DNA is wound around histones. Additions or removals of these modifications to the histone tails or to DNA can cause opening or closing of chromosomal regions and consequently activation or repression of gene transcription (Bannister and Kouzarides 2011). One example of gene regulation through epigenetic modifications is the methylation of lysine 27 on histone H3 (H3K27me). H3K27 can be mono-, di- or tri-methylated and it is a feature of facultative heterochromatin (Jamieson et al. 2016; Wiles and Selker 2017). It maintains transcriptional repression throughout development, where H3K27me3 represents the first repressive mark (Moody et al. 2017). Another important epigenetic mark in embryonic development is trimethylation of lysine 4 on histone H3 (H3K4me3) (Huang et al. 2019). While H3K27me3 represses regulatory genes during embryonic development, H3K4me3 acts like an activator of gene transcription. Together, H3K27me3 and H3K4me3 maintain and regulate cell differentiation in early embryogenesis (Vastenhouw and Schier 2012). Other methylation

marks are also involved in transcriptional regulation, where methylation of H3K9, H3K27, or H4K20 are usually associated with transcriptional repression, while methylation of H3K4, H3K36 or H3K79 are usually associated with transcriptional activation (Hyun et al. 2017; Shen et al. 2017; Wiles and Selker 2017; Eissenberg and Shilatifard 2010; Wagner and Carpenter 2012; Farooq et al. 2016; Nguyen and Zhang 2011).

DNA methylation has also a crucial role in gene expression. High levels of DNA methylation in promotors correlate with low or no transcription, which makes DNA methylation an epigenetic modification that negatively regulates gene expression (Ando et al. 2019). Another modification with an important role in transcriptional regulation is acetylation (Sterner and Berger 2000). Histone acetylation neutralizes the positive charge of a histone tail which weakens histone-DNA interactions (Norton et al. 1989). This change in the nucleosome structure enables transcription factors to access a genetic locus and to stimulate gene transcription (Sterner and Berger 2000; Hirschler-Laszkiewicz et al. 2001). A lack of acetylation marks correlates with gene repression and maintaining the appropriate levels of histone acetylation is required for regulation of cell homeostasis through gene transcription (Kuo and Allis 1998). Long non-coding RNAs (lncRNAs) also play an important role in gene transcription regulation (Guttman et al. 2011; Long et al. 2017). Their role is fulfilled through recruitment or inhibition of transcription factors. Furthermore, lncRNAs can act indirectly by building a ribonucleoprotein complex that establishes posttranslational modifications activating or repressing transcription (Smith et al. 2000; Long et al. 2017).

3.2.2. Epigenetics in DNA damage repair

DNA is subject to spontaneous damage by different environmental factors such as chemicals, ionizing radiation and UV light. Furthermore, DNA can suffer damage during DNA replication and the generation of cytotoxic DNA double strand breaks (DSB) or intracellular generation of reactive oxygen species (Richard et al. 2015). There are four different mechanisms of DNA damage repair: DNA mismatch repair (MMR), base excision repair (BER), nucleotide excision repair (NER), and double-strand break repair pathway (Li

2008; Negritto 2010; Lahtz and Pfeifer 2011; Krokan and Bjørås 2013; Schärer 2013). Epigenetic modifications like acetylation, methylation, phosphorylation and ubiquitination play important roles in DNA damage repair mechanisms (Mao and Wyrick 2016). For example, in double strand damage repair the first epigenetic signal is phosphorylation of the histone H2AX on Serine 139 initiated by the ataxia-telangiectasia mutated (ATM) protein kinase (Rass et al. 2013). This phosphorylation results in the recruitment of a number of repair proteins such as the MRN complex, which contains the meiotic recombination 11 (Mre11), Nijmegen breakage syndrome 1 (NBS1) and Rad50 protein, and which is necessary for the initial processing of double-strand DNA breaks prior to repair (Bennett 2013). H2AX phosphorylation is also required for accumulation of other repair proteins such as BRCA1 and 53BP1 (Podhorecka et al., 2010). In addition to phosphorylation, polyubiquitination of H2AX is also required for the recruitment of 53BP1 and BRCA1, the proteins involved in DNA damage repair, to DNA double strand breaks (Kocyłowski et al. 2015). Methylation is another important epigenetic modification involved in DNA damage repair. Methylation of H3K36 in the DNA repair pathway has a dual role depending on the number of the methyl groups and the cell cycle stage. H3K36me3 is necessary for homologous recombination repair (HR). Double strand breaks located in H3K36me3 rich regions or transcriptionally active genes are mostly repaired by the HR repair mechanism, while breaks in H3K36me3 scarce regions and inactive genes prefer the non-homologous end joining (NHEJ) repair mechanism (Fnu et al. 2011; Clouaire and Legube 2015). As opposed to H3K36me3, H3K36me2 functions after DNA damage repair (Amendola et al. 2017). Methylation of H4K20 and H3K79 is also important for DNA damage repair, where H3K79me and H4K20me2 recruit 53BP1 to DNA double strand breaks (Schotta et al. 2008; Huyen et al. 2004). Acetylation of histones H2A, H3 and H4 are required for DNA damage repair. By acetylating K9, K14, K18, K23, and K27 on histone H3 and K5, K8, K12, and K16 on histone H4 chromatin opens and enables the repair machinery to approach the damaged site (Tamburini and Tyler 2005).

3.2.3. Epigenetics in alternative splicing

Alternative splicing represents a regulatory process by which various exons are either kept or skipped and more different mRNA isoforms are created (Wang et al. 2015). Important factors that regulate alternative splicing are epigenetic modifications (Zhu et al. 2018). DNA methylation occurs in the alternative donor sites and mediates alternative splicing through methyl-binding domain proteins and their interaction with splicing factors (Gelfman et al. 2013; Zhu et al. 2018). Some histone modifications such as H3K4me3, H3K9me3, H3K36me3, H3K79me, H3K27ac, and H4K8ac are involved in alternative splicing (Sims et al. 2007; Piacentini et al. 2009; Xu et al. 2018). These histone modifications regulate alternative splicing by altering the RNA polymerase II elongation rate or through chromatin-adapter systems (Xu et al. 2018).

LncRNAs are also known to regulate alternative splicing through interaction with serine and arginine-rich (SR) proteins or heterogeneous nuclear ribonucleoproteins (hnRNP) (Zhu et al. 2018). SR proteins are RNA-binding proteins, while hnRNPs represent an RNA-protein complex that marks precursor mRNA (pre-mRNA) for alternative splicing (Chen et al. 1999; Jeong 2017). LncRNAs modulate the phosphorylation status of SR proteins and by doing so they affect alternative splicing (Tripathi et al. 2010). Furthermore, lncRNAs can form RNA-RNA duplexes with precursor mRNAs and through that interaction they can affect alternative splicing (Romero-Barrios et al. 2018).

3.3. Epigenetic modifications

Epigenetic control is often associated with alternative covalent modifications of either histones or DNA and it can be achieved through two main mechanisms:

1. Addition of methyl groups on DNA (Kumar et al. 2018);
2. Posttranslational modifications of amino acids in histone tails (Bannister and Kouzarides 2011).

3.3.1. DNA methylation

DNA methylation represents a heritable epigenetic change that provides regulation of gene expression through covalent addition of methyl (CH_3) group from *S*-adenyl methionine (SAM) mostly on CpG islands, changing cytosine to 5-methylcytosine. 5-methylcytosine acts mostly as regular cytosine connecting with guanine in double helix DNA (Jin et al. 2011). Addition of methyl groups to CpG islands, their establishment and maintenance is carried out by DNA methyltransferases (DNMTs). DNA methylation is spread out across the genome where some parts are more methylated than others. The regions depleted of DNA methylation are known as transcriptionally active, while highly methylated regions are known as less transcriptionally active (Jin et al. 2011; Moore et al. 2013; Kumar et al. 2018).

Next to DNA methylation, DNA demethylation has also important role in regulating DNA methylation pattern. DNA demethylation represents removing methyl group from DNA and this process is also necessary for epigenetic regulation of the genome and gene expression (Jin et al. 2011). Dynamic processes of DNA methylation and demethylation have eminent role in development. During the zygote formation DNA methylation is removed and then at the time of implantation it is re-established (Moore et al. 2013). In addition to development and gene expression, DNA methylation plays an important role in many other important processes such as X chromosome inactivation and genomic imprinting, and its misregulation can lead to various diseases including cancer (Sharp et al. 2011; Li et al. 1993).

3.3.2. Histone modifications

Histone modifications play a fundamental role in most biological processes (Strahl and Allis 2000; Bannister and Kouzarides 2011). Although histone modifications are present through the whole sequence, histone tail is usually highly modified. Modifications act as docking modules for related factors and affect inter-nucleosomal interactions and thus affect the overall chromatin structure. Different histone modifications function in different ways. The same modification can function differently at two different positions.

For example, methylated H3K9 is associated with transcriptional repression, while methylation of H3K4 associates with transcriptional activation (Eissenberg and Shilatifard 2010; Hyun et al. 2017). Also, more different modifications may occur at the same position and they can change the behavior of the nucleosome differently. For example, H3K9me is associated with transcriptional repression, while H3K9ac is associated with active transcription and it promotes transcriptional elongation (Wagner and Carpenter 2012; Gates et al. 2017; Hyun et al. 2017). This creates a large number of potentially distinct combinations and functions of various epigenetic marks. These modifications represent inherited or *de novo* molecular changes that affect the local chromatin structure and the gene expression (Zhu et al. 2011; Bannister and Kouzarides 2011). Post-translational modifications of the core histones have been shown to be essential for a large scale of cellular processes such as transcription, DNA replication, DNA damage repair, recombination, chromatin structure, cell cycle, and pre-mRNA splicing (Li et al. 2007; Kouzarides 2007; Palstra and Grosveld 2012; Towbin et al. 2013; Cabianca and Gasser 2016; Sen et al. 2016; Xu and Xie 2017; Gates et al. 2017).

Epigenetic histone modifications include methylation, acetylation, ubiquitination, phosphorylation, sumoylation, ribosylation and citrullination (Henikoff et al. 2004; Kouzarides 2007; Bannister and Kouzarides 2011; Henikoff and Smith 2015).

3.4. Histone methylation

Histone methylation is a dynamic process of adding one or more methyl groups to the lysines or arginines on the histone side chains by the enzymes called histone methyltransferases (Di Lorenzo and Bedford 2011; Greer and Shi 2012; Dong and Weng 2013). It has been reported that histidines can also be monomethylated, although it has not been further characterized (Borun et al. 1972). Histone methylation has been found to be an important posttranslational modification involved in almost all biological processes from cell cycle, transcription, DNA repair to development, differentiation and aging (Wu and Sun 2006; Greer and Shi 2012; Wei et al. 2018; Fukuda et al. 2019).

Histone methylation is a reaction of transferring a methyl group from S-adenosyl methionine to histone proteins (Greer and Shi 2012; Borun et al. 1972) (Figure 3A). Unlike other histone modifications, histone methylation does not alter the charge of the histone protein (Bannister and Kouzarides 2011). Histone methylation is mainly accomplished through specific recognition of the methylated site by effectors and transcription factors (Xin and Rohs 2018). It typically takes place on the side chains of lysines and arginines, although there are reports of histidine methylation that has not been yet characterized (Greer and Shi 2012; Borun et al. 1972). Arginine can be mono-methylated and symmetrically or asymmetrically di-methylated by enzymes arginine methyltransferases on their guanidinyl group. There are two types of arginine methyltransferase: the type I enzymes that generate mono- and asymmetrically di-methylated arginines and type II enzymes that generate mono- and symmetrically di-methylated arginines. Both classes of arginine methyltransferases transfer a methyl group from S-adenosyl methionine to the ω-guanidin group of arginine (Bannister and Kouzarides 2011). Lysines can be monomethylated, dimethylated or trimethylated and this is accomplished through lysine methyltransferases. Histone lysine methyltransferases transfer a methyl group from S-adenosyl methionine to lysine ε amine group within the N-terminal tails (Di Lorenzo and Bedford 2011; Greer and Shi 2012) (Figure 3A). All lysine histone methyltransferases contain SET domain that carries catalytical activity, except for the Dot 1 enzyme that does not contain a SET domain, and it is believed that all histone lysine methyltransferases have strict target specificity (Dillon et al. 2005).

Histone methylation regulates approachability of docking sites for different regulation factors, and by making them "open" or "closed" it regulates the binding of transcriptional factors, by means, it acts epigenetically to activate or repress gene expression (Figure 3B) (Greer and Shi 2012; Dong and Weng 2013). The most commonly methylated histone arginines are H3R2, H3R8, H3R17, H3R26 and H4R3, while histone lysine methylation can be found on histones H3 and H4, on lysines K4, K9, K27, K36, K56, K64 or K79 (Kouzarides 2007; Bannister and Kouzarides 2011; Greer and Shi 2012; Jack et al. 2013; Lange et al. 2013; Henikoff and Smith 2015; Hyun et al. 2017; Kang et al. 2018;

Huang et al. 2019). In addition to transcriptional regulation, histone methylation plays an important role in the chromatin structure. For example, heterochromatin is characterized by trimethylation of H3K9 in mammals (Nielsen et al. 2001).

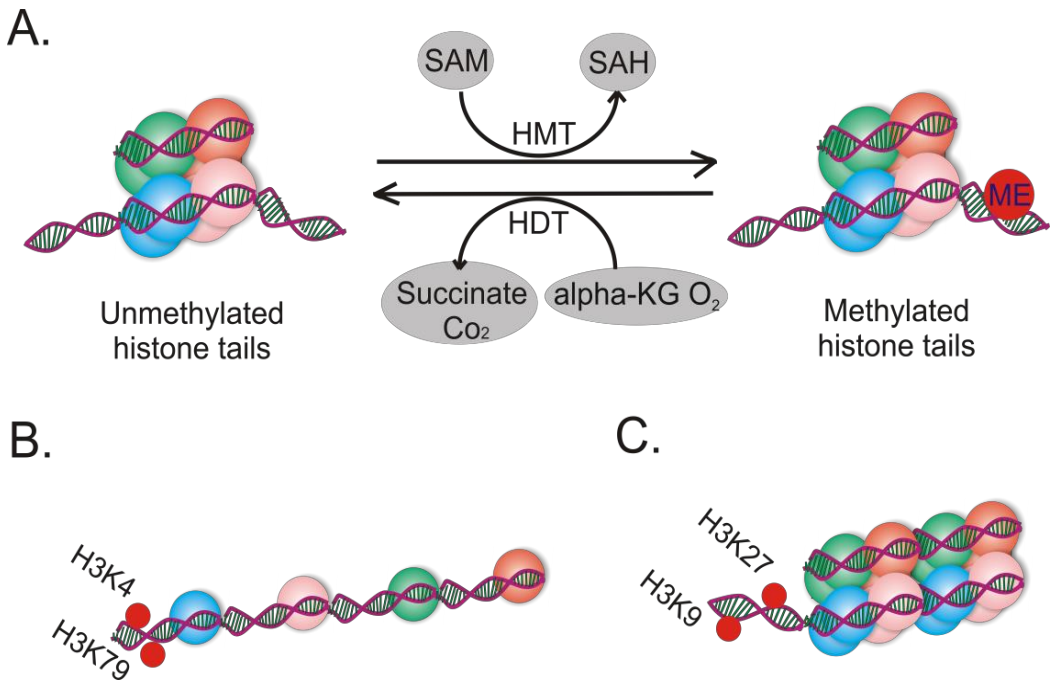

Figure 3. Histone methylation. **(A)** Histone methylation is done through the activity of histone methyl transferases (HMT) where methyl group is transferred from S-adenosylmethionine (SAM) to lysine/arginine giving S-adenosylhomocysterin (Di Lorenzo and Bedford 2011; Greer and Shi 2012). Histone demethylation represents removing of a methyl group from lysines/arginines by histone demethylases (HDMs) (Culhane and Cole 2007). **(B)** Methylation of H3K4 and H3K79, respectively induces an open histone structure (Huang et al. 2019; Farooq et al. 2016). **(C)** Methylation of H3K9 and H3K27, respectively induces closed histone structure and represses gene transcription (Hyun et al. 2017; Wiles and Selker 2017).

3.5. Histone demethylation

For a long time it was believed that histone methylation is an irreversible process. However, in 2004 Dr. Yang Shi's laboratory discovered the first histone demethylase LSD1 (LSD1) (Shi et al. 2004). While histone methyltransferases have a role in adding methyl

group, histone demethylases have a role in removing the methyl group from histones – histone demethylation, which alters the spacing of nucleosomes and changes the gene expression (Figure 3) (Kang et al. 2017; Marabelli et al. 2019). Histone demethylases constitute a big family of proteins which play essential roles in various cellular processes such as transcription, chromatin architecture, and cellular differentiation (Cloos et al. 2008; Dimitrova et al. 2015; Kang et al. 2017).

There are two families of histone demethylases, the Jumonji domain-containing (JmjC) proteins and the lysine (K)-specific demethylase proteins (D'Oto et al. 2016). The first histone demethylase to be discovered was the lysine (K)-specific demethylase 1A (LSD1, also called LSD1), which can demethylate the mono- and di-methylated lysines 4 and 9 (K4 and K9) on histone H3 (Shi et al. 2004; Matoba et al. 2014). It is an 852 amino acid (AA) long protein that contains three domains: the amine oxidase catalytic domain (AOD) (residues 272–415 and 515–852), the approximately 100 AA long insert known as the "tower" domain (residues 415–515), and the SWIRM domain (residues 172–272) (Chen et al. 2006). AOD is the catalytically active LSD1 domain whose histone demethylation activity is catalyzed through flavin adenine dinucleotide (FAD) (Forneris et al. 2005). LSD1 takes part in several complexes such as the CoREST transcriptionally repressive complex, the Mi-2/nucleosome remodeling complex, the NuRD deacetylase complex and the lysine methyltransferase mixed lineage leukemia (MLL) coactivator complex (Lee et al. 2005; Harris et al. 2012; Ouyang et al. 2013). LSD1 is highly expressed in several cancer types such as breast, lung, prostate, bladder and esophageal cancer, neuroblastoma and acute myeloid leukemia (AML) (Kong et al. 2016; Maiques-Diaz and Somervaille 2016; McGrath et al. 2016; Chen et al. 2017; Jubierre et al. 2018; Sehrawat et al. 2018). Also, LSD1 is highly expressed in undifferentiated human embryonic stem cells and it is progressively downregulated during differentiation (Myrick et al. 2017). The mouse LSD1 knockouts exhibit embryonic lethality before embryonic day 7.5 (E7.5) due to a failure in egg cylinder elongation and gastrulation (Foster et al. 2010). In addition to histone demethylation, LSD1 also has a role in demethylation of TP53, E2F1, and DNMT1 (Huang et al. 2007; Foster et al. 2010; Kontaki et al. 2010; Brenner et al. 2016).

KDM1B is a flavin-dependent histone demethylase associated with chromatin remodeling, gene silencing and it plays an important role in transcriptional regulation and genomic imprinting (Ciccone et al. 2009; Katz et al. 2014). It demethylates H3K4me1/2 in the intergenic regions of the target genes and complexes with active transcription elongation factors, as well as with the histone methyltransferases EHMT1/2 and NSD3 (Fang et al. 2010). KDM1B plays a role in transcriptional regulation of LSD1, HDAC1/2, and DNMT3B (Chen et al. 2017). In comparison to normal breast cell lines, the KDM1B protein levels are elevated in malignant breast cell lines and in basal-like breast tumors (Chen et al. 2017; Katz et al. 2014). KDM1B has an impact on cell proliferation, colony formation, motility, and invasion. Furthermore, in breast cancer cells KDM1B induces the expression of the pluripotent stem cell markers such as NANOG and SOX2 (Chen et al. 2017). LSD1 and KDM1B share the centrally located SWIRM domain, and the C-terminal oxidase domain (AOD domain). Unlike LSD1, KDM1B does not have the tower domain, but it has an N-terminal zinc finger which forms a CW-type zinc-finger domain. The CW domain binds to methylated histones and it is present in several chromatin-remodeling proteins. The demethylase activity is dependent not only on the AOD domain, but also on the N-terminal zinc-finger domain, the SWIRM domain (Fang et al. 2013).

The JmjC-containing protein family is mostly characterized by lysine demethylases (KDMs). In addition to demethylation of methylated lysines, some JmjC-domain containing proteins are also involved in hydroxylation reactions where they catalyze oxidative modifications to create chemically stable alcohol products (Markolovic et al. 2016). Recently it has been published that some JmjC domain-containing proteins (JMJD5 and JMJD7) function as proteases and can remove methylated arginine residues on histone tails (Liu et al. 2017).

JmjC domain-containing proteins have the shape of the cupin fold built of flattened beta-barrel structure. The beta-barrel contains a double-stranded antiparallel beta-sheet structure that is typical for this family of non-haeme iron (II) and 2-oxoglutarate dependent oxygenases (Meng et al. 2018). The enzymatically active pocket within the JmjC domain binds the cofactors non-haeme iron (II) and 2-oxoglutarate (2OG

Subfamily	Name	Synonym	Oxygenase	Lysine Demethylase	Arginine Demethylase	Clipping
JHDM1	JHDM1A	KDM2A		H3 (K36me1/2)		
	JHDM1B	KDM2B		H3 (K4me3/ K36me2)		
PHF2 /PHF8	JHDM1D	KDM7A		H3 (K9me2/ K27me2)		
	PHF8	KDM7B		H3 (K9me1/2) H4 (K20me1)		
	PHF2	JHDM1E		H3 (K9me1) H4 (K20me3)		
JHDM2	HR			H3 (K9me1/2)		
	JMJD1A	KDM3A		H3 (K9me1/2)		
	JMJD1B	KDM3B		H3 (K9me1/2)		
	JMJD1C	KDM3C		H3 (K9me1/2)		
UTX /UTY	JMJD3	KDM6B		H3 (K27me2/3)		
	UTX	KDM6A		H3 (K27me1/2/3)		
	UTY	KDM6C		H3 (K27me3)		
JMJD2 /JHDM3	JMJD2A	KDM4A		H3 (K4me3/ K27me3/ K36me3)	H3 (R2me2a)	
	JMJD2B	KDM4B		H3 (K9me3/ K36me3)		
	JMJD2C	KDM4C		H3 (K9me3)		
	JMJD2D	KDM4D		H3 (K9me2/3)		
JARID	JARID1A	KDM5A		H3 (K4me2/3)		
	JARID1B	KDM5B		H3 (K4me1/2/3)		
	JARID1C	KDM5C		H3 (K4me2/3)	H3 (R2me1/2a/2s/ R8me2a/2s) H4 (R3me2a/2s)	
	JARID1D	KDM5D		H3 (K4me2/3)		
	JARID2					
JmjC domain only	JMJD5	KMD8	+	H3 (K36me2)		H3 (R2me2/ K9me1) H4 (R3me2)
	JMJD7					H3 (R2me2) H4 (R3me2)
	TYW5		+			
	HSPBAP1					
	HIF1AN	FIH	+			
	JMJD4		+			
	JMJD6		+		H3 (R2me2a/2s) H4 (R3me1/2a/2s)	
	JMJD8					
	NO66	RIOX1	+	H3 (K4me1/3/ K36me2/3)		
	MINA	RIOX2	+			

Table 1. JmjC-containing protein family, their biochemical and oxygenase activities (Meng et al. 2018).

or α-ketoglutarate)-dependent oxygenases, demethylates histones and generates formaldehyde and succinate (Tsukada et al. 2006; Shmakova et al. 2014). The members of the JmjC-containing family are shown in Table 1 together with their demethylase and oxygenase functions.

3.6. Lysine demethylase KDM2A

The lysine demethylase KDM2A, also known as FBXL11 or JHDM1A, was originally identified as a dimethyl Lysine 36 histone H3 (H3K36me2) demethylase (Tsukada et al. 2006; Cheng et al. 2014). The KDM2A gene encodes an 1162-amino-acid protein containing the demethylation Jumonji C domain - JmjC (residues 148-316), the DNA binding CXXC zinc finger domain (residues 564-610), the plant homeodomain (PHD) zinc finger domain (residues 617-678), the F-box domain (residues 889-936), and the C-terminal six leucine-rich repeats domain (LRR) (residues 961-1156) (Tsukada et al. 2006; Cheng et al. 2014; Borgel et al. 2017). KDM2A binds to nonmethylated CpG islands through its ZF-CXXC DNA binding domain and using its N-terminal JmjC demethylase domain utilizes multiple cofactors to hydroxylate the methyl group and remove it from di- and mono-methylated H3K36. By demethylating H3K36me2 in transcriptionally active gene promoters, KDM2A functions as a transcriptional repressor and it has been shown to repress a number of genes, as well as the centromeric repetitive DNA and ribosomal DNA (Frescas et al. 2008; Tanaka et al. 2010; Runtao et al. 2013; Dhar et al. 2014; Kawakami et al. 2015; Tanaka et al. 2015). Furthermore, KDM2A is also involved in demethylation of lysine residues of non-histone proteins such as the NF-kB p65 subunit at lysines K218 and K221. This demethylation results in downregulation of NF-kappaB target genes (Lu et al. 2010). The nuclear beta-catenin has also been reported to be demethylated by KDM2A. This demethylation marks beta-catenin for degradation, which consequently negatively affects the transcription of canonical Wnt signaling target genes (Lu et al. 2015). KDM2A has been shown to affect canonical Wnt signaling also by repressing the transcription of the Wnt antagonist SFRP2. The loss of KDM2A leads to higher levels of H3K36me2 and H3K4me3 in the *SFRP2* promoter, and therefore to higher

levels of the *SFRP2* mRNA (Yu et al. 2016). KDM2A also plays an important role in DNA damage repair. Methylation of H3K36 is necessary for recruiting the MRE complex to damaged DNA and therefore for the DNA damage repair process. KDM2A has to be thus removed from DNA double-strand brakes in order to increase levels of H3K36me2 and to attract the MRE complex. This removal is mediated by ataxia-telangiectasia mutated (ATM) protein that phosphorylates KDM2A at threonine 632 (T632) near DNA damage sites. (Cao et al. 2016). KDM2A further affects DNA damage repair by interacting with and stabilizing p53-binding protein 1 (53BP1) (Panier et al. 2014; Bueno et al. 2018).

Even though the *in vitro* histone demethylation assay and the crystal structure showed that KDM2A has just H3K36me2/1 demethylation activity, it has been reported that knockdown of KDM2A causes an increase also in the levels of H3K4me3 on the *SFRP2, SOX2, and NANOG* promotors of (Tsukada et al. 2006; Dong et al. 2013; Cheng et al. 2014; Tsai et al. 2014; Yu et al. 2016). It is possible that KDM2A has an impact on the level of H3K4me3 through some other proteins that are attracted by demethylated H3K36. There is also a possibility that cell type specific factors interacting with KDM2A can affect its substrate specificity.

In addition, KDM2A has been found to be misregulated in various cancers which results in downregulation of the Polycomb group protein (PcG) Ezh2, PcG mediated H2A ubiquitination and upregulation of the cyclin-dependent kinase inhibitor p21Cip1 (Wagner et al. 2013; Dhar et al. 2014; Kawakami et al. 2015).

3.7. Lysine demethylase KDM2B

KDM2B is a paralogue of KDM2A that also contains the JmjC, CXXC zinc finger, PHD zinc finger, F-box, and LRR domain (Jin et al. 2004). KDM2B has been reported to act as a transcriptional repressor through demethylation of H3K36me1/me2 and H3K4me3 but reports on its activity toward H3K4me3 are conflicting (Frescas et al. 2007; He et al. 2008; Tzatsos et al. 2009). Also, KDM2B has a role in the self-renewal of stem cells, organization of the Polycomb Repressive Complexes and regulation of histone H2A ubiquitination

(Frescas et al. 2007; He et al. 2011; Tian et al. 2013; Kottakis et al. 2014; Wu et al. 2014; D'Oto et al. 2016). It has been shown that KDM2B can act also as an oncogene by preventing senescence in some cells and it can promote or antagonize tumor progression depending on the cellular context (He et al. 2008). Moreover, KDM2B is regulating NOTCH and WNT signaling pathways that are essential for embryonic development (Lu et al. 2015; Andricovich et al. 2016).

3.8. Demethylation deficient histone demethylases

Most single-gene loci can encode multiple protein isoforms and this ability is causing diversity of the mammalian proteome (Davuluri et al. 2008; Barbosa et al. 2013; Vacik and Raska 2017). Mechanisms involved in these processes include alternative splicing, alternative start codone usage, alternative polyadenylation and alternative promotor usage (Ayoubi and Van De Ven 1996; Kochetov 2008; Wang et al. 2015; Tian and Manley 2018). Protein isoforms created by one of the alternative mechanisms can have different spatio-temporal expression patterns or they can even differ in function, since they can lack certain domains or some functional structure (Vacik and Raska 2017). The genes of histone demethylases can also give rise to alternative mRNA and protein isoforms.

KDM2A and KDM2B histone demethylases have been extensively studied, however, little attention has been paid to their naturally occurring alternative isoforms. KDM2A and KDM2B have several described alternative protein isoforms lacking some part or even domain of the full-length protein (Vacik et al. 2018). The KDM2A isoform KDM2A-N782 (GenBank: JQ710741.1), which has the JmjC, CXXC and PHD domain, but lacks the F-box and LRR domain, can stimulate proliferation of human embryonic stem cell-derived keratinocytes while other isoforms cannot (Iuchi and Green 2012). This implies that even though the JmjC domain is essential for most of the functions of KDM2A, its activity can be affected also by other domains in the protein structure. Furthermore, the KDM2A and KDM2B loci also produce short alternative mRNA isoforms that are initiated from still uncharacterized alternative intronic promoters (Vacik et al. 2018). However, in the

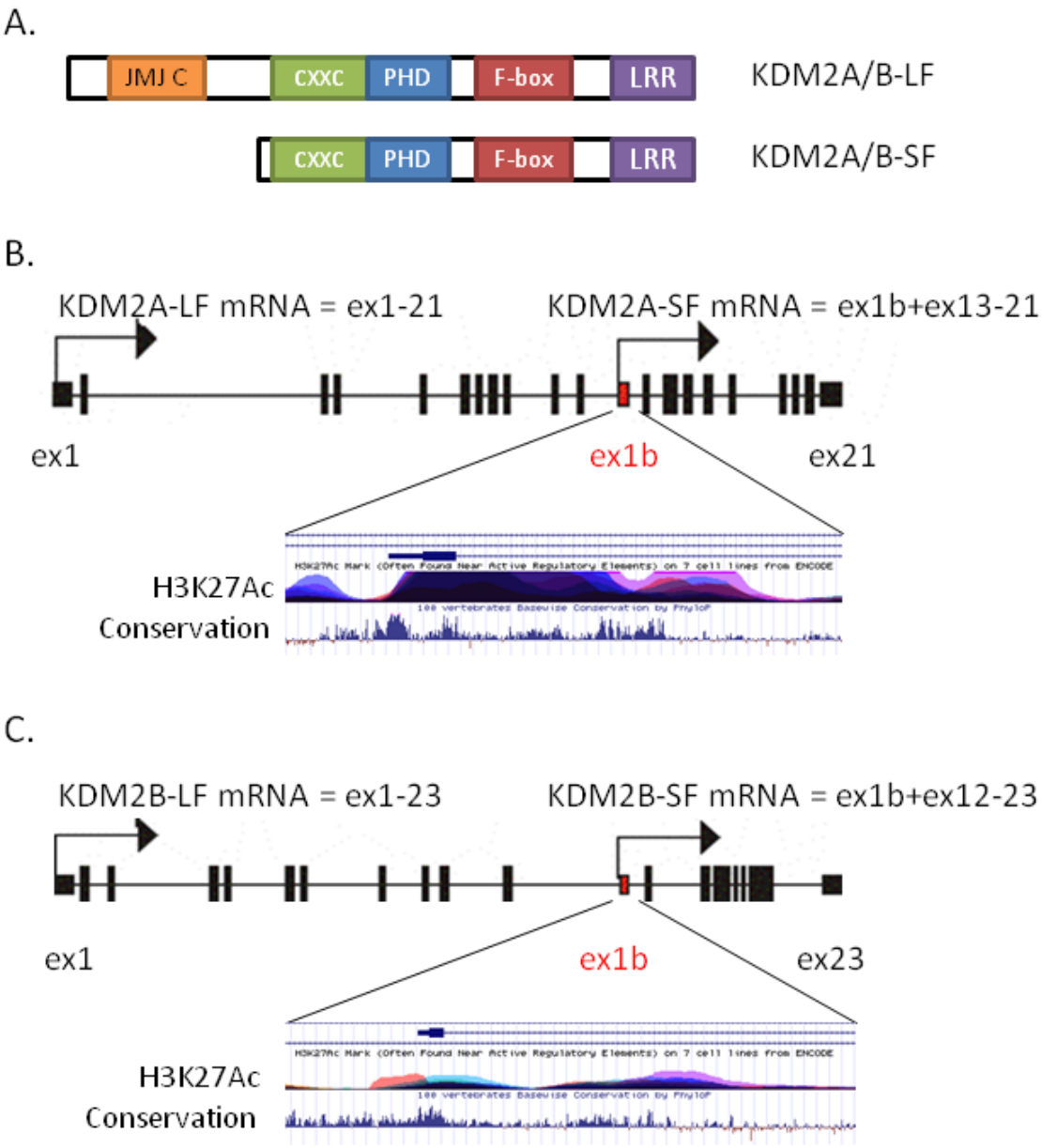

Figure 4. *KDM2A* and *KDM2B gene* locus. **(A)** KDM2A/B-LF and KDM2A/B-SF domain structure. **(B)** *KDM2A* gene locus with exon structure with elevated H3K27Ac at the human short isoform promoter regions and its conservation bar. **(C)** *KDM2B* gene locus with exon structure with elevated H3K27Ac at the human short isoform promoter regions and its conservation bar (Vacik et al. 2018)

publicly available UCSC genome browser these alternative promoters can be found to be clearly defined by the presence of the alternative first exons and of elevated levels of epigenetic marks H3K4me3 and H3K27Ac which are associated with transcriptionally active promoter regions (Kent et al. 2002; Gates et al. 2017) (Figures 4B, 4C).

Alternative promoters located in gene introns drive the expression of the alternative mRNAs from alternative transcription start sites (TSS) and are frequently regulated in a spatio-temporal manner. Given that alternative intronic promoters are located downstream of the original start site, they drive the expression of alternative mRNAs that lack the upstream exons. These short isoforms (KDM2A-SF and KDM2B-SF) lack the N-terminal JmjC enzymatic domain and therefore they are unable to function as demethylases. However, they share all the other functional domains (the CXXC, PHD, F-box, and LRR domain) with the full length long isoforms (KDM2A-LF and KDM2B-LF) (Inagaki et al. 2015; Liu et al. 2016; Lađinović et al. 2017) (Figure 4A). KDM2A-SF encodes a 723-amino-acid protein with 10 exons, while KDM2B-SF encodes 776 amino acid protein and both begin with the CXXC DNA binding domain (Vacik et al. 2018) (Figure 4A).

3.9. Wnt signaling pathway

A recent study emphasized the role of KDM2A and KDM2B in canonical Wnt/beta-catenin dependent signaling (Lu et al. 2015). Wnt signaling is an evolutionary conserved pathway that is essential for cellular regulation, cellular differentiation, cell migration, as well as for development and organogenesis (Sokol 2011; Steinhart and Angers 2018; Wang et al. 2018). In the presence of Wnt proteins bound to the Frizzled receptors on the surface of the cell, Dishevelled proteins are activated (Vikram et al. 2014). Dishevelled proteins and casein kinase 1 inhibit phosphorylation and degradation of beta-catenin by inactivation of Glycogen Synthase Kinase-3 (GSK-3). Beta-catenin is therefore not phosphorylated and enters the nucleus by a mechanism that remains poorly understood (Mannava and Tolwinski 2015). In the nucleus canonical Wnt signaling target genes are kept inactive through the DNA-binding transcription TCF/LEF factors and their co-repressor Groucho proteins. When no-phosphorylated beta-catenin enters nucleus, it

replaces the Groucho co-repressors proteins on the TCF/LEF proteins, acts as a co-activator and induces the transcription of canonical Wnt signaling target genes (Daniels and Weis 2005; Vijayakumar et al. 2011). These target genes include c-Myc, Cyclin D1, Axin 2, c-Jun, Telomerase, FGF9 and many more (Shtutman et al. 1999; Gan et al. 2008; Ramakrishnan and Cadigan 2017). The histone demethylases KDM2A and KDM2B have been reported to inhibit Wnt signaling through the interaction with and demethylation of the nuclear beta-catenin, which results in its ubiquitilation and proteosomal degradation. Using its JmjC demethylase domain KDM2A/B demethylate beta-catenin lysines in the region around fourth and fifth Armadillo repeat. This degradation indirectly inhibits the transcription of canonical Wnt signaling target genes by disabling beta-catenin and TCF/LEF interaction (Lu et al. 2015).

4. Thesis goals

Considering the above-mentioned possible differences between protein isoforms and the lack of research on the KDM2A and KDM2B demethylation deficient isoforms, this thesis was focused on the alternative demethylase-inactive KDM2A and KDM2B isoforms, on their characterization and on their function.

1. Characterization of the short isoform of the lysine demethylase KDM2A

Elevated levels of the epigenetic marks H3K4me3 and H3K27Ac are associated with transcriptionally active promoter regions and their presence suggests that the expression of the *KDM2A-SF* mRNA is driven by the alternative promoter located in an intron. This alternative promoter is located in *KDM2A* intron 13 in the region where the alternative first KDM2A exon was detected. Characterization of the KDM2A-SF coding region and of the transcription start site, was one of the thesis goals.

2. Characterization of chromatin regions bound by the short KDM2A-SF isoform

The structural differences between the KDM2A-SF and KDM2A-LF protein isoforms are likely to result in the two proteins assuming different conformations and consequently in KDM2A-SF being involved in different protein complexes than KDM2A-LF. Although both KDM2A isoforms should theoretically bind to the same DNA regions through their identical zinc finger CXXC DNA-binding domain, it is possible that KDM2A-SF, as a conformationally different protein, can complex differently from KDM2A-LF, and interacts with DNA regions different from those bound by KDM2A-LF.

3. Characterization of the role of KDM2A-SF and KDM2B-SF in canonical Wnt signaling

Although KDM2A-SF and KDM2B-SF lack the JmjC demethylase domain, they contain all the other functional protein domains including the DNA CXXC binding domain. KDM2A-SF and KDM2B-SF are thus likely to interact with the same proteins and DNA regions as their full-length KDM2A and KDM2B counterparts. One of the goals of this thesis was therefore to elucidate the role of KDM2A-SF and KDM2B-SF in canonical Wnt signaling.

5. Material and Methods

5.1. Cell cultures

Human cell lines (HEK293T, U2OS, HeLa, and MCF-7) and mouse cell lines (NIH3T3) were grown in DMEM (Thermo Fisher Scientific 31966047) with 10% fetal bovine serum (ThermoFisher 10270106) and 1% antibiotics/antimycotics – Penicillin/Streptomycin (ThermoFisher 15140122) in 5% CO2 at +37˚C. Cell transfections were performed using Fugene 6 (Promega E2691). Gene specific and control Silencer Select siRNAs (Thermo Fisher Scientific) were transfected into various cell lines using Lipofectamine 3000 (Thermo Fisher Scientific L3000008) or RNAiMAX (Thermo Fisher Scientific 56532) and after 48hrs the cells were harvested and processed for the downstream applications. Wnt activation was achieved by treating cells with BIO Reagent (Biovision 1673) at a final concentration of 1 μM for 24 hrs before harvest.

5.2. Plasmids and constructs

The KDM2A, KDM2B and beta-catenin coding regions were amplified by PCR using the primers listed in Table 2. The RT-PCR products were cloned into the pCS2 expression plasmids and the constructs were verified by sequencing.

5.3. RNA analysis

5.3.1. Isolation of total RNA

For total RNA isolation the cells were lysed directly in a culture dish using TRIzol Reagent (Thermo Fisher Scientific 15596026) and resuspended several times through a pipette. Chloroform (Sigma Aldrich 25666) was used for phase separation 0.2ml per 1ml of TRIzol. Samples were vortexed vigorously for 20 seconds and incubated at room temperature for 2 minutes. This step was followed by centrifuging the samples at 21.380 x g for 10 minutes at +4˚C. The mixture separates into three phases 1 – lower red, phenol-chloroform phase, organic phase with proteins and lipids; 2 – white interphase with DNA; 3 – colorless upper aqueous phase with RNA. The upper aqueous phase was carefully transferred into a fresh tube without disturbing the interphase. This TRIzol step was

repeated one more time and the second aqueous phase was transferred into a new tube and RNA was precipitated by 0.7V of isopropyl alcohol for 10 minutes at room temperature. The precipitated RNA was then centrifuged at 21.380 x g for 20 minutes at +4˚C. The precipitated RNA would form pellet on the bottom of the tube. The supernatant was removed carefully not to disturb the pellet and the pellet was washed with 1mL of 75% ethanol. Samples were shortly vortexed and span down. All ethanol was removed and RNA pellet was air-dried for 2 minutes at room temperature. RNA was dissolved in ultra-pure H_2O and its quality was determined by a spectrophotometric analysis and on agarose gel.

5.3.2. Spectrophotometric analysis of RNA

Purines (A,G) a pyrimidines (C,T,U) of nucleic acids absorb the 260 nm wavelength light, whereas proteins and various contaminants (organic chemicals, salts) absorb the 280 nm or 230 nm wavelength light. Thus, it is possible to determine the concentration and purity of nucleic acids spectrophotometrically as follows: 1 ml of aqueous RNA solution contains 40 µg of RNA when A260 = 1, which means that the concentration of RNA (µg/ml) = A260 x 40. To determine the purity of RNA samples two absorbance ratios were used: High quality RNA gives the A260/A280 ratio of 1.8 – 2.0 and A260/A230 ratio of 2.0 – 2.5 (Gallagher and Desjardins 2008). Absorbance was measured on spectrophotometer Eppendorf BioPhotometer® D30.

5.3.3. Elektrophoretic analysis of RNA

Since the phosphate groups of nucleic acids are charged negatively, RNA and DNA molecules migrate in an electric field towards the positively charged electrode. Electrophoretic separation of nucleic acids is done in 1% agarose gel. For nucleic acids detection gels are stained with intercalating agent, ethidium bromide (EtBr). EtBr absorbs UV light at 285 nm and after binding to a nucleic acid it emits orange light at 605 nm with 20x higher intensity then when not bound to nucleic acids. EtBr is charged positively and therefore migrates towards the negatively charged electrode (Petrov et al. 2013).

5.3.4. Isolation of mRNA

mRNA was isolated from total RNA using the GeneElute mRNA Miniprep Kit (Sigma MRN10–1KT). 300µg of total RNA was mixed with 1V of the 2x Binding Solution and 15µl of the Oligo dT beads, and then incubated at +70˚C for 3 minutes. This was followed by incubation for 10 minutes at room temperature and centrifugation at 16.000 x g for 2 minutes. The supernatant was discarded and the pellet was resuspended in 500µl of Wash Solution. mRNA was collected in the Gene Elute spin collection tube by centrifugation at 16.000 x g for 2 minutes. The flow through was discarded and the column was washed with 500µl of the Wash Solution. mRNA was eluted from the column by centrifugation for 1 minute at 16.000 x g with 50µl of the Elution Solution prewarmed at +70˚C for 5 minutes.

5.3.5. Reverse trancription

1µg of total RNA was reverse transcribed into complementary DNA (cDNA) using the Superscript III kit system (Thermo Fisher Scientific 18080051). 1µg of total RNA was mixed with 2.5 ng/µl Random Hexamer primers and 0.5mM dNTP, vortexed and incubated for 5 minutes at +65˚C. cDNA synthesis mix was made and added to sample mixes with final concentrations 1x First Strand Buffer; 5mM DTT; 2U/µl RNase OUT and 10 U/µl SuperScript III. The incubation program was run on a PCR cycler (1.) 10 min at +24˚C; (2.) 60 min at +50˚C; (3.) 15 min at +70˚C. cDNA was diluted with 40 µl of ultra-pure H_2O.

5.4. Northern Blot

Northern blot was performed using Northern Max kit (Thermo Fischer Scientific, Ambion; AM1940). mRNA was mixed with 3 volumes Formaldehyde Load Dye, denaturized at 70˚C for 10 minutes and run on 1% agarose gel with Denaturing Gel Buffer in MOPS gel run buffer. mRNA was transferred to Bright Star-Plus membrane (Thermo Fisher Scientific, AM10100) or Zeta-Probe Blotting membrane (BioRad cat #162-0165). Transfer setup was made of paper towels, chromatography paper, membrane, gel, chromatography paper, chromatography paper bridge submerged into the Transfer buffer reservoir and cover. The transfer was done for 15-20 min per mm of gel thickness. The membrane was washed in 1x MOPS gel running buffer and crosslinked with

Ultraviolet light (radiant exposure (He) = 120mJ/cm2; 254 nm; 50 s). Hybridization with probes prepared using the T7 RNA Polymerase (Sigma Aldrich 10881767001) and the Biotin RNA labeling mix (Sigma Aldrich 11685597910) was performed 16hrs (overnight) at 68 ˚C. Membranes were washed and the non-radioactive signal was developed using Chemiluminescent Detection Module (Thermo Fischer Scientific #89880) on films.

5.5. Quantitative RT-PCR

QRT-PCR was performed using the CFX96 Touch Real-Time PCR Detection System (BIO-RAD) and iQ SYBR Green Supermix (BIO-RAD; 1708880). Q-PCR reactions were run in duplicates on at least two biological samples yielding the minimum of 4 values per condition. The relative mRNA levels were determined as $2^{Ct(ref)-Ct(test)}$, where Ct(ref) is the Ct of the reference gene and Ct(test) is the Ct of the tested gene. The Q-PCR primer sequences are listed in Table 2.

Name	Assay	Target	Sequence (5´to 3´)
F1	QRT-PCR	human *ACTNB* exon 4	TCTTCCAGCCTTCCTTCCTG
R1	QRT-PCR	human *ACTNB* exon 5	CAATGCCAGGGTACATGGTG
F2	QRT-PCR	human *GAPDH* exon 7	TGCACCACCAACTGCTTAGC
R2	QRT-PCR	human *GAPDH* exon 8	GCCATCCACAGTCTTCTGGG
F3	QRT-PCR	human *KDM2A* exon 12	TCGCTGCCTTGTAGATAAGTTGG
F3b	QRT-PCR	human *KDM2A* exon 1b	ACAGAAAACAAAACAAAGACGCTG
R3	QRT-PCR	human *KDM2A* exon 13	ATAGGAACTCCAGTGAGGGCTAAC
F4	QRT-PCR	human *HP1α* exon 3	AACAGTGCCGATGACATCAAATC
R4	QRT-PCR	human *HP1α* exon 5	AAGAACCAGGTCAGCTTCATCTG
F5	qRT-PCR	human Cyclin D1 exon 3	AACAGATCATCCGCAAACACG
R5	qRT-PCR	human Cyclin D1 exon 4	GTTGTTGGGGCTCCTCAGG
F6	qRT-PCR	*human Axin 2 exon 8*	CTGACGGATGATTCCATGTCC
R6	qRT-PCR	*human Axin 2 exon 9*	GGGAAATGAGGTAGAGACACTTGG

Table 2. – Primers and siRNAs (Continuing on the next page)

F7	qRT-PCR	*human C-Myc exon 1*	CGCTTCTCTGAAAGGCTCTCC
R7	qRT-PCR	*human C-Myc exon 2*	TTCTCCTCCTCGTCGCAGTAG
F8	qRT-PCR	*mouse Gapdh exon 4*	CTGGCCAAGGTCATCCATG
R8	qRT-PCR	*mouse Gapdh exon 5*	TGGCAGCACCAGTGGATG
F9	qRT-PCR	mouse *Actnb* exon 4	GAAATCGTGCGTGACATCAAAG
R9	qRT-PCR	mouse *Actnb* exon 5	TGTAGTTTCATGGATGCCACAG
F10	qRT-PCR	mouse *Hprt* exon 4	TCAGTCAACGGGGGACATAAA
R10	qRT-PCR	mouse *Hprt* exon 6	GGGGCTGTACTGCTTAACCAG
F11	qRT-PCR	mouse *Kdm2a* exon 12	GTGCATCTCACCCATTTTGAAC
F11b	qRT-PCR	mouse *Kdm2a* exon 1b	AGCAGAAAAGCTAACTCCTTCCG
R11	qRT-PCR	mouse *Kdm2a* exon 13	ATCGCTACTGGCAAGTTCTTCC
F12	qRT-PCR	mouse *Kdm2b* exon 12	CACGTGGATGACGACCCC
F12b	qRT-PCR	mouse *Kdm2b* exon 1b	TATGAATCGGAGCCCGACC
R12	qRT-PCR	mouse *Kdm2b* exon 13	CTGCTGTTGTTCGGTTGGC
F13	qRT-PCR	mouse Cyclin D1 exon 1	TGCGTGCAGAAGGAGATTGT
R13	qRT-PCR	mouse Cyclin D1 exon 2	CGGTCCAGGTAGTTCATGGC
F14	qRT-PCR	mouse Axin 2 exon 2	CAAAACTCTTCGGGCCACC
R14	qRT-PCR	mouse Axin 2 exon 3	GAATCGTCGGTCAGTGCGT
F15	qRT-PCR	mouse C-Myc exon 1	GAGCTCCTCGAGCTGTTTGAA
R15	qRT-PCR	mouse C-Myc exon 2	GGCTGTACGGAGTCGTAGTCG
R16	5´RACE	human *KDM2A* exon 13	GCTAACTTGGGATCGCTGTTGGC
R16b	5´RACE	human *KDM2A* exon 13	GGATCGCTGTTGGCAAGCTCCTC
R17	5´RACE	mouse *Kdm2a* exon 13	AGTGAGGGCTAACTTGGGATCGCT
R17b	5´RACE	mouse *Kdm2a* exon 13	ACTTGGGATCGCTACTGGCAAGTTC
siRNA 1	knock down	mouse Kdm2b exon 11	UCACCUUACCGAAUUUGAA
siRNA 2	knock down	mouse Kdm2b exon 1b	CGACGACUAUGAAUCGGAG
siRNA 6	knock down	mouse Kdm2a exons 11-12	GCAUGGAUAUGGAGUUAAA

Table 2. – Primers and siRNAs (Continuing on the next page)

siRNA 7	knock down	mouse Kdm2a exon 1b	AGCUAACUCCUUCCGCACA
siRNA 3	knock down	human *KDM2A* exon 2	GAAGAAGAAAGGAUUCGUU
siRNA 5	knock down	human *KDM2A* exon 1b	GGAUUUUCCCAGAGGCAGA
siRNA 9	knock down	human exon 3	GCAGAGCAAUGAUAUCGCU
F18	ChIP-Q-PCR	human chr. 1 region 1	AAGGTCAATGGCAGAAAAGGAA
R18	ChIP-Q-PCR	human chr. 1 region 1	CAACGAAGGCCACAAGATGTC
F19	ChIP-Q-PCR	human chr. 1 region 2	CGAAGAAGGTTCTAAGAATGCTTCTG
R19	ChIP-Q-PCR	human chr. 1 region 2	GGATGGAGGAGTTTCAAAACACAC
F20	ChIP-Q-PCR	human chr. 1 region 3	AATGTTCAACTCTGTGAGTTGCATG
R20	ChIP-Q-PCR	human chr. 1 region 3	TGGATATTTGGAGCACTTTGTGG
F21	ChIP-Q-PCR	human chr. 5	TCAACTCACAGAGTTGAACCTTCC
R21	ChIP-Q-PCR	human chr. 5	GAAGTTTCTGAGAATGCTTCTGGC
F22	ChIP-Q-PCR	human chr. 8 region 1	CTACTTTGTGAGTTTTGCATTCAATTAAC
R22	ChIP-Q-PCR	human chr. 8 region 1	GTGTTTCAAAACTACTCTATCGAAAGGAAC
F23	ChIP-Q-PCR	human chr. 8 region 2	GTGTGATTCTGTGAGGAACCACC
R23	ChIP-Q-PCR	human chr. 8 region 2	TCCTCCGATATGGCTTTCATAAC
F24	ChIP-Q-PCR	human chr. 10	TGATAGAGCAGTTTAGAAACACTCTTTTTG
R24	ChIP-Q-PCR	human chr. 10	TCTGTCTTGTTTTATATGAAAAATTCCCG
F25	ChIP-Q-PCR	human chr. 15	TGAGAATGCTTCTGTCAAG
R25	ChIP-Q-PCR	human chr. 15	CACAGAGTTGAAGATACCTTTC
F26	ChIP-Q-PCR	human chr. 18	GGATAGTTGGATAGCTCTCACTATTTCG
R26	ChIP-Q-PCR	human chr. 18	AAAGCGCTCCAAGTGTCCACAT
F27	ChIP-Q-PCR	human chr. X region 1	GGCTCAGAAGAAAGAGAGAGACTCTATCC
R27	ChIP-Q-PCR	human chr. X region 1	ATAGCGGTACCACTCTGATGGTCTTG
F28	ChIP-Q-PCR	human chr. X region 2	TGCTGGAAAAGGGGCGTTCA
R28	ChIP-Q-PCR	human chr. X region 2	ACCTAGAAGCAATCAAACTCCAAATGGT
F29	ChIP-Q-PCR	human chr. X region 3	GAGACCCATAAACTTGCAGGCTTTAG

Table 2. – Primers and siRNAs (Continuing on the next page)

R29	ChIP-Q-PCR	human chr. X region 3	CCCCTGTAGACAAGTTGGTACCTAAGG
F30	ChIP-Q-PCR	human *FBXO7* promoter	CCTAAGGCTTCTCAGAGCAGATG
R30	ChIP-Q-PCR	human *FBXO7* promoter	CCAGTACTTACTCCCTGTGTGCG
F31	ChIP-Q-PCR	human *CTNNA1* promoter	GGGAGGAAGGAATTCTGAGGTG
R31	ChIP-Q-PCR	human *CTNNA1* promoter	GCTTTTGGGGAAAGGGAAGG
F32	ChIP-Q-PCR	human *LSD1* promoter	GGAGGAAATGGTCACCTTCG
R32	ChIP-Q-PCR	human *LSD1* promoter	GCCATAGAGCGGCGTTCTC
F33	cloning	human KDM2A exon 1	ATGGAACCCGAAGAAGAAAGGATTC
F33b	cloning	human *KDM2A* exon 1b	ATGTGCTCTGGGAGATTCCAGAATA
F33c	cloning	human *KDM2A* exon 14	ATGAAACCAGCTCCACGGTTAACA
R33	cloning	human *KDM2A* exon 21	TTAGCTGATCTTCTGTATCAGCTTC
F34	cloning	mouse Kdm2b exon 1	GGAATTCCATGGAGGCAGAGAAAGACTCTGG
F34b	cloning	mouse Kdm2b exon 1b	GGAATTCCATGGCCATGTCCGTGAGCGCC
R34	cloning	mouse Kdm2b exon 22	GCTCTAGACATACTTGTCCTGGAACTAACTTAG
F35	northern	human *KDM2A* exon 13	GCGCAATTAACCCTCACTAAAGGGTTTGCTGGAGGAGCTTGCCAACAG
R35	northern	human *KDM2A* exon 14	GCGCGTAATACGACTCACTATAGGGTTGCACACAGGCTTTGCATTTTCG
F36	northern	human *KDM2A* exon 1b	GCGCAATTAACCCTCACTAAAGGGGTTGCAAAGCATTTCTGGGAGCTG
R36	northern	human *KDM2A* exon 1b	GCGCGTAATACGACTCACTATAGGGCTTTCGTTTCCCGTCGCTCTGG
R37	northern	human *KDM2A* exon 12	GCGCGTAATACGACTCACTATAGGGGCAGCGAAGGCCTTCAAGCTCAAA
F37	northern	human *KDM2A* exon 12	GCGCAATTAACCCTCACTAAAGGGATTTGGAGTTAAATGGGTTGGAGTC

Table 2. Primers and siRNAs

5.6. Chromatin immunoprecipitation

Chromatin immunoprecipitation was done from the MCF-7 cells using the Magnify ChIP system (Life Technologies 492024) and as described previously (Vacik et al. 2011; Lađinović et al. 2017). The following antibodies: anti-pan-KDM2A (anti-JHDM1A, Bethyl A301–475A), anti- H3K36me2 (Abcam ab9049), rabbit control IgG (Abcam ab46540) were coupled to the Dynabeads for 1hr at 4°C. Dynabeads coupled with antibodies were rotated for 2 hrs at 4 °C in Chromatin Extract. Bound Chromatin was washed three times rotating for 5 minutes at 4 °C in IP Buffer 1. This wash was followed by wash in IP Buffer 2 twice rotating for 5 minutes at 4 °C. Reverse Crosslinking Buffer was loaded onto beads together with Proteinase K and incubated 15 minutes at 55 °C. Using magnetic stand beads were separated from the sample and the sample was incubated 15 minutes at 65 °C. Procedure was continued with DNA purification. The immunoprecipitated DNA was analyzed by quantitative PCR (ChIP Q-PCR) using using the CFX96 Touch Real-Time PCR Detection System (BIO-RAD), iQ SYBR Green Supermix (BIO-RAD; 1708880) and the primers listed in Table 2.

5.7. Protein analysis

Cytoplasmic protein extracts were prepared by bursting the cells in the hypotonic cell lysis buffer (10mM HEPES; 10mM KCl; 1mM DTT; 1mM EDTA; 0.5% Igepal CA-630; 1x Protein inhibitors) for 20 minutes on ice. This step was followed by spinning down the nuclei for 5 minutes at 1000 x g at +4˚C. The nuclear pellet was washed 3 times in 1mL of the hypotonic cell lysis buffer and span down for 5 minutes at 1000 x g at +4˚C. The nuclear pellet was then resuspended in the high salt extraction buffer (20mM HEPES pH 7.5; 400mM NaCl; 1mM DTT; 10mM EDTA; 1x Protein Inhibitors) and incubated 40 minutes on ice with vortexing every 10 minutes. The nuclear proteins were separated from the cell debris by centrifugation for 10 minutes at 21.000 x g at +4˚C. The protein concentration was measured using Quick Start Bradford 1x Dye Reagent (BIO-RAD 500-0205) and the spectrophotometer Eppendorf BioPhotometer® D30.

5.8. Western Blot

The protein extracts were denatured for 5 minutes at +100˚C in Major Science Dry bath incubator and separated on a 10% polyacrylamide gel (1 x Stacking gel buffer: 0.5M Tris-Cl pH6.8, 0.4% SDS, 1 x Running-separating gel buffer: 1.5M Tris-Cl pH8.8, 0.4% SDS) in 1 x Tris-Glycine-SDS running buffer (25 mM Tris, 191.8 mM Glycine, 0.1% SDS). Proteins were transferred to a PVDF Membrane (Immobilon-P Millipore, IPVH00010: 0.45 µm, 26.5 cm x 3.75 m roll or IPVH07850: PVDF, 0.45 µm, 7 x 8.4 cm sheet, 50). The membrane was activated for 15 seconds in Methanol and washed in H_2O for 2 minutes and then in 1 x Tris-Glycine transfer buffer (25 mM Tris, 191.8 mM Glycine, 20% methanol) for 10 minutes. The transfer was run at the constant current of 0.35A for 1hr. The membrane was blocked for 30 minutes in 5% BSA blocking buffer (5% Bovine serum albumin, 0.1% NaAz in TBST) and incubated in the primary antibody for 16hrs (overnight) at +4˚C. The overnight incubation with the primary antibody was followed by two rinses in 1 x PBS (137 mM NaCl, 2.7 mM KCl, 10 mM Na_2HPO_4, KH_2PO_4, pH of 7.4) and three 5 minute washes in 1x TBST (20 mM Tris, 150 mM NaCl, 0.1%, Tween® 20). The membrane was then incubated (1hr at RT) in the corresponding secondary antibody diluted 1:5000 in non-fat milk buffer (0.2% non-fat milk powder in TBST). This was followed by two rinses in 1 x PBS, three 5 minute washes in 1x TBST and one rinse in 1x PBS. The membrane was then incubated in the (Thermo Fischer Scientific #34580) ECL horseradish peroxidase (HRP) substrate and the signals were developed on Medical X-ray Film Blue CP-BU NEW (AGFA #EXTVX). The following antibodies were used: anti-KDM2A (Bethyl A301–475A) and anti-FLAG (Sigma F1804).

5.9. Microscopy

Immunofluorescence experiments were performed using confocal microscopy. Cells were fixed with 2% paraformaldehyde for 10 minutes, washed in 1x PBS permeabilized with Triton X-100 for 5 minutes, washed in 1x PBS, blocked 30 min in 3% BSA in PBS and immunolabelled as previously described (Paige Taylor. Immunofluorescence of Cultured Cells. Nature Publishing Group. 2015.

doi:10.1038/protex.2015.021). Fluorophores were visualized on the Leica TCS SP5 confocal microscope. The following primary antibodies were used: anti-pan-KDM2A (anti-JHDM1A, Bethyl A301–475A), anti-HP1α (Abcam ab77256), anti-H3K9me3 (Millipore 05–1250), anti-CENP-A (Abcam ab13939). The images and intensity plots were analyzed using the Fiji software (Schindelin et al. 2012).

5.10. Luciferase assay

The TCF/LEF luciferase reporter plasmids pNL1.1-TOP5/FOP5 and the pGL4.53 [luc2/PGK] vector were co-transfected together with the pCS2-KDM2A/B constructs. After 48hrs the luciferase assay was performed and activity was measured using Nano-Glo Dual-Luciferase Reporter Assay System (Promega; N1610) on Infinite 200 with Tecan i-control, 1.12.4.0.

6. Results

6.1. KDM2A mRNA isoforms

To confirm the sequence of both the human (RefSeq: NM_001256405.1) and the mouse (RefSeq: NM_001001984.2) *KDM2A* alternative first exon 1b, we performed a 5´ RACE experiment. The 5´ RACE was done with primers specific for the *KDM2A* exon 13 (Table 2) (Figure 5A). The results of the 5´RACE experiment confirmed that the *KDM2A* alternative first exon 1b is present in both human and in mouse and that it corresponds to several mouse ESTs that are present in the GenBank database (BQ931182.1, BI689076, BY272589).

To further characterize the *KDM2A-LF* and *KDM2A-SF* mRNAs, we performed a northern blot analysis of the mRNA from the MCF-7 cells (Figure 5B). We used 3 different antisense RNA probes to detect both *KDM2A* mRNA isoforms, just the *KDM2A-LF* mRNA or just the *KDM2A-SF* mRNA. Together with the 5´RACE experiment, this northern blot analysis confirmed that the *KDM2A-SF* mRNA is not a product of alternative splicing, but that it is an alternative variant of mRNA that originates in the *KDM2A* intron 12 (Figure 5B). The transcription of this alternative *KDM2A-SF* mRNA is most likely driven by a yet uncharacterized intronic promoter whose presence is supported by the publicly available ChIP-seq data. The ChIP-seq data can be visualized in the UCSC genome browser and show enrichment of H3K27Ac and H3K4me3, the histone modifications associated with transcriptionally active promoters, in the region around the first *KDM2A-SF* exon (Figure 4B) (Kent et al. 2002).

To analyze the *KDM2A-LF* mRNA level separately from that of the short *KDM2A-SF* isoform, we designed Q-PCR primers specific for each isoform. Based on the sequence of the human *KDM2A* mRNA (RefSeq: NM_012308.2), we designed a pair of Q-PCR primers in *KDM2A* exon 12 and exon 13 (Figure 5A). We further designed a pair of Q-PCR primers specific for the human *KDM2A-SF* mRNA (RefSeq: NM_001256405.1), the forward primer in the alternative first exon 1b and the reverse primer in the exon that corresponds to exon 13 of the long *KDMA-LF* isoform (Figure 5A). These primers were used in a

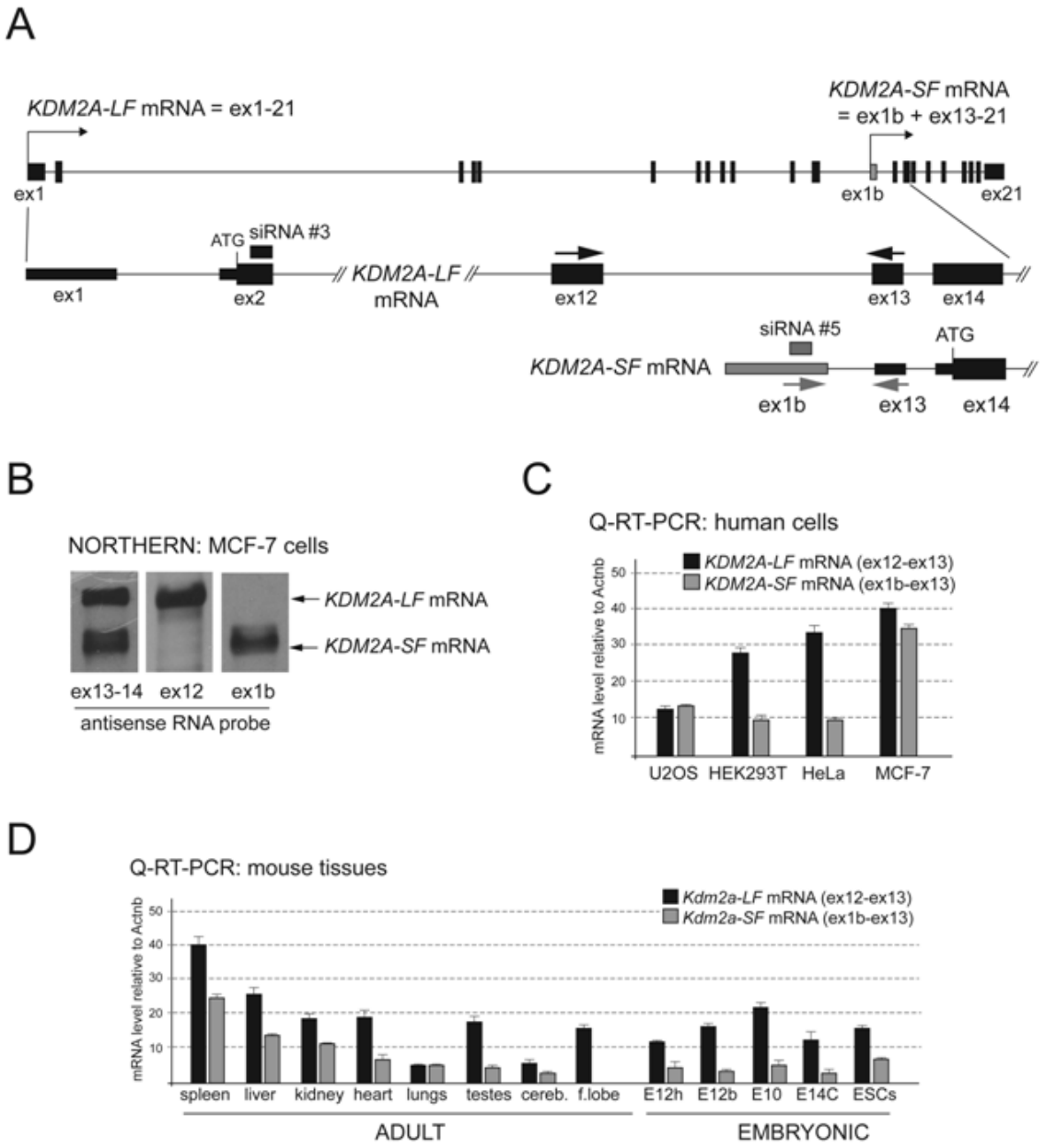

Figure 5. The *KDM2A* mRNA isoforms. **(A)** The KDM2A-LF and KDM2A-SF mRNA exon structure, with alternative first exon 1b in intron 12 that represents the start of the *KDM2A-SF* mRNA. The QRT-PCR primers and siRNAs are shown in the shape of arrows. **(B)** The human *KDM2A* mRNA isoforms were detected in the MCF-7 cells by northern blot using three probes: 1. ex13-14: a probe against KDM2A exons 13–14 that detects both mRNA isoforms, 2. ex12: a probe against KDM2A exon 12 that detects just the KDM2A-LF mRNA, and 3. ex1b: a probe against KDM2A exon 1b that detects just the KDM2A-SF

mRNA. **(C)** The levels of the human *KDM2A-SF* (gray bars) and *KDM2A-LF* (black bars) mRNAs determined by QRT-PCR in 3 independent experiments and related to the levels of the *b-actin* mRNA (Actnb). ***(D)*** *The levels of the mouse Kdm2a-SF* (gray bars) and *Kdm2a-LF* (black bars) mRNAs analyzed as in C. cereb.: cerebellum, f.lobe: front lobe, E12h: embryonic day 12 head, E12b: embryonic day 12 body, E10: embryonic day 10 whole embryo, E14c: embryonic day 14 cortex, ESCs: ebmryonic stem cells.

quantitative RT-PCR assay. We analyzed the levels of the *KDM2A-LF* and *KDM2A-SF* mRNAs in the U2OS, HEK293T, MCF-7 and HeLa cells, and we detected the highest mRNA levels in the MCF-7 cells (Figure 5C).

We detected very high levels of the *KDM2A-LF* and *KDM2A-SF* mRNAs in the human breast cancer MCF-7 cells correspond to the previously published expression levels in various breast cancer cells (Liu et al. 2016) (Figure 5C). We also analyzed the levels of the mouse KDM2A-LF and KDM2A-SF mRNAs in various adult and embryonic mouse tissues (Figure 5D). The results showed that KDM2A-LF, as well as KDM2A-SF are expressed in most of the tested mouse tissues. We detected the highest expression of both mRNAs in the mouse spleen, while the lowest expression of the *KDM2A-LF* and *KDM2A-SF* mRNAs was detected in the cerebellum and the frontal lobe, respectively. During mouse embryonic development the levels of the *KDM2A-LF* mRNA peak at embryonic day 10 (E10), while the *KDM2A-SF* mRNA levels do not change very much during the tested stages. Furthermore, the *KDM2A-LF* and *KDM2A-SF* mRNAs are both expressed even in mouse embryonic stem cells (mESCs) (Figure 5D). These data, together with the data in the USCS genome browser (e.g. the conservation tracks, the GeneBank EST tracks) imply that KDM2A-SF is a naturally occurring and evolutionary conserved isoform.

6.2. KDM2A-SF protein isoforms

To analyze KDM2A-SF and KDM2A-LF on the protein level, we designed an siRNA against *KDM2A* exon 2 and an siRNA against *KDM2A* exon 1b to knock down specifically just the *KDM2A-LF* mRNA or just the *KDM2A-SF* mRNA. We confirmed the knockdown

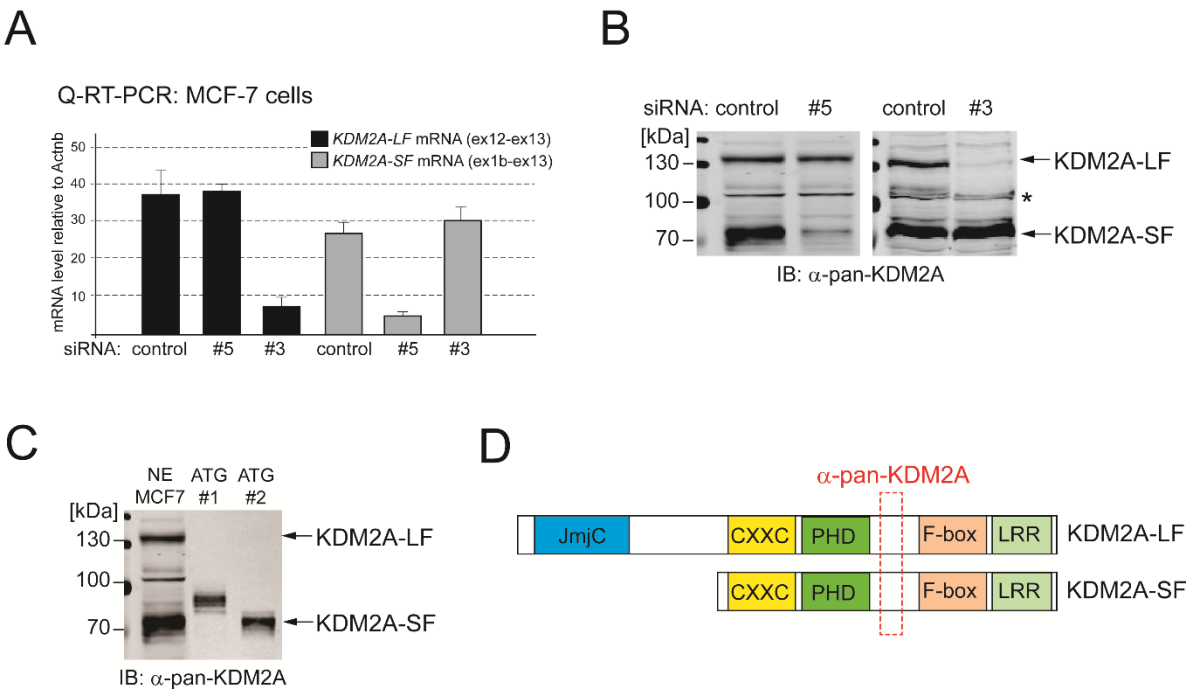

Figure 6. KDM2A isoform-specific knockdown. **(A)** The *KDM2A-SF (gray bars) and KDM2A-LF* (black bars) mRNAs were knocked down with siRNA #5 and siRNA #3. The mRNA levels, relative to the level of the b-actin mRNA, were determined by QRT-PCR in 3 independent experiments. **(B)** Downregulation of *KDM2A-SF* and *KDM2A-LF* by siRNA #5 and siRNA #3, was confirmed by a western blot analysis of the nuclear extract from the treated MCF-7 cells using the anti-pan-KDM2A antibody. The asterisk marks a cross-reactive band recognized by the KDM2A antibody. **(C)** In vitro translation from an ATG in KDM2A exon 14 (ATG #2) yields a protein of the same size as that of the endogenous KDM2A-SF protein detected by the anti-pan-KDM2A antibody in the nuclear extracts from the MCF-7 cells (NE MCF-7). **(D)** The full length KDM2A protein (KDM2A-LF, AA1–1162) contains all the functional domains, while the shorter KDM2A-SF isoform (KDM2A AA543–

1162) lacks the N-terminal demethylation JmjC jumonji domain (in blue). The DNA binding domain is in yellow and the plant homeodomain (PHD) is in green. The epitope of the anti-pan-KDM2A antibody (Bethyl A301–475A) is shown with the red dashed rectangle.

downregulation in the MCF-7 cells first by QRT-PCR (Figure 6A) and then also by a western blot analysis (Figure 6B).

In order to better characterize the translational start of KDM2A-SF, we analyzed the sequence of the *KDM2A-SF* mRNA (RefSeq: NM_001256405.1) for potential start codons in. We found two potential start codons that are in-frame with the downstream amino acid sequence whose usage would create a protein with an intact DNA binding domain, one in alternative first exon 1b and one in exon 14. To distinguish between the two potential start sites, we cloned the two potential coding regions into an expression plasmid and *in vitro* translated two different proteins: one starting with the start codon in *KDM2A* exon 1b (the first *KDM2A-SF* exon) and the other one starting with the start codon in exon 14 (the third *KDM2A-SF* exon). We then analyzed these *in vitro* translated proteins by western together with the nuclear protein extract from the MCF-7 cells using the anti-pan-KDM2A antibody that recognizes both the long and the short KDM2A isoform (Figures 6C and 6D). This western blot analysis showed that the size of the protein translated from the start codon in *KDM2A* exon 14 corresponds to the endogeneous approximately 75 kDa protein that is strongly downregulated after knocking down the short KDM2A-SF mRNA (Figures 6B and 6C). Even though the alternative first *KDM2A* exon 1b is annotated as coding (RefSeq: NM_001256405.1), our results show that the translation of KDM2A-SF starts at the start codon in the third exon of the *KDM2A-SF* mRNA which corresponds to *KDM2A* exon 14. This conclusion is further supported by a comparison of the two potential start codons with the Kozak consensus sequence, a sequence at which translation starts most favorably (Antonarakis and Cooper 2019; Kozak 1986). The sequence around the start codon in exon 14 showed a higher similarity to the Kozak consensus sequence then that in exon 1b (Figure 7).

Figure 7. Alignment of the KDM2A-LF and KDM2A-SF start codons with the Kozak consensus sequence. The bases of the Kozak consensus sequence are aligned in a descending manner where the highest and the biggest one is the most abundant base at the given position. The sequences around the ATGs in KDM2A exon1, exon 1b and exon14 were aligned with the Kozak sequence and the bases corresponding to one of the two most common bases in the Kozak sequence are highlighted in pink.

6.3. Nuclear localization of KDM2A

To analyze the nuclear pattern of the KDM2A isoforms, we used the anti-pan-KDM2A antibody (recognizes both KDM2A-LF and KDM2A-SF, Figure 6D) for immunostaining of the MCF-7 and U2OS cells. The data obtained with this experiment showed that KDM2A forms distinct structures in both cell types (Figure 8A). To further characterize these KDM2A structures we performed a series of immunofluorescence experiments. Taking into consideration that KDM2A has been reported to interact with HP1α protein – a chromosomal protein prominently connected to pericentromeric heterochromatin (Borgel et al. 2017), we also tested co-localization of KDM2A and HP1α. Our results show that the KDM2A foci partially co-localize with HP1α, as well as with H3K9me3 - an epigenetic mark of transcriptionally silent heterochromatin (Figures 9B and 9C). Both HP1α and H3K9me3 are known to be involved transcriptional repression and to be associated with transcriptionally silent pericentromeric and telomeric heterochromatin (Eissenberg and Elgin 2014; Hyun et al. 2017). Therefore, we tested whether the KDM2A foci colocalize with CENP-A, a human histone H3-like nucleosomal protein that is specifically found in the nucleosome core of the centromeric chromatin. Our immunofluorescent data revealed that KDM2A structures localize next to CENP-A, a

histone variant associated with centromeric heterochromatin (Sullivan et al. 2004) (Figure 8D). Taken together, these colocalization experiments show that the KDM2A structures are formed on pericentromeric heterochromatin.

To distinguish whether the KDM2A structures are formed by KDM2A-LF or by KDM2A-SF, we performed more immunofluorescence experiments. KDM2A-LF or KDM2A-SF were knocked down using the siRNAs that specifically knocks down KDM2A-LF or KDM2A-SF (Figures 6A and 6B). After knocking down specifically just KDM2A-LF the KDM2A structures remained present (Figure 8F), while the KDM2A structures were not detected after knocking down specifically just KDM2A-SF (Figure 8E). These results show that the KDM2A structures are formed at pericentromeric heterochromatin by KDM2A-SF and not by KDM2A-LF.

Since pericentromeric heterochromatin is not rich in genes and CpG islands (Babenko et al. 2017). KDM2A-SF as a CpG island binding protein is not likely to directly interact with it. The deposition of KDM2A-SF to pericentromeric heterochromatin that we detected in the MCF-7 cells is thus likely to be mediated by some additional protein. Based on the facts that first, HP1α is known to directly interact with KDM2A (Borgel et al. 2017), second, HP1α facilitates the interaction between KDM2A and H3K9me3 (Mishima, Y. et al. 2013; Borgel et al. 2017), and third, both HP1α and H3K9me3 are known components of the pericentromeric heterochromatin, we hypothesized that KDM2A-SF is forming specific structures on pericentromeric heterochromatin through interaction with HP1α. To confirm this hypothesis, HP1α was knocked down in the MCF-7 cells using an siRNA against *HP1α* exon 3. We confirmed downregulation of the *HP1α* mRNA by QRT-PCR (Figure 9A) and downregulation of the HP1α protein by western blot (Figure 9B). We then analyzed the KDM2A nuclear pattern in the knockdown cells by immunofluorescence and found out that KDM2A-SF structures do not form in the absence of HP1α. Our results show that KDM2A-SF forms specific foci on pericentromeric heterochromatin in an HP1α dependent manner (Figure 8G).

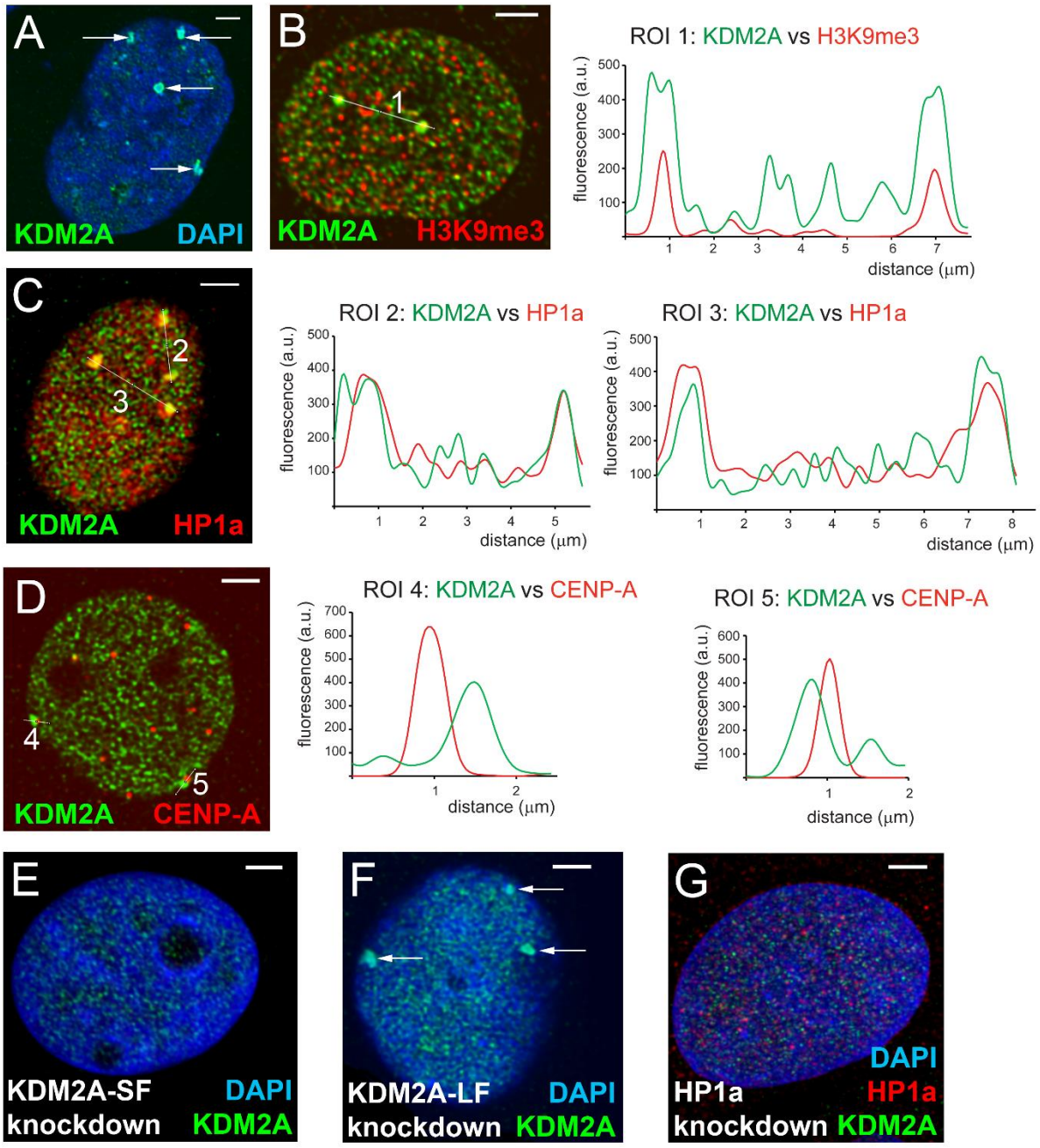

Figure 8. KDM2A-SF forms distinct heterochromatic structures. **(A)** The disctinct KDM2A nuclear bodies (arrows) were detected by the anti-pan-KDM2A antibody on a confocal slice through a cell nucleus. **(B)** The KDM2A foci partially co-localize with H3K9me3 and **(C)** with HP1α and are formed just next to the centromeric heterochromatin marked by CENP-A **(D)**. **(E)** A maximal intensity projection of 52 z-stacks through a cell nucleus lacking KDM2A-SF shows that the KDM2A bodies are not formed in

the absence of KDM2A-SF. **(F)** A single confocal z-stack shows that the KDM2A structures (arrows) remain intact in the MCF-7 cells lacking KDM2A-LF. **(G)** A maximal intensity projection of 46 z-stacks through a cell nucleus lacking HP1α shows that the KDM2A-SF bodies are not formed in the absence of HP1α. The shown images are representative images selected out of at least 5 analyzed nuclei for each condition. The images and intensity plots were processed using the Fiji software. Scale bar = 3µm.

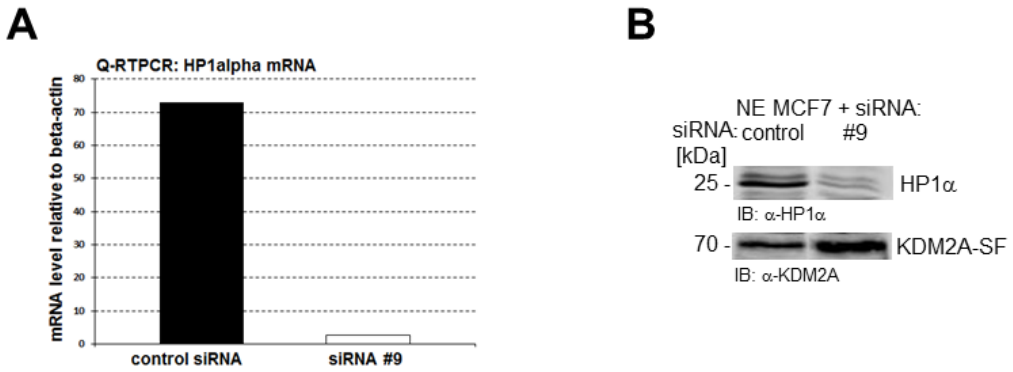

Figure 9. HP1α knockdown. **(A)** The HP1α mRNAs were knocked down with siRNA #9. The HP1α mRNA levels were determined by QRT-PCR relatively to the level of the b-actin mRNA. **(B)** Downregulation of HP1α by siRNA #9 was confirmed by a western blot analysis of the nuclear extract from the treated MCF-7 cells using the anti-pan- HP1α antibody.

6.4. KDM2A on pericentromeric heterochromatin

To complement our immunofluorescence data (Figure 8), we analyzed the levels of KDM2A on the selected pericentromeric regions using chromatin immunoprecipitation (ChIP). Our ChIP experiments showed that the tested pericentromeric regions exhibited even higher levels of KDM2A then the ones detected on the several selected CpG island promoters (Figure 10A). Using ChIP we also tested the levels of H3K36me2, the substrate of the demethylation activity of KDM2A-LF (Cheng et al. 2014), and our experiment revealed that the pericentromeric regions exhibit extremely high levels of H3K36me2, higher even than those of the tested KDM2A bound CpG island promoter regions (Figure 10B). As positive control were used FBXO7 and CTNNA1 promoter regions. These results

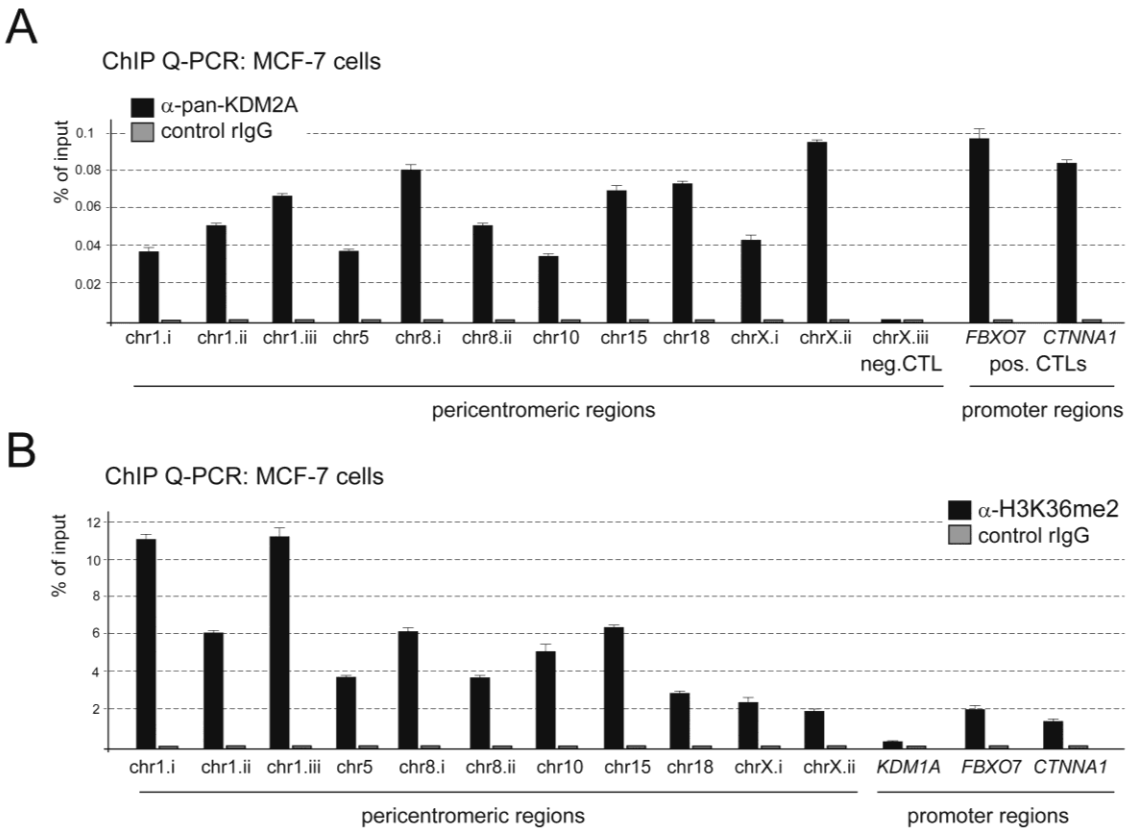

Figure 10. KDM2A bound regions and their H3K36me2 levels. **(A)** The elevated levels of KDM2A (black bars) on the tested pericentromeric regions were determined by 2 independent ChIP experiments and 2 independent Q-PCR reactions from each ChIP. ChIP with the control IgG did not yield any enrichment of the tested regions (gray bars). One of the regions on chromosome X (chrX.iii) does not exhibit any KDM2A binding and serves as the negative control, whereas the 2 promoter regions (FBXO7, CTNNA1) known to be bound by KDM2A serve as the positive controls. **(B)** The high levels of H3K36me2 (black bars) on the tested pericentromeric regions were quantified by ChIP Q-PCR as in A. No enrichment with the rabbit IgG (gray bars) confirms the specificity of the assay. In comparison to the extremely high H3K36me2 levels on the tested pericentromeric regions H3K36me2 is virtually absent on the LSD1 promoter, which thus serves as the negative comparison point.

imply that the KDM2A isoform bound to the tested pericentromeric regions is KDM2A-SF and not the KDM2A-LF, which supports our immunofluorescence data (Figure 8). Further, to analyze more directly which KDM2A isoform is bound to the pericentromeric regions we performed similar ChIP experiments on the MCF-7 cells in which knocked down either KDM2A-LF or KDM2A-SF. However, this experiment turned out to be technically challenging and the results were not reproducible and hardly interpretable (data not shown).

6.5. KDM2A/B-LF/-SF repress canonical Wnt signaling target genes

KDM2A/B have been reported to interfere with canonical Wnt signaling by interacting with and demethylating the nuclear beta-catenin (Lu et al. 2015). Therefore, we asked wether KDM2A/B-SF could also interfere with the transcription of canonical Wnt signaling target genes. We used an siRNA against *KDM2A and Kdm2b* exon 2 and an siRNA against *KDM2A* and *Kdm2b* exon 1b to knock down specifically just the *KDM2A-LF and Kdm2b-LF* mRNA or just the *KDM2A-SF and Kdm2b-SF* mRNA in MCF-7 and NIH3T3 cells. We confirmed the knockdown downregulation by Q-RT-PCR (Figure 11A) and analyzed the levels of the canonical Wnt signaling target genes *Axin 2*, *Cyclin D1* and *C-Myc* mRNA. Our Q-RT-PCR data show that knockdown of KDM2A-LF as well as of KDM2A-SF induces the transcription of *Axin2* mRNA in MCF-7 cells and transcription of *Cyclin D1* mRNA in NIH3T3 cells, while the *C-Myc* mRNA levels were not significantly changed (Figure 11B). However, no change in Wnt signaling target genes was observed in Kdm2b-LF/SF knockdown in NIH3T3 cells (Figure 11B).

To complement the loss-of-function siRNA experiments, we performed gain-of-function analyses, in which we overexpressed KDM2A-LF/SF and KDM2B-LF/SF in HEK293T cells and analyzed the *Axin 2* and *Cyclin D1* mRNA levels. To activate the transcription of the Axin2 and *CyclinD1* genes, we treated the cells with BIO, a Wnt signaling agonists that inhibits the function of the GSK3 degradation complex (Lee et al. 2016; Marchand et al. 2011). Our results showed that KDM2A, as well as KDM2B long and short isoforms repress Axin 2 and Cyclin D1 in HEK293T cells.

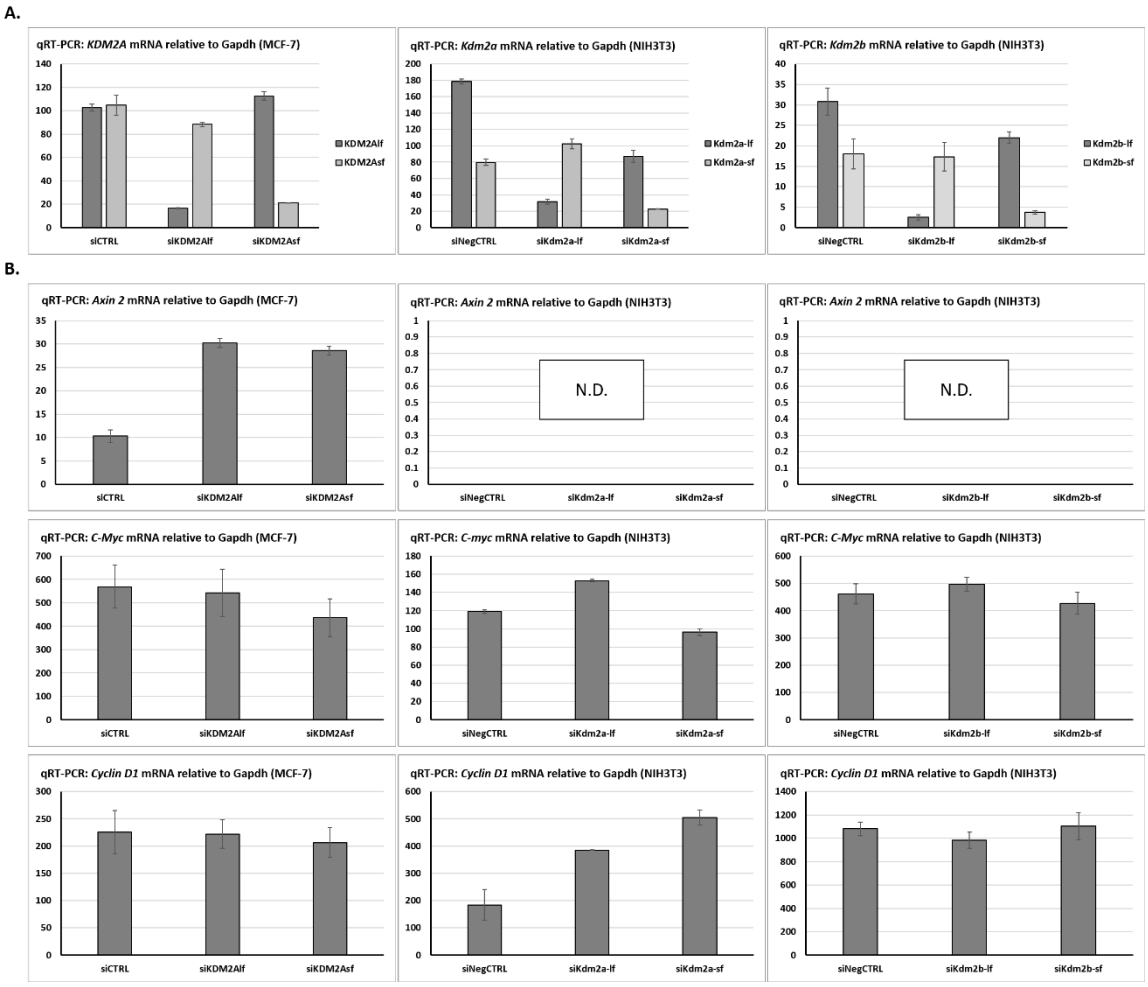

Figure 11. KDM2A and KDM2B knock down affects Wnt target genes transcription. **(A)** The *KDM2A-LF* and *KDM2B-LF* (dark gray bars) and *KDM2A-SF* and *KDM2B-SF* (lignt gray bars) mRNAs were knocked down with isoform specific siRNAs. **(B)** Wnt signaling target genes (*Axin2, C-Myc and Cyclin D1*) mRNA levels in KDM2A-LF/SF or KDM2B-LF/SF knock down cells. The mRNA levels, relative to the level of the *Gapdh* mRNA, were determined by QRT-PCR in 3 independent experiments.

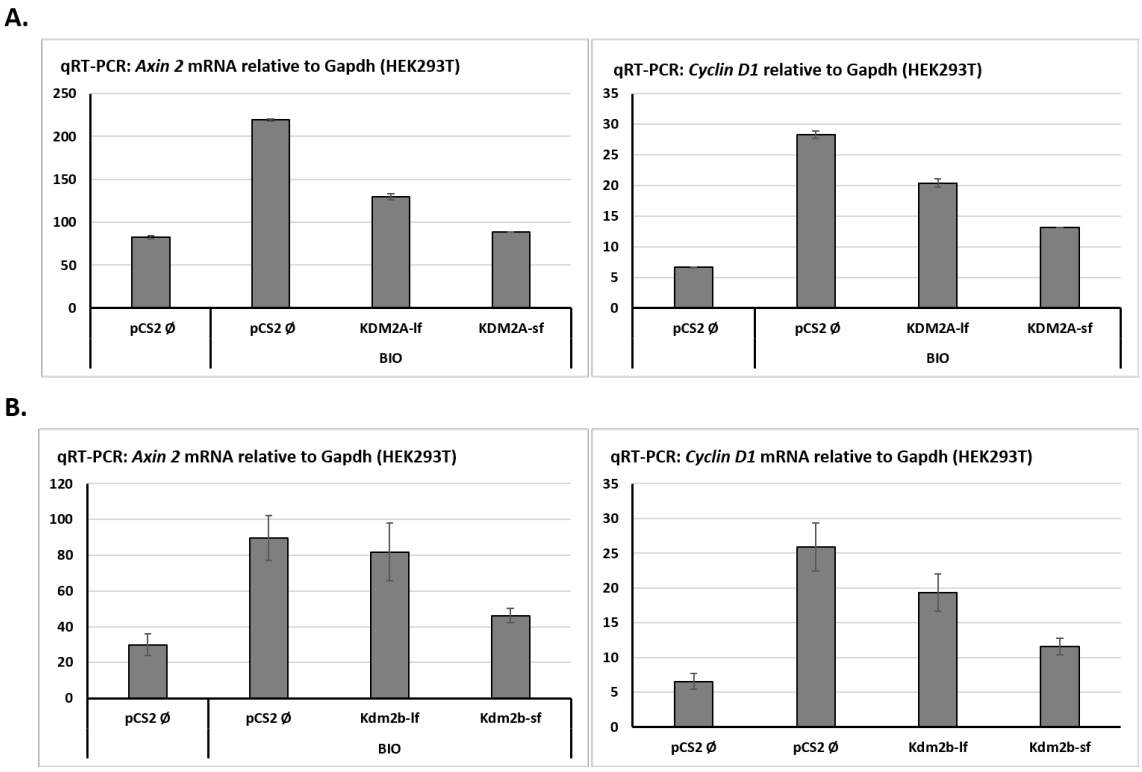

Figure 12. KDM2A-LF/SF and KDM2B-LF/SF overexpression **(A)** *Axin 2* and *Cyclin D1* mRNA levels in HEK293T cells overexpressed with KDM2A-LF or KDM2A-SF. **(B)** *Axin 2* and *Cyclin D1* mRNA levels in HEK293T cells overexpressed with Kdm2b-LF or Kdm2b-SF. The mRNA levels, relative to the level of the *Gapdh* mRNA, were determined by QRT-PCR in 3 independent experiments.

This conclusion is further supported by the luciferase assay we performed. We overexpressed KDM2A or KDM2B in the presence of the TCF/LEF luciferase reporter TOP5. The TOP5 plasmid contains five TCF/LEF binding sites in front of the minimal promoter that drives the transcription of the luciferase gene (Vacik et al. 2011). When a TCF/LEF transcription factor binds to the five TCF/LEF sites it activates the transcription of the luciferase gene if it is co-activated with the nuclear beta-catenin. Wnt signaling was induced using the BIO reagent. Our luciferase assay results showed that KDM2A-LF, KDM2A-SF and KDM2B-SF repress the stimulated TCF/LEF luciferase reporter. However, KDM2B-LF did not.

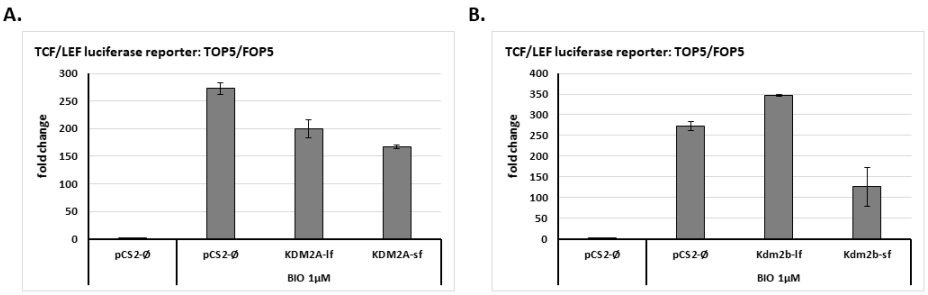

Figure 13. Wnt/beta-catenin responsive luciferase assay. **(A)** Overexpressed KDM2A-LF and KDM2A-SF repress the luciferase reporter. **(B)** Overexpressed KDM2B-LF is not repressing luciferase reporter, while KDM2B-SF does. The results are expressed as the ratio between the normalized luciferase signal from the wild type TOP5 reporter and that of the mutant FOP5 plasmid, whose TCF/LEF binding sites are mutated (Vacik et al. 2011).

7. Discussion

Histone methylation is one of the fundamental histone modifications responsible for controlling transcription, chromatin architecture, and cellular differentiation (Bannister and Kouzarides 2011; Greer and Shi 2012; Fiszbein and Kornblihtt 2016). Since histone methylation has a critical role in almost all cellular processes, its misregulation can lead to various diseases including cancer (Borun et al. 1972; Ciccone et al. 2009; Dong et al. 2013; Brenner et al. 2016; McCabe et al. 2017; Bueno et al. 2018). Homeostasis of histone methylation is maintained through histone methylation and demethylation, the processes mediated by histone methyltransferases and histone demethylases, respectively (Greer and Shi 2012; D'Oto et al. 2016). The main focus of this work was to characterize in detail the lysine demethylase KDM2A and its short isoform, KDM2A-SF, whose transcription is driven by an alternative intronic promoter and to find out more about the possible role of KDM2A/B-LF and KDM2A/B-SF in canonical Wnt signaling (Lađinović et al. 2017; Vacik et al. 2018).

The number of known genes that contain alternative promoters has increased dramatically in the past decade. Alternative promoters can influence gene expression in a number of different ways (Davuluri et al. 2008). Alternative promoters can be tissue and time specific, and alternative promoter usage can also lead to generation of protein isoforms that differ at the amino terminus (Scohy et al. 2000; Flemr et al. 2013).

Example of alternative promotor located in gene intron that is regulating time and space expression is α-fetoprotein (AFP) (Figure 14C). In a study of Scohy, S. et al., (2000) it is showed that the AFP mRNAs is controlled by two promoters P1 and P2 that are subject to different regulation mechanisms. Transponsable elements can also act as alternative promoters for a subset of host genes. Such transcripts are identical to mRNA sequences of known host genes but with alternative transcription element-derived 5' end (Peaston et al. 2004). Example of retrotransposon driven alternative promoter located in

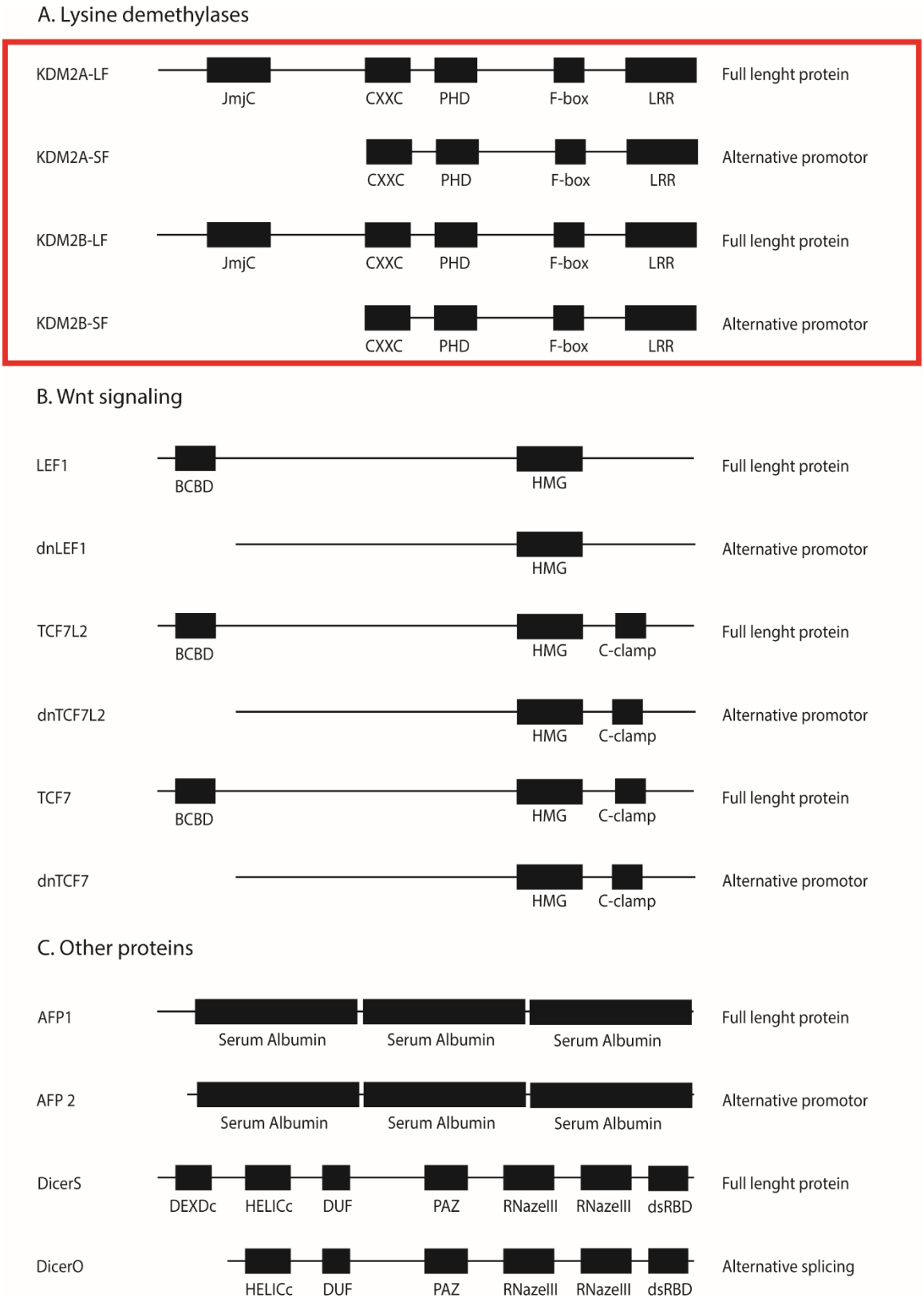
A. Lysine demethylases
KDM2A-LF
JmjC
CXXC
PHD
F-box
LRR
Full lenght protein
KDM2A-SF
CXXC
PHD
F-box
LRR
Alternative promotor
KDM2B-LF
JmjC
CXXC
PHD
F-box
LRR
Full lenght protein
KDM2B-SF
CXXC
PHD
F-box
LRR
Alternative promotor
B. Wnt signaling
LEF1
BCBD
HMG
Full lenght protein
dnLEF1
HMG
Alternative promotor
TCF7L2
BCBD
HMG
C-clamp
Full lenght protein
dnTCF7L2
HMG
C-clamp
Alternative promotor
TCF7
BCBD
HMG
C-clamp
Full lenght protein
dnTCF7
HMG
C-clamp
Alternative promotor
C. Other proteins
AFP1
Serum Albumin
Serum Albumin
Serum Albumin
Full lenght protein
AFP 2
Serum Albumin
Serum Albumin
Serum Albumin
Alternative promotor
DicerS
DEXDc
HELICc
DUF
PAZ
RNazeIII
RNazeIII
dsRBD
Full lenght protein
DicerO
HELICc
DUF
PAZ
RNazeIII
RNazeIII
dsRBD
Alternative splicing

Figure 14. Alternative promotor usage. **(A)** Lysine demethylases and their protein isoforms derived from alternative promotors. **(B)** Wnt signaling proteins and their protein isoforms derived from alternative promotors. **(C)** Other proteins with alternative isoforms derived from intronic promotors. Black box represents functional domain structures in the protein.

gene intron is oocyte-specific Dicer isoform (DicerO) (Figure 14C). Due to downstream alternative intronic promotor, DicerO lacks the N-terminal DExD helicase domain. DicerO, short isoform of DicerS, has higher cleavage activity in somatic cells and it is specific for oocytes (Flemr et al. 2013). Another example of important factors created by alternative promoter usage are dominant negative isoforms of TCF/LEF proteins (Figure 14B). Wnt signaling is extremely important and these dominant negative isoforms always repress the canonical Wnt signaling target genes. (Vacik and Raška 2017, Vacik and Lemke 2011).

The transcription of the *KDM2A-SF* mRNA appears to be driven by an alternative intronic promoter located in *KDM2A* intron 12. Using the publicly available ChIP-seq data we found that the first *KDM2A-SF* exon is surrounded by elevated levels of various transcription factors and the epigenetic marks H3K4me3 and H3K27Ac. Since these epigenetic marks are known to be associated with active promoter regions, this strongly suggests the presence of an active promoter region (Stasevich et al. 2014; Huang et al. 2019). This is further supported by the presence of elevated levels of TBP and RNA-polymerase II and other transcription factors. The alternative intronic promoter that drives the expression of KDM2A-SF is still uncharacterized and the regulation of KDM2A-LF or KDM2A-SF expression is not yet elucidated in detail, but several KDM2A-LF regulators have been reported. The regulation of the *KDM2A* mRNA transcription has been shown to be affected by hypoxia (Batie et al. 2017). In the cellular environment with decreased levels of available oxygen, hypoxia-inducible factors (HIFs) are activated. Hypoxia-inducible factor 1 (HIF-1) is reported to bind to the *KDM2A* promotor, where it facilitates recruitment of RNA polymerase II and stimulates transcription of the *KDM2A*

mRNA (Batie et al. 2017). It has been shown that KDM2A is also regulated by miR-29b, a microRNA precursor that directly targets the *KDM2A* 3'-UTR region, which results in downregulation of KDM2A and consequently in suppression of proliferation and metastasis of gastric cancer (Kong et al. 2016).

We showed that the translation start site of *KDM2A-SF* corresponds to ATG site located in *KDM2A* exon 14, which results in the protein that contains the same functional domains as KDM2A-LF with one but big difference, it lacks the N-terminal demethylase domain (Figure 14A). Even though KDM2A-SF lacks the JmjC demethylase domain and therefore also the demethylation function, it has been shown that it is expressed in several breast cancer cell lines, in some of which it is even more abundant then KDM2A-LF (Liu et al. 2016; Okamoto et al. 2017). However, KDM2A-SF has not been studied in details. Our work shows that KDM2A-SF is expressed not just in cancer cell lines, but also in other human and mouse cell lines, in adult and embryonic mouse tissues, and also in mouse ESCs (Lađinović et al. 2017). Furthermore, we showed that KDM2A-SF, unlike its full length canonical KDM2A-LF counterpart, binds to pericentromeric heterochromatin and by doing so it forms distinct nuclear heterochromatic bodies dependently on HP1α (Lađinović et al. 2017). These results are consistent with the results published by Boegel et al. (2017) and Frescas et al. (2008) showing that KDM2A directly interacts with HP1α and is involved in the formation of pericentromeric heterochromatin, respectively. In 2008 Frescas et al. reported that knock down of KDM2A in HEK293 cells caused an increase of the H3K36me2 levels on one pericentromeric region of chromosome 4, while it remained unchanged on the *GAPDH* promoter (Frescas et al. 2008). These results suggested that KDM2A demethylates pericentromeric H3K36me2 using its Jumonji C domain and by doing so it maintains the closed chromatin state to prevent transcription. Frescas et al. showed that knocking down KDM2A results in transcriptional de-repression of pericentromeric regions in NIH3T3 cells (Frescas et al. 2008). Although we used a different cell type, we did not detect any transcriptional activity of the KDM2A-bound pericentromeric regions after knocking down either or both KDM2A isoforms in the MCF-7 cells (data not shown). It is possible thus that KDM2A mediated repression of

pericentromeric heterochromatin is cell type dependent and that there is another factor that can substitute for KDM2A in the MCF-7 cells. What is the role of either KDM2A-LF or KDM2A-SF in this transcriptional repression of pericentromeric heterochromatin remains to be elucidated and will have to be studied using also other cell types such as the above mentioned NIH3T3 cells.

A recent study has emphasized the role of KDM2A and KDM2B in canonical Wnt/beta-catenin dependent signaling (Lu et al. 2015). Histone demethylase KDM2A, as well as its paralogue KDM2B, have been reported to inhibit canonical Wnt signaling by interacting with and demethylating beta-catenin in the nucleus, which marks it for ubiquitination and degradation. Using its JmjC demethylase domain KDM2A/B demethylate the beta-catenin lysines in the region around fourth and fifth Armadillo repeat. This degradation is shown to indirectly inhibit the transcription of canonical Wnt target genes (Lu et al. 2015). We tested the influence of the demethylation deficient isoforms KDM2A-SF and KDM2B-SF on Axin2 and CyclinD1, two well established canonical Wnt signaling target genes. Our results show that KDM2A-LF, KDM2A-SF, as well as KDM2B-SF have the ability to repress canonical Wnt signaling target genes. On the other hand, KDM2B-LF mediated repression is cell type dependent and it should be studied more in the future. Considering that KDM2A-SF and KDM2B-SF lack the demethylase domain, further experiments are required to explain their mechanism of action. It has been shown that KDM2A-LF and KDM2B-LF interact with beta-catenin, as well as with TCF7L1 (Lu et al. 2015). It is possible that KDM2A-SF and KDM2B-SF retained the ability to interact with these proteins, which would explain our results.

KDM2A is also involved in transcriptional regulation of microRNAs. Ou et al. (2018) showed that KDM2A represses the transcription of miR-132 in cervical cancer by direct interaction with its promotor where it removes mono and dimethyl marks from H3K36. By repressing miR-132 that represses cancer cell proliferation, KDM2A functions as a stimulator of cell proliferation and tumor activator. KDM2A has been shown to be involved in the regulation of the cell proliferation and osteodentinogenic differentiation of the mesenchymal stem cells (MCSs) (Yu et al. 2016). It represses the transcription of

the *SOX2* and *NANOG* genes which results in lower adipogenic and chondrogenic differentiation potentials (Donget al. 2013). Later, the *SOX2* gene was shown to be a direct target of KDM2A also in breast cancer cells. Through *SOX2* repression, KDM2A is fulfilling its function in cancer stemness promotion (Chen et al. 2016). Further, it has been demonstrated in stem cells from apical papilla that KDM2A can promote cell proliferation through the cyclin-dependent kinase inhibitors, p15INK4B and p27Kip1 (cyclin-dependent kinase inhibitor 1B) (Gao et al. 2013). During embryonic development KDM2A downregulates the cyclin dependent kinase inhibitor p21Cip1, but no global changes of H3K36 mono-, di-, and tri-methylation were detected (Kawakami et al. 2015). Under starvation KDM2A has been shown to affect cell proliferation by repressing the production of ribosomal RNA (rRNA) (Tanaka et al. 2015, Tanaka et al. 2010). Another target of KDM2A is TET2, dioxygenase that plays a key role in active DNA demethylation. KDM2A represses the TET2 transcription by binding to the *TET2* gene promotor together with RelA. Even though the mechanism by which KDM2A represses the *TET2* gene is not known yet, by repressing TET2 KDM2A is involved in the DNA methylation status (Chen et al. 2017). Next to DNA methylation, KDM2A indirectly affects also histone acetylation. By removing methyl groups from the gene activation mark H3K36me2 on the *histone deacetylase 3 (HDAC3)* promotor, KDM2A represses the HDAC3 gene transcription. This repression results in the induction of the expression levels of cell cycle-associated genes (e.g. CDK6) and cell invasion-related genes (e.g. NANOS1), which stimulates proliferation and invasiveness of non-small cell lung cancer (NSCLC) cells (Dhar et al. 2014). Several independent groups showed that knocking down KDM2A results in cell arrest. In stem cells from the apical papilla (SCAPs) KDM2A depletion causes an increased percentage of cells in the G1/S cell cycle phase through the cyclin-dependent kinase inhibitors p15INK4B and p27Kip1 (Gao et al. 2013). In HEK293T cells depletion of KDM2A leads to a decreased percentage of cells in the G1 phase and increased percentage of cells in S and G2/M cell cycle phase through TGF- β signaling (Gao et al. 2013; Xu et al. 2019). However, another study showed that KDM2A depletion leads to a reduction of the number of cells in the S cycle phase without affecting the number of cells in the G1 or G2/M population (Dhar et

al. 2014). Contradictory results concerning the cell migration and proliferation were obtained also in breast cancer tissue (Rizwani et al. 2014). These cell lines exhibit tumor-suppressive and anti-angiogenic properties and also high levels of KDM2A. With progression of disease to metastasis, KDM2A expression decreases. The anti-angiogenic effects are caused by the interaction between KDM2A and E2F1 in a cell cycle dependent manner, which affects the E2F1-mediated expression of vascular endothelial growth factor (VEGF) receptors (Rizwani et al. 2014). Since the molecular mechanism of action of KDM2A is not known here, it cannot be clearly said which KDM2A isoform is responsible for anti-proliferative effects in these cells.

KDM2A has been reported to be indirectly involved in several signaling pathways and in repression of their target genes. KDM2A binds to the *JAG1* and *PDGFA* promoters and represses their expression by demethylating H3K36me2 (Chen et al. 2016). Since JAG1 is a NOTCH signaling ligand, KDM2A negatively affects also the whole NOTCH signaling pathway. NOTCH signaling is not the only signaling pathway KDM2A has been reported to affect. Furthermore, KDM2A has been reported to be a negative regulator of the NF-kappaB signaling pathway as well (Lu et al. 2009; Lu et al. 2010). By interacting with the NF-kappaB subunit p65, KDM2A disrupts the binding of NF-kappaB to DNA. (Lu et al. 2010). Dual-specificity phosphatase 3 (DUSP3) was also identified as a KDM2A target gene. DUSP3 is a protein phosphatase that dephosphorylates ERK1/2 in NSCLC cells. By demethylating H3K36me2 at the *DUSP3* locus, KDM2A represses the transcription of DUSP3. KDM2A indirectly affects protein phosphorylation and in the case of protein phosphatase DUSP3 repression, it activates ERK1/2 signaling pathway (Wagner et al. 2013). PI3K/AKT/mTOR pathway is found to be affected by KDM2A too. KDM2A knock down is shown to down regulate the expression of phospho (p)-PI3K, p-AKT and p-mTOR and by that suppressing and PI3K/AKT/mTOR pathway itself (Lu et al. 2019). The PI3K/AKT/mTOR pathway plays an important role in regulating the cell cycle and in regulating the cellular quiescence, proliferation, cancer, and longevity (Gao et al. 2003). Lu et al. (2019) revealed that KDM2A is involved in apoptosis, cell proliferation, migration and invasion of tumor cells in epithelial ovarian cancer. Even though, KDM2A is known as

a transcriptional repressor, it has been reported that knocking down KDM2A leads to downregulation of TGF-β1 and TGF-β2 and KDM2A thus downregulates the TGF-β pathway (Xu et al. 2019). TGF-β signaling is known for its role in G1 cell cycle arrest, stopping proliferation, inducing differentiation and promotion of apoptosis (Iordanskaia and Nawshad 2011; Massagué and Xi 2012; Ramesh et al., 2009). The exact molecular mechanism of how KDM2A regulates the TGF-β pathway is still unknown. However, TGF-β signaling is activated by CXXC5 in hepatocellular carcinoma and KDM2A is also a member of the CXXC-type zinc finger domain containing protein family (Yan et al. 2018; Xu et al., 2019). This implicates that KDM2A possibly regulates the TGF-β expression in a CXXC domain-dependent manner, which means that KDM2A-SF could also have a similar impact on TGF-β signaling.

KDM2A has been shown to play an important role also in DNA damage repair (Fnu et al. 2011; Cao et al. 2016; Bueno et al. 2018). During homologous recombination repair histone methylation plays an important role in attracting 53BP1 to a DNA double-strand break (DSB). After a DSB has occurred, the major event is generation of H3K36me2 (Fnu et al. 2011). KDM2A, with its demethylation catalytic activity, has an important role in DNA damage repair by demethylating H3K36me2 on DSBs, which decreases DNA DSB repair by NHEJ (Fnu et al. 2011). H3K36me2 on DSBs sites serves also as a platform to recruit the MRE11 complex which results in the efficient homologous recombination DNA damage repair and enhanced cell survival. KDM2A inhibits DNA damage repair by demethylating H3K36me2, which prevents the MRE11 complex from binding to DSBs sites. Ataxia-telangiectasia mutated (ATM) protein is a regulator of this process and KDM2A is its direct phosphorylation target. ATM phosphorylates KDM2A at threonine 632 (T632) located in the PHD zinc finger domain and this phosphorylation significantly deteriorates the KDM2A chromatin-binding capacity and consequently leads to increased levels of H3K36me2 near DNA damage sites (Cao et al. 2016). Not only does KDM2A inhibit DNA damage repair by binding to DSBs and by demethylating H3K36 dimethylation, it also mediates the ubiquitination of 53BP1. Through this ubiquitination of 53BP1, KDM2A negatively regulates recruitment of 53BP1 to double strand brakes

(DSBs) and inhibits DNA damage repair. KDM2A-mediated ubiquitination of 53BP1 has been shown to depend on the KDM2A demethylase activity and the CXXC zinc finger domain (Bueno. et al. 2018). Given that KDM2A-SF also contains the CXXC zinc finger domain, KDM2A-SF could also be involved in DNA damage repair and hypothetically could "protect" 53BP1 from ubuquitination and stimulate DNA damage repair.

All the above mentioned research was done with KDM2A-LF and most of the presented functions are JmjC demethylation domain dependent. Even though KDM2A-SF does not have the JmjC demethylation domain, it contains all the other domains including the DNA and protein interaction domains, which suggests that KDM2A-SF could also interact with the same DNA regions and proteins as KDM2A-LF. However, KDM2A-SF would likely act in a different way here, since it is missing the demethylation activity. Besides the zinc finger binding domains, KDM2A-SF has also an F-box domain. F-box domain is known as E3 ubiquitin ligase adaptor in SCF ubiquitin ligase complex, which mediates the ubiquitination of proteins involved in transcription, signal transduction and cell cycle progression. (Schulman et al. 2000). Considering this, KDM2A-SF could also have a ubiquitination function.

KDM2A-SF is highly expressed in several breast cancer cell lines and it has been reported to be required for maintaining cell proliferation, as well as for the colony-forming and invasive abilities of breast cancer cells *in vitro* (Liu et al. 2016). Furthermore, KDM2A has been reported to be involved in circadian rhythm control as a negative regulator of CLOCK/BMAL1-regulated genes, whose promoters are bound by KDM2A in a circadian phase-dependent manner (Reischl and Kramer 2015). Considering that the JmjC demethylase domain is not required for this negative regulation, there is a high possibility that KDM2A-SF is involved in the regulation of circadian rhythm as well. It has been reported that KDM2A is reducing the ribosomal RNA production in response to starvation by binding to the CpG island of the rDNA promotor. This binding is detected independently of the demethylase activity, which suggests that KDM2A-SF might also have a role in the rDNA transcriptional regulation (Tsuneoka et al. 2015). Later, Okamoto et al. (2017) indeed confirmed that KDM2A-SF is required for the rRNA transcription and

that it binds to the rDNA promoter while KDM2A-LF does not. It has been also reported that a reduced level of KDM2A-SF leads to increased levels of H4K20me3 (Okamoto et al. 2017).

Using various KDM2A isoforms Iuchi and Green (2012) showed that that the KDM2A-N782 isoform that encodes a protein containing the JmjC demethylation, CXXC and PHD zinc finger domains, but lacking the F-box and LRR domains plays a role in keratinocyte proliferation, while the full length protein KDM2A-LF does not. This research highlights the importance of the domain structure in the protein function. Iuchi and Green (2012) emphasize how different transcripts from the same gene encode proteins with different or opposite functions, but also present critical evidence of the complicated activities of KDM2A.

KDM2B, a paralog of KDM2A, is another lysine demethylase that has an alternative short isoform derived from an alternative intronic promotor and lacking thus the JmjC demethylation domain. KDM2B-LF has been reported to be involved in similar processes to KDM2A-LF and to promote cell proliferation. KDM2B affects cell proliferation by repressing the p16Ink4a and p19Arf inducers of cellular senescence (Tzatsos et al. 2009). In the same cell line, KDM2B has been shown to induce cellular proliferation and to inhibit cellular senescence through direct transcriptional silencing of p15Ink4b (He et al. 2008). Furthermore, KDM2B has been reported to regulate cell growth by repressing p19Arf (Fukuda et al. 2011). KDM2B has been also shown to repress the ribosomal DNA transcription. This transcriptional repression of the ribosomal genes is dependent on the KDM2B JmjC demethylation domain. Due to the connection between the ribosomal RNA synthesis and cell growth, KDM2B has a negative effect on the cell size and proliferation through this repression (Frescas et al. 2007). In addtition to the JmjC domain dependent roles, KDM2B has a role also in ubiquitination through its F-box domain acting as a subunit of the CUL-RING ubiquitin ligase (CRL1/SCFKDM2B) complex (Han et al. 2016).

Although the KDM2B long (KDM2B-LF) and short (KDM2B-SF) isoforms have been both described to be expressed in early mouse embryos and in various adult tissues,

KDM2B-SF is the more predominant isoform (Boulard et al. 2015; Inagaki et al. 2015). KDM2B-SF is induced during the early differentiation stages and it is expressed in white adipose tissue. Also, it has been shown that the KDM2B JmjC catalytic domain is not required for adipogenesis and that KDM2B-SF plays a role in fat differentiation and pathophysiology (Inagaki et al. 2015).

Further, KDM2B specifically recognizes non-methylated CpG islands in gene promoters and recruits the polycomb repressive complex 1 (PRC1) which contributes to gene repression (Farcas et al. 2012). This discovery lead to another surprising discovery that showed that KDM2B was the first reported factor whose loss leads to dense de novo genomic DNA methylation (Boulard et al. 2015).

Loss of both KDM2B isoforms in mice has been shown to result in completely penetrant lethal developmental defects around embryonic day E10.5 – E13.5. In addition to a reduced size of the embryos, developmental defects included a failure of the neural tube closure, a malformation of the anterior neural tube, a kinked and tortuous posterior neural tube, limb and craniofacial malformations, as well as abnormal somitogenesis and heart defects (Boulard et al. 2015; Andricovich et al. 2016). The mouse mutants with the loss of function of either KDM2B-LF or KDM2B-SF have remarkably different phenotypes (Fukuda et al. 2011; Boulard et al. 2016). The KDM2B-LF mutants gave offspring with a weakly penetrant phenotype characterized by exencephaly, coloboma, and kinked tails, while most offspring were born viable and without visible phenotype (Fukuda et al. 2011). On the other hand, the KDM2B-SF mutants showed craniofacial abnormalities, compression of the anterior portion of the head and eyes open at birth, while prenatally dead mutants exhibited craniofacial and neural tube abnormalities (Boulard et al. 2016). KDM2A-LF and KDM2A-SF are thus very likely to have different functions in embryonal development.

The other important members of the JmjC domain-containing protein family are JARID1 and JARID2. Both proteins contain the JmjC, JmjN, AT-rich interaction (ARID), and CXXC zinc finger domain. The JmjC domain of JARID1 and JARID2 differ in several amino

acids, which gives JARID1 the ability to remove methyl groups from di- and trimethylated histone H3K4, while JARID2 does not have any demethylase activity (Landeira and Fisher 2011). The JmjC-domain demethylation function is established through interaction with cofactors non-haeme iron (II) and 2-oxoglutarate (2OG or α-ketoglutarate)-dependent oxygenases (Shmakova et al. 2014). Substitutions in amino acid sequence of JARID2 block binding of cofactors iron and α-ketoglutarate, which eradicates the demethylase function (Landeira and Fisher 2011). Both JARID1 and JARID2 loss of function homozygotes are embryonically lethal, except that the JARID1 mutants die at the day E4.5, while the JARID2 mutants are still detected at E15.5 (Catchpole et al. 2011; Takeuchi et al. 1995). Even though JARID2 lacks the demethylation activity it is connected with various defects like non-syndromic cleft lip, spina bifida, congenital heart defects and schizophrenia (Scapoli et al. 2010; Volcik et al. 2004; Liu et al. 2009; Pedrosa et al. 2007).

These differences between the Kdm2b-lf and Kdm2b-sf, JARID1 and JARID2 mutant phenotypes emphasize the importance of distinguishing between not just KDM2B-LF and KDM2B-SF or JARID1 and JARID2, but also between the KDM2A-LF and KDM2A-SF functions and their molecular mechanisms. It has been found that the loss of function of both KDM2A-LF and KDM2A-SF increases apoptosis and decreases cell proliferation leading to embryonic lethality at embryonic days E10.5–12.5. However, it is not clear which isoform is responsible for the phenotype (Kawakami et al. 2015).

Another member of F-box family of proteins is FBXL19 shares the domain structure with KDM2A-SF and KDM2B-SF, since it contains the CXXC, PHD zinc finger, F-box and LRR domain, but it lacks the JmjC demethylase domain (Katoh and Katoh 2004). It is a member of Skp1-Cullin-F-box family of E3 ubiquitin ligases and it binds to the transmembrane receptor interleukin 1 receptor-like 1 and regulates its ubiquitination and degradation (Zhao et al. 2012). FBXL19 has been reported to play a role in TGF-β-induced E-cadherin down-regulation by decreasing the endogenous and overexpressed levels of Rac3 (Dong et al. 2014). Furthermore, FBXL19 has been recently shown to be essential for mouse development (Dimitrova et al. 2018). This function of FBXL19 that shares the

domain structure with KDM2A-SF draws attention to possible functions of KDM2A-SF that should be further examined.

Alternative splicing of the *LSD1/LSD1* pre-mRNA results in several alternative mRNA and consequently also protein isoforms. One of the LSD1/LSD1 isoforms is LSD1/LSD1n. Unlike its non-spliced variant LSD1/LSD1 that demethylates either H3K4me2 or H3K9me2, LSD1/LSD1n demethylates H4K20me1/2 (mono- and di-methylated lysine K20 of histone H4) (Wang et al. 2015). Second isoform LSD1/LSD1 gene can give rise is LSD1+8a that lacks the H3K4me2 demethylation activity but retains the H3K9me2 demethylation activity (Laurent et al. 2015). These three isoforms due to their different demethylation target have and different function, where LSD1 isoform through demethylation of H3K4me2 or H3K9me2 functions as transcriptional activator or repressor and LSD1n and LSD1+8a isoforms by demethylating H3K4me2 or H3K9me2 can function just as transcriptional activators (Shi et al. 2004; Metzger et al. 2005; Wang et al. 2007; Foster et al. 2010; Laurent et al. 2015; Wang et al. 2015).

All these protein isoforms, KDM2B-SF, JARID1, JARID2, FBXL19, LSD1n, and LSD1+8a, as well as many other protein isoforms that lack a certain domain due to alternative splicing or alternative promotor usage, emphasize the importance of distinguishing between KDM2A-LF and KDM2A-SF. Even though KDM2A-SF lacks the catalytical Jumonji C demethylase domain, there are multiple reasons to believe that KDM2A-SF has an important role in many cellular processes, in development and that its misregulation can lead to severe diseases and cancer.

8. Conclusions

KDM2A is a lysine demethylase that binds directly to CpG islands through its CXXC zinc-finger DNA binding domain and demethylates H3K36 using its Jumonji C demethylation domain. The same gene locus encodes a shorter KDM2A isoform that contains the DNA binding CXXC zinc finger, protein binding PHD zinc finger, F-box, and six leucine-rich repeats domain, but lacks the JmjC demethylation domain. One of the goals of this thesis was to characterize this demethylation deficient KDM2A isoform more in detail and to focus on the chromatin regions it is associated with. KDM2A-SF is produced by the action of an alternative intronic promotor characterized by elevated levels of the epigenetic marks H3K4me3 and H3K27Ac. This promotor and the alternative first exon of KDM2A are located in *KDM2A* intron 12. As opposed to the starting hypothesis, we showed that the first coding exon of KDM2A-SF is its third exon, which corresponds to *KDM2A* exon 14 and that the alternative first exon 1b is not coding. Despite lacking the Jumonji C demethylase domain KDM2A-SF retains its ability to bind CpG islands through its CXXC zinc finger DNA binding domain, which makes it a competitor of KDM2A-LF for binding to the same CpG islands. Considering that H3K36me2 is mostly associated with active gene promoters and its demethylation leads to transcriptional repression, KDM2A-SF could function as an activator by preventing KDM2A-LF from binding to and demethylating a CpG island containing promoter. However, KDM2A-LF and KDM2A-SF have been found to directly interact with HP1α which is involved in transcriptional silencing of pericentromeric heterochromatin. Even though pericentromeric heterochromatin is not transcriptionally active, it has been found that KDM2A bound pericentromeric regions exhibit high levels of H3K36me2 (Lađinović, D. et al., 2017). Taking into account that H3K36me2 is the KDM2A-LF demethylation substrate, these results suggests that pericentromeric regions are occupied by KDM2A-SF which lacks the demethylation function and not by KDM2A-LF. Since we failed to detect any transcriptional activity of the KDM2A-bound pericentromeric regions after knocking down both KDM2A isoforms, it can be hypothesized that H3K36me2 does not have a role in transcriptional regulation of these regions. It is possible, however, that H3K36me2

functions as a repression mark in pericentromeric heterochromatin and therefore it should not be removed by the demethylase domain of KDM2A-LF. But, because some of the other KDM2A domains are necessary here in pericentromeric chromatin for currently unknown reason (e.g. structural integrity, transcriptional co-repressors), KDM2A-SF binds here. The exact function and mechanism of KDM2A-SF in the formation of pericentromeric heterochromatin remains poorly defined and in the future, it should be studied more in detail. In this research we also discovered that KDM2A-SF is a naturally occurring isoform that is expressed in various adult mouse tissues, in developing mouse embryo and in mouse ES cells. Based on the publicly available GenBank EST and RNA-seq data, KDM2A-SF is likely to be expressed also in healthy human tissues including human ES cells. Another goal of this thesis was to analyze the role of KDM2A-SF and KDM2B-SF in canonical Wnt signaling. We showed that KDM2A-SF and KDM2B-SF repress the canonical Wnt signaling target genes Axin2 and CyclinD1, although the mechanism of action is still unknown. This research highlighted the possible functional difference between KDM2A/B-LF and KDM2A/B-SF and opened new questions about KDM2A/B-SF, their functions and the role in pericentromeric heterochromatin, as well as its involvement in transcriptional regulation and signaling pathways.

9. References

Abdelsamed, H. A., Zebley, C. C., Youngblood, B. Epigenetic Maintenance of Acquired Gene Expression Programs during Memory CD8 T Cell Homeostasis. Front Immunol. 2018; 9:6.

Alaskhar Alhamwe, B., Khalaila, R., Wolf, J., et al. Histone modifications and their role in epigenetics of atopy and allergic diseases. Allergy Asthma Clin Immunol. 2018; 14:39.

Alberts, B., Johnson, A., Lewis, J., et al. Molecular Biology of the Cell. 4th edition. New York: Garland Science; The Global Structure of Chromosomes. 2002.

Amendola, P. G., Zaghet, N., Ramalho, J. J., Vilstrup Johansen, J., Boxem, M., Salcini, A. E. JMJD-5/KDM8 regulates H3K36me2 and is required for late steps of homologous recombination and genome integrity. PLoS Genet. 2017; 13(2):e1006632.

Ando, M., Saito, Y., Xu, G., Bui, N. Q., Medetgul-Ernar, K., Pu, M., et al. Chromatin dysregulation and DNA methylation at transcription start sites associated with transcriptional repression in cancers. Nature Communications, (2019). 10(1).

Andricovich, J., Kai, Y., Peng, W., Foudi, A., Tzatsos, A. Histone demethylase KDM2B regulates lineage commitment in normal and malignant hematopoiesis. J Clin Invest. 2016. 216(3): 905-920.

Annunziato, A. DNA Packaging: Nucleosomes and Chromatin. Nature Education. 2008. 1(1):26.

Antonarakis, S. E. and Cooper, D. N. Human Genomic Variants and Inherited Disease: Molecular Mechanisms and Clinical Consequences. Emery and Rimoin's Principles and Practice of Medical Genetics and Genomics (Seventh Edition). 2019, Pages 125-200.

Ashapkin, V. V., Kutueva, L. I., Vanyushin, B. F. Aging as an Epigenetic Phenomenon. Curr Genomics. 2017; 18(5):385–407.

Atlasi, Y., Stunnenberg, H. G. The interplay of epigenetic marks during stem cell differentiation and development. Nature Reviews Genetics. 2017; 18: 643–658.

Ayoubi, T. A., Van De Ven, W. J. Regulation of gene expression by alternative promoters. FASEB J. 1996. 10(4):453-60.

Babenko, V. N., Chadaeva, I. V., Orlov, Y. L. Genomic landscape of CpG rich elements in human. BMC Evol Biol. 2017; 17:19.

Bannister, A. J., Kouzarides, T. Regulation of chromatin by histone modifications. Cell Res. 2011; 21(3):381–395.

Barbosa, C., Peixeiro, I., Romao, L. Gene expression regulation by upstream open reading frames and human disease. PLoS Genet. 2013. 9:e1003529.

Barros, S. P., Offenbacher S. Epigenetics: connecting environment and genotype to phenotype and disease. J Dent Res. 2009; 88(5):400–408.

Batie, M., Druker, J., D'Ignazio, L., Rocha, S. KDM2 Family Members are Regulated by HIF-1 in Hypoxia. Cells. 2017; 6(1):8.

Beerman, I. Rossi, D. J. Epigenetic Control of Stem Cell Potential during Homeostasis, Aging, and Disease. Cell Stem Cell. 2015; 16(6):613–625.

Bennett, G., Papamichos-Chronakis, M., Peterson, C. L. DNA repair choice defines a common pathway for recruitment of chromatin regulators. Nat Commun. 2013; 4:2084.

Bernhard, H. A critical view on transgenerational epigenetic inheritance in humans. Nature Communications. 2018. 9(1):2973

Borgel, J., Tyl, M., Schiller, K., et al. KDM2A integrates DNA and histone modification signals through a CXXC/PHD module and direct interaction with HP1. Nucleic Acids Research. 2017; 45(3):1114-1129.

Borun, T. W., Pearson, D., Paik, W. K. Studies of histone methylation during the HeLa S-3 cell cycle. J Biol Chem. 1972; 247(13):4288-98.

Boulard, M., Edwards J. R., Bestor T. H. Abnormal X chromosome inactivation and sex-specific gene dysregulation after ablation of FBXL10. Epigenetics Chromatin. 2016; 9:22.

Boulard, M., Edwards, J. R., Bestor, T. H. FBXL10 protects Polycomb-bound genes from hypermethylation. Nat Genet. 2015; 47(5):479-85.

Brenner, C., Luciani, J., Bizet, M., et al. The interplay between the lysine demethylase KDM1A and DNA methyltransferases in cancer cells is cell cycle dependent. Oncotarget. 2016; 7(37):58939–58952.

Bueno, M. T. D., Baldascini, M., Richard, S., Lowndes, N. F. Recruitment of lysine demethylase 2A to DNA double strand breaks and its interaction with 53BP1 ensures genome stability. Oncotarget, 2018; 9(22): 15915-15930.

Burggren, W. Epigenetic Inheritance and Its Role in Evolutionary Biology: Re-Evaluation and New Perspectives. Biology (Basel). 2016; 5(2):24.

Butler, A. A., Webb, W. M., Lubin, F. D. Regulatory RNAs and control of epigenetic mechanisms: expectations for cognition and cognitive dysfunction. Epigenomics. 2016; 8(1):135–151.

Cabianca, D. S. and S. M. Gasser. Spatial segregation of heterochromatin: Uncovering functionality in a multicellular organism. Nucleus, 2016; 7(3): 301-7.

Calvanese, V., Fraga, M. F. Epigenetics of embryonic stem cells. Adv Exp Med Biol. 2012. 741:231-53.

Cao, L. L., Wei, F., Du, Y., Song, B., Wang, D., Shen, C., Lu, X., Cao, Z., Yang, Q., Gao, Y., Wang, L., Zhao, Y., Wang, H., Yang, Y., Zhu, W. G. ATM-mediated KDM2A phosphorylation is required for the DNA damage repair. Oncogene. 2016; 35 (3): 301-313.

Castelnovo, M. and Grauwin, S. Electrophoresis of positioned nucleosomes. Biophys J. 2007; 92(9):3022–3031.

Catchpole, S., Spencer-Dene, B., Hal,l D., Santangelo, S., Rosewell, I., Guenatri, M., Beatson, R., Scibetta, A. G., Burchell, J. M., Taylor-Papadimitriou, J. PLU-1/JARID1B/KDM5B is required for embryonic survival and contributes to cell proliferation in the mammary gland and in ER+ breast cancer cells. Int J Oncol. 2011; 38: 1267–1277.

Chen, C. D., Kobayashi, R., Helfman, D. M. Binding of hnRNP H to an exonic splicing silencer is involved in the regulation of alternative splicing of the rat β-tropomyosin gene. Genes & Dev. 1999. 13: 593-606.

Chen, J. Y., Li, C. F., Chu, P. Y., et al. Lysine demethylase 2A promotes stemness and angiogenesis of breast cancer by upregulating Jagged1. Oncotarget. 2016; 7(19): 27689–27710.

Chen, J. Y., Luo, C. W., Lai, Y. S., Wu, C. C., Hung, W. C. Lysine demethylase KDM2A inhibits TET2 to promote DNA methylation and silencing of tumor suppressor genes in breast cancer. Oncogenesis. 2017; 6(8):e369.

Chen, L., Vasilatos, S. N., Qin, Y., et al. Functional characterization of lysine-specific demethylase 2 (LSD2/KDM1B) in breast cancer progression. Oncotarget. 2017; 8(47):81737–81753.

Chen, Y., Yang, Y., Wang, F., et al. Crystal structure of human histone lysine-specific demethylase 1 (LSD1). Proc Natl Acad Sci U S A. 2006; 103(38):13956–13961.

Cheng, Z., Cheung, P., Kuo, A. J., et al. A molecular threading mechanism underlies Jumonji lysine demethylase KDM2A regulation of methylated H3K36. Genes & Development. 2014; 28(16): 1758-1771.

Ciccone D. N., Su, H., Hevi, S., Gay, F., Lei, H., Bajko, J., Xu, G., Li, E. and Chen, T. KDM1B is a histone H3K4 demethylase required to establish maternal genomic imprints. Nature. 2009. 461: 415–418.

Cleveland, D. W., Mao, Y., Sullivan, K. F. Centromeres and Kinetochores. Cell. 2003; 112(4): 407-421.

Cloos, P. A., Christensen, J., Agger, K., Helin, K. Erasing the methyl mark: histone demethylases at the center of cellular differentiation and disease. Genes Dev. 2008; 22(9):1115–1140.

Clouaire, T., Legube, G. DNA double strand break repair pathway choice: a chromatin based decision? Nucleus. 2015; 6(2):107–113.

Coleman, W. B. Chapter 6 - The Human Genome: Understanding Human Disease in the Post-Genomic Era. Molecular Pathology (Second Edition). 2018, Pages 121-134.

Cubiles, M. D., Barroso, S., Vaquero-Sedas, M. I., Enguix, A., Aguilera, A., Vega-Palas, M. A. Epigenetic features of human telomeres. Nucleic Acids Res. 2018; 46(5):2347–2355.

Culhane, J. C., Cole, P. A. LSD1 and the chemistry of histone demethylation. Curr Opin Chem Biol. 2007; 11(5):561–568.

D'Oto, A., Tian, Q., Davidoff, A. M., Yang, J. Histone demethylases and their roles in cancer epigenetics. Journal of medical oncology and therapeutics. 2016; 1(2):34-40.

Daniels DL, Weis WI. Beta-catenin directly displaces Groucho/TLE repressors from Tcf/Lef in Wnt-mediated transcription activation. Nat Struct Mol Biol. 2005; 12(4):364-71.

Davuluri, R. V., Suzuki, Y., Sugano, S., Plass, C., Huang, T. H. The functional consequences of alternative promoter use in mammalian genomes. Trends Genet. 2008. 24:167–177.

Dhar, S. S., Alam, H., Li, N., et al. Transcriptional Repression of Histone Deacetylase 3 by the Histone Demethylase KDM2A Is Coupled to Tumorigenicity of Lung Cancer Cells. The Journal of Biological Chemistry. 2014; 289(11):7483-7496.

Di Lorenzo, A., Bedford, M. T. Histone arginine methylation. FEBS Lett. 2011; 585(13):2024–2031.

Dillon. S. C., Zhang, X., Trievel, R. C., Cheng, X. The SET-domain protein superfamily: protein lysine methyltransferases. Genome Biol. 2005; 6(8):227.

Dimitrova, E., Kondo, T., Feldmann, A., et al. FBXL19 recruits CDK-Mediator to CpG islands of developmental genes priming them for activation during lineage commitment. Elife, 2018. 7:e37084.

Dimitrova, E., Turberfield, A. H., Klose, R. J. Histone demethylases in chromatin biology and beyond. EMBO Rep. 2015; 16(12):1620–1639.

Dong, R., Yao, R., Du, J., Wang, S., Fan, Z. Depletion of histone demethylase KDM2A enhanced the adipogenic and chondrogenic differentiation potentials of stem cells from apical papilla. Exp Cell Res. 2013; 319(18):2874-82

Dong, S., Zhao, J., Wei, J., et al. F-box protein complex FBXL19 regulates TGFβ1-induced E-cadherin down-regulation by mediating Rac3 ubiquitination and degradation. Mol Cancer. 2014; 13:76.

Dong, X., Weng, Z. The correlation between histone modifications and gene expression. Epigenomics. 2013; 5(2):113–116.

Eissenberg, J. C. and A. Shilatifard. Histone H3 lysine 4 (H3K4) methylation in development and differentiation. Dev Biol, 2010. 339(2): 240-9.

Eissenberg, J. C., Elgin, S. C. HP1a: a structural chromosomal protein regulating transcription. Trends Genet. 2014; 30(3):103–110.

Fang, R., Barbera, A. J., Xu, Y., et al. Human LSD2/KDM1b/AOF1 regulates gene transcription by modulating intragenic H3K4me2 methylation. Mol Cell. 2010; 39(2):222–233.

Fang, R., Chen, F., Dong, Z., et al. LSD2/KDM1B and its cofactor NPAC/GLYR1 endow a structural and molecular model for regulation of H3K4 demethylation. Mol Cell. 2013; 49(3):558–570.

Farcas, A. M., Blackledge, N. P., Sudbery, I., et al. KDM2B links the Polycomb Repressive Complex 1 (PRC1) to recognition of CpG islands. Elife. 2012; 1:e00205.

Farooq, Z., Banday, S., Pandita, T. K., Altaf, M. The many faces of histone H3K79 methylation. Mutat Res, 2016. 768: 46-52.

Felsenfeld, G. and Groudine, M. Controlling the double helix. Nature. 2003; 421(6921):448-53.

Fiszbein, A., Kornblihtt, A. R. Histone methylation, alternative splicing and neuronal differentiation. Neurogenesis (Austin). 2016; 3(1):e1204844.

Flemr, M., Malik, R., Franke, V., Nejepinska, J., Sedlacek, R., Vlahovicek, K., & Svoboda, P. A Retrotransposon-Driven Dicer Isoform Directs Endogenous Small Interfering RNA Production in Mouse Oocytes. Cell. 2013; 155(4), 807–816.

Fnu, S., Williamson, E. A., De Haro, L. P., et al. Methylation of histone H3 lysine 36 enhances DNA repair by nonhomologous end-joining. Proc Natl Acad Sci U S A. 2011; 108(2):540–545.

Forneris, F., Binda, C., Vanoni, M. A., Mattevi, A., Battaglioli, E. Histone demethylation catalysed by LSD1 is a flavin-dependent oxidative process. FEBS Lett. 2005; 579(10):2203-7.

Foster, C.T., Dovey, O.M., Lezina, L., et al. Lysine-specific demethylase 1 regulates the embryonic transcriptome and CoREST stability. Mol Cell Biol. 2010; 30(20):4851–4863.

Frescas, D., Guardavaccaro, D., Bassermann, F., Koyama-Nasu, R., Pagano, M. JHDM1B/FBXL10 is a nucleolar protein that represses transcription of ribosomal RNA genes. Nature. 2007. 450(7167):309–13.

Frescas, D., Guardavaccaro, D., Kato, H., Poleshko, A., Katz, R. A., Pagano, M. KDM2A represses transcription of centromeric satellite repeats and maintains the heterochromatic state. Cell cycle. 2008; 7(22):3539-3547.

Fukuda, M., Sakaue-Sawano, A., Shimura, C., Tachibana, M., Miyawaki, A. & Shinkai, Y. G9a-dependent histone methylation can be induced in G1 phase of cell cycle. Scientific Reports. 2019. 9: 956

Fukuda, T., Tokunaga, A., Sakamoto, R., Yoshida, N. Fbxl10/Kdm2b deficiency accelerates neural progenitor cell death and leads to exencephaly. Mol Cell Neurosci. 2011. 46(3): 614-24.

Galati, A., Micheli, E., Cacchione, S. Chromatin structure in telomere dynamics. Front Oncol. 2013; 3:46.

Gallagher, S. R. and Desjardins, P. R. Quantitation of DNA and RNA with Absorption and Fluorescence Spectroscopy. Current Protocols in Protein Science. 2008.

Gan XQ, Wang JY, Xi Y, Wu ZL, Li YP, Li L. Nuclear Dvl, c-Jun, beta-catenin, and TCF form a complex leading to stabilization of beta-catenin-TCF interaction. J Cell Biol. 2008; 180(6):1087–1100.

Gao, N., Zhang, Z., Jiang, B., Shi, X. Role of PI3K/AKT/mTOR signaling in the cell cycle progression of human prostate cancer. Biochemical and Biophysical Research Communications. 2003. 310(4): 1124-1132

Gao, R., Dong, R., Du, J., Ma, P., Wang, S., Fan, Z. Depletion of histone demethylase KDM2A inhibited cell proliferation of stem cells from apical papilla by de-repression of p15INK4B and p27Kip1. Mol Cell Biochem. 2013; 379(1-2):115-22.

Gates, L. A., Foulds, C. E., O'Malley, B. W. Histone Marks in the 'Driver's Seat': functional Roles in Steering the Transcription Cycle. Trends Biochem Sci. 2017; 42 (12):977–989.

Gates, L. A., Shi, J., Rohira, A. D., et al. Acetylation on histone H3 lysine 9 mediates a switch from transcription initiation to elongation. J Biol Chem. 2017; 292(35):14456–14472.

Gelfman, S., Cohen, N., Yearim, A., Ast, G. DNA-methylation effect on cotranscriptional splicing is dependent on GC architecture of the exon-intron structure. Genome Res. 2013; 23:789–799.

Gibney, E. R. and Nolan, C. M. Epigenetics and gene expression. Heredity. 2010. 105: 4–13

Greer, E. L. and Y. Shi. Histone methylation: a dynamic mark in health, disease and inheritance. Nature Reviews Genetics. 2012; 13: 343.

Guttman, M., Donaghey, J., Carey, B. W., et al. lincRNAs act in the circuitry controlling pluripotency and differentiation. Nature. 2011; 477(7364):295–300.

Hall LL, Lawrence JB. RNA as a fundamental component of interphase chromosomes: could repeats prove key? Curr Opin Genet Dev. 2016; 37:137–147.

Hall, L. E., Mitchell, S. E., & O'Neill, R. J. Pericentric and centromeric transcription: a perfect balance required. Chromosome Research. 2012; 20(5), 535–546.

Han, X. R., Zha, Z., Yuan, H. X., et al. KDM2B/FBXL10 targets c-Fos for ubiquitylation and degradation in response to mitogenic stimulation. Oncogene. 2016; 35(32):4179–4190.

Harris, W. J., Huang, X., Lynch, J. T., et al. The histone demethylase KDM1A sustains the oncogenic potential of MLL-AF9 leukemia stem cells. Cancer Cell. 2012; 21(4):473-87.

He, J., Kallin, E. M., Tsukada, Y., Zhang, Y. The H3K36 demethylase Jhdm1b/Kdm2b regulates cell proliferation and senescence through p15 (Ink4b). Nature Structural & Molecular Biology. 2008. 15 (11): 1169–75

He, J., Nguyen, A. T., Zhang, Y. KDM2b/JHDM1b, an H3K36me2-specific demethylase, is required for initiation and maintenance of acute myeloid leukemia. Blood. 2011. 117(14):3869-3880.

Heard, E., Martienssen, R. A. Transgenerational epigenetic inheritance: myths and mechanisms. Cell. 2014; 157(1):95–109.

Henikoff, S., McKittrick, E., Ahmad, K.. Epigenetics, histone H3 variants, and the inheritance of chromatin states. Cold Spring Harb Symp Quant Biol. 2004; 69:235–243.

Henikoff, S., Smith, M. M. Histone variants and epigenetics. Cold Spring Harb Perspect Biol. 2015; 7(1):a019364.

Hirano, T. Condensins: universal organizers of chromosomes with diverse functions. Genes Dev. 2012; 26(15):1659–1678.

Hirschler-Laszkiewicz, I., Cavanaugh, A., Hu, Q., Catania, J., Avantaggiati, M. L., Rothblum, L. I. The role of acetylation in rDNA transcription. Nucleic Acids Res. 2001; 29(20):4114–4124.

Holliday, R. Epigenetics: an overview. Dev. Genet; 1994. 15: 453–457.

Holliday, R., Pugh, J. E. DNA modification mechanisms and gene activity during development. Science. 1975; 187:226-23.

Huang, J., Sengupta, R., Espejo, A. B., et al. P53 is regulated by the lysine demethylase LSD1. Nature. 2007; 449(7158):105-8

Huang, X., Gao, X., Li, W., et al. Stable H3K4me3 is associated with transcription initiation during early embryo development. Bioinformatics, 2019. btz173.

Huyen, Y., Zgheib, O., Ditullio Jr, R. A., Gorgoulis, V. G., Zacharatos, P., Petty, T. J., et al. Methylated lysine 79 of histone H3 targets 53BP1 to DNA double-strand breaks. Nature 2004; 432:406–11.

Hyun, K., Jeon, J., Park, K., Kim, J. Writing, erasing and reading histone lysine methylations. Exp Mol Med, 2017. 49(4): e324.

Inagaki, T., Iwasaki, S., Matsumura, Y., et al. The FBXL10/KDM2B Scaffolding Protein Associates with Novel Polycomb Repressive Complex-1 to Regulate Adipogenesis. The Journal of Biological Chemistry. 2015; 290(7):4163-4177.

Iordanskaia, T., Nawshad, A. Mechanisms of transforming growth factor β induced cell cycle arrest in palate development. J Cell Physiol. 2011; 226(5):1415–1424.

Iuchi, S., Green, H. Lysine-specific demethylase 2A (KDM2A) normalizes human embryonic stem cell derived keratinocytes. Proceedings of the National Academy of Sciences of the United States of America. 2012; 109(24):9442-9447.

Jachowicz, J. W., Santenard, A., Bender, A., Muller, J., Torres-Padilla, M. E. Heterochromatin establishment at pericentromeres depends on nuclear position. Genes Dev. 2013; 27(22):2427–2432.

Jack, A. P., Bussemer, S., Hahn, M., et al., H3K56me3 is a novel, conserved heterochromatic mark that largely but not completely overlaps with H3K9me3 in both regulation and localization. PLoS One, 2013. 8(2): e51765.

Jaenisch, R., Bird, A. Epigenetic regulation of gene expression: how the genome integrates intrinsic and environmental signals. Nature Genetics. 2003. 33: 245–254.

Jamieson, K., Wiles, E. T., McNaught, K. J., et al. Loss of HP1 causes depletion of H3K27me3 from facultative heterochromatin and gain of H3K27me2 at constitutive heterochromatin. Genome Res. 2016; 26(1):97–107.

Janssen, A., Colmenares, S. U., and Karpen, G. H. Heterochromatin: Guardian of the Genome. Annual Review of Cell and Developmental Biology. 2018. 34:265-288.

Jasencakova, Z., Meister, A., Walter, J., Turner, B. M., Schubert, I. Histone H4 acetylation of euchromatin and heterochromatin is cell cycle dependent and correlated with replication rather than with transcription. Plant Cell. 2000; 12(11):2087–2100.

Jeong, S. SR Proteins: Binders, Regulators, and Connectors of RNA. Mol Cells. 2017; 40(1):1–9.

Jin, B., Li, Y., Robertson, K. D. DNA methylation: superior or subordinate in the epigenetic hierarchy?. Genes Cancer. 2011; 2(6):607–617.

Jin, J., Cardozo, T., Lovering, R. C., Elledge, S. J., Pagano, M., Harper, J. W. Systematic analysis and nomenclature of mammalian F-box proteins. Genes Dev. 2004; 18: 2573-2580.

Kang, J. Y., Kim, J. Y., Kim, K. B. et al., KDM2B is a histone H3K79 demethylase and induces transcriptional repression via sirtuin-1-mediated chromatin silencing. FASEB J, 2018. 32(10):5737-5750

Kang, M. K., Mehrazarin, S., Park, N. H., Wang, C. Y. Epigenetic gene regulation by histone demethylases: emerging role in oncogenesis and inflammation. Oral Dis. 2017; 23(6):709–720.

Katoh, M. and Katoh, M. Identification and characterization of FBXL19 gene in silico. Int J Mol Med. 2004; 14(6):1109-14.

Katz, T. A., Vasilatos, S. N., Harrington, E., Oesterreich, S., Davidson, N. E,. Huang, Y. Inhibition of histone demethylase, LSD2 (KDM1B), attenuates DNA methylation and increases sensitivity to DNMT inhibitor-induced apoptosis in breast cancer cells. Breast Cancer Res Treat. 2014 Jul; 146(1):99-108.

Kawakami, E., Tokunaga, A., Ozawa, M., Sakamoto, R., Yoshida, N. The histone demethylase Fbxl11/Kdm2a plays an essential role in embryonic development by repressing cell-cycle regulators. Mechanisms of Development. 2015; 135:31-42,

Kent, W. J., Sugnet, C. W., Furey, T. S., Roskin, K. M., Pringle, T. H, Zahler, A. M., Haussler, D. The human genome browser at UCSC. Genome Res. 2002. 12(6): 996-1006

Kochetov, A. V. Alternative translation start sites and hidden coding potential of eukaryotic mRNAs. BioEssays. 2008. 30:683 –691.

Kocyłowski, M. K., Rey, A. J., Stewart, G. S., Halazonetis TD. Ubiquitin-H2AX fusions render 53BP1 recruitment to DNA damage sites independent of RNF8 or RNF168. Cell Cycle. 2015; 14(11):1748–1758.

Kong, Y., Zou, S., Yang, F., Xu, X., Bu, W., Jia, J., Liu, Z. RUNX3-mediated up-regulation of miR-29b suppresses the proliferation and migration of gastric cancer cells by targeting KDM2A. Cancer Lett. 2016; 381(1):138-48.

Kontaki, H., Talianidis, I. Lysine methylation regulates E2F1-induced cell death. Mol Cell. 2010; 39(1):152-60.

Kornberg. R. D. Structure of chromatin. Annu Rev Biochem. 1977; 46:931-54.

Kottakis, F., Foltopoulou, P., Sanidas, I., Keller, P., Wronski, A., Dake, B. T., Ezell, S. A., Shen, Z., Naber, S. P., Hinds, P. W., McNiel, E., Kuperwasser, C., Tsichlis, P. N. NDY1/KDM2B functions as a master regulator of polycomb complexes and controls self-renewal of breast cancer stem cells. Cancer Res. 2014. 74(14):3935–46.

Kouzarides, T. Chromatin modifications and their function. Cell. 2007; 128(4):693–705.

Kozak, M. Point mutations define a sequence flanking the AUG initiator codon that modulates translation by eukaryotic ribosomes. Cell. 1986. 44(2):283-92.

Krokan, H. E.and Bjørås, M. Base excision repair. Cold Spring Harb Perspect Biol. 2013; 5(4):a012583.

Kumar, S., Chinnusamy, V., Mohapatra, T. Epigenetics of Modified DNA Bases: 5-Methylcytosine and Beyond. Front Genet. 2018; 9:640.

Kuo, M. H. And Allis, C. D. Roles of histone acetyltransferases and deacetylases in gene regulation. BioEssays. 1998. 20(8):615–626.

Lacal, I., Ventura, R. Epigenetic Inheritance: Concepts, Mechanisms and Perspectives. Front Mol Neurosci. 2018; 11:292.

Lađinović, D., Novotná, J., Jakšová, S., Raška, I., Vacík, T. A demethylation deficient isoform of the lysine demethylase KDM2A interacts with pericentromeric heterochromatin in an HP1a-dependent manner. Nucleus. 2017; 8(5): 563-572.

Lahtz, C., Pfeifer G. P. Epigenetic changes of DNA repair genes in cancer. Journal of Molecular Cell Biology. 2011. 3(1): 51–58.

Landeira, D., Fisher, A. G. Inactive yet indispensable: the tale of Jarid2. Trends Cell Biol. 2011; 21(2):74–80.

Lange, U. C., Siebert, S., Wossidlo, M. et al., Dissecting the role of H3K64me3 in mouse pericentromeric heterochromatin. Nat Commun, 2013. 4: 2233.

Laurent, B., Ruitu, L., Murn, J., et al. A specific LSD1/KDM1A isoform regulates neuronal differentiation through H3K9 demethylation. Mol Cell. 2015; 57(6):957–970.

Lee, H. C., Lim S., Han J. Y. Wnt/β-catenin signaling pathway activation is required for proliferation of chicken primordial germ cells in vitro. Sci Rep. 2016; 6:34510.

Lee, M. G., Wynder, C., Cooch, N., Shiekhattar, R. An essential role for CoREST in nucleosomal histone 3 lysine 4 demethylation. Nature. 2005; 437(7057):432-5.

Lester, B. M., Conradt, E., Marsit, C. Introduction to the Special Section on Epigenetics. Child Dev. 2016; 87(1):29–37.

Leuba, S. H. and Brewer, L. R. Chapter 5 - Single Molecule Studies of Chromatin Structure and Dynamics. Single Molecule Biology. 2009, Pages 143-171.

Li, B., Carey, M., and Workman, J.L. The role of chromatin during transcription. Cell, 2007. 128(4): 707-19.

Li, E., Beard, C. and Jaenisch, R. Role for DNA methylation in genomic imprinting. Nature. 1993; 366:362–365

Li, G. Mechanisms and functions of DNA mismatch repair. Cell Research. 2008. 18:85–98.

Liu, H., Liu, L., Holowatyj, A., Jiang, Y., Yang, Z-Q. Integrated genomic and functional analyses of histone demethylases identify oncogenic KDM2A isoform in breast cancer. Molecular carcinogenesis. 2016; 55(5):977-990.

Liu, H., Wang, C., Lee, S., et al. Clipping of arginine-methylated histone tails by JMJD5 and JMJD7. Proc Natl Acad Sci U S A. 2017; 114(37):E7717–E7726.

Liu, Y., Chen, G., Norton, N., et al. Whole genome association study in a homogenous population in Shandong peninsula of China reveals JARID2 as a susceptibility gene for schizophrenia. J Biomed Biotechnol. 2009; 2009:536918.

Long, Y., Wang, X., Youmans, D. T., Cech, T. R. How do lncRNAs regulate transcription? Sci Adv. 2017; 3(9):eaao2110.

Lu, D. H., Yang, J., Gao, L. K., Min, J., Tang, J. M., Hu, M., Li, Y., Li, S. T., Chen, J., Hong, L. Lysine demethylase 2A promotes the progression of ovarian cancer by regulating the PI3K pathway and reversing epithelialmesenchymal transition. ONCOLOGY REPORTS. 2019 41(2): 917-927.

Lu, L., Gao, Y., Zhang, Z., Cao, Q., Zhang, X., Zou, J., Cao, Y. Kdm2a/b Lysine Demethylases Regulate canonical wnt signaling by modulating the stability of nuclear beta-Catenin. Dev Cell, 2015. 33(6):660-74.

Lu, T., Jackson, M. W., Singhi, A. D, et al. Validation-based insertional mutagenesis identifies lysine demethylase FBXL11 as a negative regulator of NFkappaB. Proc Natl Acad Sci U S A. 2009; 106(38):16339–16344.

Lu, T., Jackson, M. W., Wang, B., Yang, M., Chance, M. R., Miyagi, M., Gudkov, A. V., Stark, G. R. Regulation of NF-kappaB by NSD1/FBXL11-dependent reversible lysine methylation of p65. Proc Natl AcadSci U S A, 2010. 107(1): 46- 51.

Lu, W., Zhang, Y., Liu, D., Songyang, Z., Wan, M. Telomeres-structure, function, and regulation. Exp Cell Res. 2013; 319(2):133–141.

Ma, Y., Kanakousaki, K., Buttitta, L. How the cell cycle impacts chromatin architecture and influences cell fate. Front Genet. 2015; 6:19.

Mannava AG, Tolwinski NS. Membrane bound GSK-3 activates Wnt signaling through disheveled and arrow. PLoS One. 2015; 10(4):e0121879.

Mao, P. and Wyrick, J. J. Emerging roles for histone modifications in DNA excision repair. FEMS Yeast Res. 2016; 16(7):fow090.

Marabelli, C., Marrocco, B., Pilotto, S., Chittori, S., Picaud, S., Marchese, S., Ciossani, G., Forneris, F., Filippakopoulos, P., Schoehn, G., Rhodes, D., Subramaniam, S., Mattevi, A. A Tail-Based Mechanism Drives Nucleosome Demethylation by the LSD2/NPAC Multimeric Complex. Cell Rep. 2019; 27(2):387-399.

Marchand A, Atassi F, Gaaya A, et al. The Wnt/beta-catenin pathway is activated during advanced arterial aging in humans. Aging cell. 2011; 10(2): 220-232.

Mariño-Ramírez, L., Kann, M. G., Shoemaker, B. A., Landsman, D. Histone structure and nucleosome stability. Expert Rev Proteomics. 2005; 2(5):719–729.

Markolovic, S., Leissing, T. M., Chowdhury, R., Wilkins, S. E., Lu, X., Schofield, C. J. Structure-function relationships of human JmjC oxygenases-demethylases versus hydroxylases. Curr Opin Struct Biol. 2016; 41:62-72.

Massagué, J., Xi, Q. TGF-β control of stem cell differentiation genes. FEBS Lett. 2012; 586(14):1953–1958.

Matoba, S., Liu, Y., Lu, F., et al. Embryonic development following somatic cell nuclear transfer impeded by persisting histone methylation. Cell. 2014; 159(4):884–895.

McCabe, M. T., Mohammad, H. P., Barbash, O., Kruger, R. G. Targeting Histone Methylation in Cancer. Cancer J. 2017; 23(5):292-301.

Meng, Y., Li, H., Liu, C., Zheng, L., Shen, B. Jumonji domain-containing protein family: the functions beyond lysine demethylation. J Mol Cell Biol. 2018; 10(4):371–373.

Metzger, E., Wissmann, M., Yin, N., et al., LSD1 demethylates repressive histone marks to promote androgen-receptor-dependent transcription. Nature, 2005. 437(7057): 436-9.

Mishima, Y., Watanabe, M., Suetake, I. Hinge and chromoshadow of HP1α participate in recognition of K9 methylated histone H3 in nucleosomes. J. Mol. Biol. 2013; 425:54–70.

Moody, J. D., Levy, S., Mathieu, J., et al. First critical repressive H3K27me3 marks in embryonic stem cells identified using designed protein inhibitor. Proc Natl Acad Sci U S A. 2017; 114(38):10125–10130.

Moore, L. D., Le, T., Fan, G. DNA methylation and its basic function. Neuropsychopharmacology. 2013; 38(1):23–38.

Moosavi, A., Motevalizadeh Ardekani, A. Role of Epigenetics in Biology and Human Diseases. Iran Biomed J. 2016; 20(5):246–258.

Myrick, D. A., Christopher, M. A., Scott, A. M., et al. KDM1A/LSD1 regulates the differentiation and maintenance of spermatogonia in mice. PLoS One. 2017; 12(5):e0177473.

Negritto, M. C. Repairing Double-Strand DNA Breaks. Nature Education. 2010. 3(9):26.

Nguyen, A. T. and Zhang, Y. The diverse functions of Dot1 and H3K79 methylation. Genes Dev, 2011. 25(13): 1345-58.

Nielsen, A. L., Oulad-Abdelghani, M., Ortiz, J.A., Remboutsika, E., Chambon, P., Losson, R. Heterochromatin Formation in Mammalian Cells. Molecular Cell. 2001. 7(4): 729-739.

Norton, V. G., Imai, B. S., Yau, P., Bradbury, E. M. Histone acetylation reduces nucleosome core particle linking number change. Cell. 1989. 57(3):449-57.

O'Connor, C. Chromosome segregation in mitosis: The role of centromeres. Nature Education. 2008. 1(1):28

Okamoto, K., Tanaka, Y., & Tsuneoka, M. SF-KDM2A binds to ribosomal RNA gene promoter, reduces H4K20me3 level, and elevates ribosomal RNA transcription in breast cancer cells. International Journal of Oncology. 2017. 50: 1372-1382.

Ou, R., Zhu, L., Zhao, L., Li, W., Tao, F., Lu, Y., He, Q., Li, J., Ren, Y., Xu, Y. HPV16 E7-induced upregulation of KDM2A promotes cervical cancer progression by regulating miR-132-radixin pathway. J Cell Physiol. 2019; 234(3):2659-2671.

Ouyang, H., Qin, Y,, Liu, Y., Xie, Y., Liu, J. Prox1 directly interacts with LSD1 and recruits the LSD1/NuRD complex to epigenetically co-repress CYP7A1 transcription. PLoS One. 2013; 8(4):e62192.

Palstra, R. J. and Grosveld, F. Transcription factor binding at enhancers: shaping a genomic regulatory landscape in flux. Front Genet, 2012. 3: 195.

Panier, S. and Boulton S. J., Double-strand break repair: 53BP1 comes into focus. Nat Rev Mol Cell Biol, 2014. 15(1): p. 7-18.

Peaston, A. E., Evsikov, A. V., Graber, J. H., de Vries, W. N., Holbrook, A. E., Solter, D., & Knowles, B. B. Retrotransposons Regulate Host Genes in Mouse Oocytes and Preimplantation Embryos. Developmental Cell. 2004; 7(4), 597–606.

Pedrosa, E., Ye, K., Nolan, K. A., et al. Positive association of schizophrenia to JARID2 gene. Am. J. Med. Genet. B Neuropsychiatr. Genet. 2007; 144B:45–51

Peschansky, V. J. and Wahlestedt, C. Non-coding RNAs as direct and indirect modulators of epigenetic regulation. Epigenetics. 2014. 9:3–12.

Petrov, A., Tsa, A., Puglisi, J. D. Chapter Sixteen - Analysis of RNA by Analytical Polyacrylamide Gel Electrophoresis. Methods in Enzymology. Volume 530, 2013, Pages 301-313.

Piacentini, L., Fanti, L., Negri, R., Del Vescovo, V., Fatica, A., Altieri, F., et al. Heterochromatin Protein 1 (HP1a) Positively Regulates Euchromatic Gene Expression through RNA Transcript Association and Interaction with hnRNPs in Drosophila. PLoS Genet. 2009; 5:e1000670

Podhorecka, M., Skladanowski, A., Bozko, P. H2AX Phosphorylation: Its Role in DNA Damage Response and Cancer Therapy. J Nucleic Acids. 2010; 2010:920161.

Poonperm R, Takata H, Hamano T, et al. Chromosome Scaffold is a Double-Stranded Assembly of Scaffold Proteins. Sci Rep. 2015; 5:11916. Published 2015 Jul 1. doi:10.1038/srep11916

Ramakrishnan AB, Cadigan KM. Wnt target genes and where to find them. F1000Res. 2017; 6:746.

Ramesh, S., Wildey, G. M., Howe, P. H. Transforming growth factor beta (TGFbeta)-induced apoptosis: the rise & fall of Bim. Cell Cycle. 2009;8(1):11–17. doi:10.4161/cc.8.1.7291

Rass, E., Chandramouly, G., Zha, S., Alt, F. W., Xie, A. Ataxia telangiectasia mutated (ATM) is dispensable for endonuclease I-SceI-induced homologous recombination in mouse embryonic stem cells. J Biol Chem. 2013; 288(10):7086–7095.

Razin, A. and Kantor, B. DNA methylation in epigenetic control of gene expression. Prog Mol Subcell Biol. 2005; 38:151-67.

Redon, C., Pilch, D., Rogakou, E., Sedelnikova, O., Newrock, K., Bonner, W. Histone H2A variants H2AX and H2AZ. Curr Opin Genet Dev. 2002; 12(2):162-9.

Reik, W. Stability and flexibility of epigenetic gene regulation in mammalian development. Nature. 2007; 447: 425–432.

Reischl, S., Kramer, A. Fbxl11 Is a Novel Negative Element of the Mammalian Circadian Clock. Journal of Biological Rhythms, 2015: 30(4), 291–301.

Richard, D. J., Bolderson, E., Baird, A.-M., O'Byrne, K. J. Epigenetics Underpinning DNA Damage Repair. Epigenetic Cancer Therapy. 2015. 595–612.

Riggs, A. D., Porter, T. N. Overview of Epigenetic Mechanisms. Epigenetic Mechanisms of Gene Regulation. 1996. 32:29-45.

Ris, H. and Mirsky, A. E. The state of the chromosomes in the interphase nucleus. J Gen Physiol. 1949; 32(4):489–502.

Rivenbark, A. G. Chapter 6 - The Human Genome: Implications for the Understanding of Human Disease. Essential Concepts in Molecular Pathology. 2010, Pages 77-87.

Rizwani, W., Schaal, C., Kunigal, S., Coppola, D., Chellappan, S. Mammalian lysine histone demethylase KDM2A regulates E2F1-mediated gene transcription in breast cancer cells. PLoS One. 2014; 9(7):e100888.

Romero-Barrios, N., Legascue, M. F., Benhamed, M., Ariel, F., Crespi, M. Splicing regulation by long noncoding RNAs. Nucleic Acids Res. 2018; 46(5):2169–2184.

Runtao, G., Dong, R., Du, J., et al. Depletion of histone demethylase KDM2A inhibited cell proliferation of stem cells from apical papilla by de-repression of p15INK4B and p27Kip1. Mol Cell Biochem. 2013; 379: 115-122.

Saurin, A. J., Shiels, C., Williamson, J., et al. The human polycomb group complex associates with pericentromeric heterochromatin to form a novel nuclear domain. *J Cell Biol*. 1998; 142(4):887–898.

Scapoli, L., Martinelli, M/, Pezzetti. F. et al. Expression and association data strongly support JARID2 involvement in nonsyndromic cleft lip with or without cleft palate. Hum. Mutat. 2010; 31:794–800

Schärer, O. D. Nucleotide excision repair in eukaryotes. Cold Spring Harb Perspect Biol. 2013 ;5(10):a012609.

Schindelin, J., Arganda-Carreras, I., Frise, E., Kaynig, V., Longair, M., Pietzsch, T., Preibisch, S., Rueden, C., Saalfeld, S., Schmid, B. Fiji: an open-source platform for biological-image analysis. Nat Methods. 2012; 9(7):676-82;

Schotta, G, Sengupta, R., Kubicek, S., Malin, S., Kauer, M., Callén, E., et al. A chromatin-wide transition to H4K20 monomethylation impairs genome integrity

and programmed DNA rearrangements in the mouse. Genes Dev 2008; 22:2048–2061.

Schulman, B. A., Carrano, A. C., Jeffrey, P. D., Bowen, Z., Kinnucan, E. R., Finnin, M. S., Elledge, S. J., Harper, J. W., Pagano, M., Pavletich, N. P. Insights into SCF ubiquitin ligases from the structure of the Skp1-Skp2 complex. Nature. 2000; 408(6810):381-6.

Scohy, S., Gabant, P., Szpirer, C., Szpirer, J. Identification of an enhancer and an alternative promoter in the first intron of the alpha-fetoprotein gene. Nucleic Acids Res. 2000; 28(19):3743–3751.

Sen, P., Shah, P. P., Nativio, R., Berger, S. L. Epigenetic Mechanisms of Longevity and Aging. Cell, 2016. 166(4): p. 822-839.

Sokol, S. Y. Maintaining embryonic stem cell pluripotency with Wnt signaling. Development. 2011; 138: 4341-4350

Shammas, M. A. Telomeres, lifestyle, cancer, and aging. Curr Opin Clin Nutr Metab Care. 2011; 14(1):28–34.

Sharakhov, I. V., Sharakhova, M. V. Heterochromatin, histone modifications, and nuclear architecture in disease vectors. Curr Opin Insect Sci. 2015; 10:110–117.

Sharma, S., Kelly, T. K., Jones, P. A. Epigenetics in cancer. Carcinogenesis. 2010; 31(1):27–36.

Sharp, A. J., Stathaki, E., Migliavacca, E., et al. DNA methylation profiles of human active and inactive X chromosomes. Genome Res. 2011; 21(10):1592–1600.

Shen, H., W. Xu, and F. Lan, Histone lysine demethylases in mammalian embryonic development. Exp Mol Med, 2017. 49(4): p. e325.

Shi, Y., Lan, F., Matson, C., Mulligan, P., Whetstine, J. R., Cole, P. A., Casero, R. A., Shi, Y. Histone demethylation mediated by the nuclear amine oxidase homolog LSD1. Cell. 2004; 119(7):941-53.

Shmakova, A., Batie, M., Druker, J., Rocha, S. Chromatin and oxygen sensing in the context of JmjC histone demethylases. Biochem J. 2014; 462(3):385–395.

Shtutman M, Zhurinsky J, Simcha I, et al. The cyclin D1 gene is a target of the beta-catenin/LEF-1 pathway. Proc Natl Acad Sci. 1999; 96(10):5522–5527.

Sims, R. J., Millhouse, S., Chen, C. F., Lewis, B. A., Erdjument-Bromage, H., Tempst, P., et al. Recognition of trimethylated histone h3 lysine 4 facilitates the recruitment of transcription postinitiation factors and pre-mRNA splicing. Mol Cell. 2007; 28:665–76.

Skinner, M. K. Role of epigenetics in developmental biology and transgenerational inheritance. Birth Defects Res C Embryo Today. 2011; 93(1):51–55.

Skvortsova, K., Iovino, N., Bogdanović, O. Functions and mechanisms of epigenetic inheritance in animals. Nature Reviews Molecular Cell Biology. 2018. 19, 774–790

Smith, E. R., Pannuti, A., Gu, W., et al. The drosophila MSL complex acetylates histone H4 at lysine 16, a chromatin modification linked to dosage compensation. Mol Cell Biol. 2000; 20(1):312–318.

Smith, Z. D. and Meissner, A. DNA methylation: roles in mammalian development. Nat Rev Genet. 2013. 14:204–220.

Srivastava, S., Zasadzińska, E., Foltz, D. R. Posttranslational mechanisms controlling centromere function and assembly. Curr Opin Cell Biol. 2018; 52:126–135.

Stasevich, T. J., Hayashi-Takanaka, Y., Sato, Y. et al., Regulation of RNA polymerase II activation by histone acetylation in single living cells. Nature volume.2014. 516, pages 272–275.

Steinhart Z, Angers S. Wnt signaling in development and tissue homeostasis. Development. 2018; 145(11)

Sterner, D. E. and Berger, S. L. Acetylation of histones and transcription-related factors. Microbiol Mol Biol Rev. 2000; 64(2):435–459.

Sterner, D. E., Berger, S. L. Acetylation of histones and transcription-related factors. Microbiol Mol Biol Rev. 2000; 64(2):435–459.

Strahl, B. D., Allis, C. D. The language of covalent histone modifications. Nature. 2000. 403(6765):41-5.

Sullivan, B. A., Karpen, G. H. Centromeric chromatin exhibits a histone modification pattern that is distinct from both euchromatin and heterochromatin. Nat Struct Mol Biol. 2004; 11(11):1076–1083.

Takeuchi, T., Yamazaki, Y., Katoh-Fukui, Y., Tsuchiya, R., Kondo, S., Motoyama, J., and Higashinakagawa, T. Gene trap capture of a novel mouse gene, jumonji, required for neural tube formation. GENES & DEVELOPMENT. 1995; 9:1211-12229

Tamburini, B. A., Tyler, J. K. Localized histone acetylation and deacetylation triggered by the homologous recombination pathway of double-strand DNA repair. Mol Cell Biol 2005; 25:4903–13.

Tanaka, T. U., Clayton, L., Natsume, T. Three wise centromere functions: see no error, hear no break, speak no delay. EMBO Rep. 2013; 14(12):1073–1083.

Tanaka, Y., Okamoto, K., Teye, K., et al. JmjC enzyme KDM2A is a regulator of rRNA transcription in response to starvation. EMBO J. 2010; 29(9):1510–1522.

Tanaka, Y., Yano, H., Ogasawara, S., et al. Mild Glucose Starvation Induces KDM2A-Mediated H3K36me2 Demethylation through AMPK To Reduce rRNA Transcription and Cell Proliferation. Molecular and Cellular Biology. 2015; 35(24):4170-4184.

Tian, B., Manley, J. L. Alternative polyadenylation of mRNA precursors. Nature Reviews Molecular Cell Biology. 2017; 18: 18–30.

Tian, X., Zhang, S., Liu, H. M., Zhang, Y. B., Blair, C. A., Mercola, D., Sassone-Corsi, P., Zi, X. Histone Lysine-Specific Methyltransferases and Demethylases in Carcinogenesis: New Targets for Cancer Therapy and Prevention. Current cancer drug targets. 2013. 13(5):558-579.

Towbin, B. D., Gonzalez-Sandoval, A., and Gasser, S.M., Mechanisms of heterochromatin subnuclear localization. Trends Biochem Sci, 2013. 38(7): p. 356-63

Tripathi, V., Ellis, J. D., Shen, Z., Song, D. Y., Pan, Q., et al. The nuclear-retained noncoding RNA MALAT1 regulates alternative splicing by modulating SR splicing factor phosphorylation. Mol Cell. 2010; 39:925–938.

Trojer, P., Reinberg, D. Facultative heterochromatin: is there a distinctive molecular signature? Mol Cell. 2007; 28(1):1-13.

Tsai, C., Shi, Y. and Tainer, J. A. How substrate specificity is imposed on a histone demethylase-lessons from KDM2A. Genes & Dev. 2014. 28: 1735-1738.

Tsukada, Y., Fang, J., Erdjument-Bromage, H., Warren, M. E., Borchers, C. H., Tempst, P. & Zhang, Y. Histone demethylation by a family of JmjC domain-containing proteins. 2006; 439(7078):811-816.

Tsuneoka, M., Tanaka, T., and Okamoto, K.. A CxxC Domain That Binds to Unmethylated CpG Is Required for KDM2A to Control rDNA Transcription. YAKUGAKU ZASSHI. 2015, 135(1):11-21

Turner, B. M. Cellular memory and the histone code. Cell. 2002. 111:285–291.

Tzatsos, A., Pfau, R., Kampranis, S. C., Tsichlis, P. N. Ndy1/KDM2B immortalizes mouse embryonic fibroblasts by repressing the Ink4a/Arf locus. Proceedings of the National Academy of Sciences of the United States of America. 2009; 106(8):2641-2646.

Vacik, T. and Lemke, G. Dominant-negative isoforms of Tcf/Lef proteins in development and disease. Cell Cycle. 2011. 10(24): 4199-4200

Vacik, T. and Raska, I. Alternative intronic promoters in development and disease. Protoplasma, 2017. 254(3): 1201-1206.

Vacik, T., Ladinovic, D., Raska, I. KDM2A/B lysine demethylases and their alternative isoforms in development and disease. Nucleus. 2018. 9(1): 431-441.

Vacik, T., Stubbs, J. L., Lemke, G. A novel mechanism for the transcriptional regulation of Wnt signaling in development. Genes Dev 2011; 25(17):1783-95.

Vastenhouw, N. L. and Schier, A. F. Bivalent histone modifications in early embryogenesis. Curr Opin Cell Biol. 2012; 24(3):374–386.

Vijayakumar S, Liu G, Rus IA, et al. High-frequency canonical Wnt activation in multiple sarcoma subtypes drives proliferation through a TCF/β-catenin target gene, CDC25A. Cancer Cell. 2011; 19(5):601–612.

Vikram A, Kim YR, Kumar S, et al. Canonical Wnt signaling induces vascular endothelial dysfunction via p66Shc-regulated reactive oxygen species. Arterioscler Thromb Vasc Biol. 2014; 34(10):2301–2309.

Volcik, K. A., Zhu, H., Finnell, R. H., et al. Evaluation of the jumonji gene and risk for spina bifida and congenital heart defects. Am. J. Med. Genet. A. 2004; 126A:215–217

Waddington, C. H. An Introduction to Modern Genetics. Proceedings of the Royal Entomological Society of London. Series A, General Entomology. 1939. 14(4-6): 82-82

Waghmare I, Page-McCaw A. Wnt Signaling in Stem Cell Maintenance and Differentiation in the Drosophila Germarium. Genes. 2018; 9(3):127.

Wagner, E. J. and P.B. Carpenter. Understanding the language of Lys36 methylation at histone H3. Nat Rev Mol Cell Biol, 2012. 13(2): 115-26.

Wagner, K. W., Alam, H., Dhar, S. S., Giri, U., Li, N., Wei, Y., Giri, D., Cascone, T., Kim, J. H., Ye, Y. KDM2A promotes lung tumorigenesis by epigenetically enhancing ERK1/2 signaling. J Clin Invest, 2013. 123(12): 5231-46.

Wang X, Wang X, Liu Y, et al. LGR5 regulates gastric adenocarcinoma cell proliferation and invasion via activating Wnt signaling pathway. Oncogenesis. 2018; 7(8):57.

Wang, J., Scully, K., Zhu, X., et al., Opposing LSD1 complexes function in developmental gene activation and repression programmes. Nature, 2007. 446(7138): 882-7. 24.

Wang, J., Telese, F., Tan, Y., et al. LSD1n is an H4K20 demethylase regulating memory formation via transcriptional elongation control. Nat Neurosci. 2015; 18(9):1256–1264.

Wang, Y., Liu, J., Huang, B. O., et al. Mechanism of alternative splicing and its regulation. Biomed Rep. 2015; 3(2):152–158.

Wei, S., Li, C., Yin, Z., et al. Histone methylation in DNA repair and clinical practice: new findings during the past 5-years. J Cancer. 2018; 9(12):2072–2081.

Westhorpe, F. G., Straight, A. F. The centromere: epigenetic control of chromosome segregation during mitosis. Cold Spring HarbPerspect Biol. 2014; 7(1):a015818.

White, C. L., Suto, R, K., Luger, K. Structure of the yeast nucleosome core particle reveals fundamental changes in internucleosome interactions. EMBO J. 2001; 20(18):5207–5218.

Wiles, E. T. and E. U. Selker, H3K27 methylation: a promiscuous repressive chromatin mark. Curr Opin Genet Dev, 2017. 43: 31-37.

Wong, S. J., Gearhart, M. D., Taylor, A. B., et al. KDM2B Recruitment of the Polycomb Group Complex, PRC1.1, Requires Cooperation between PCGF1 and BCORL1. Structure. 2016; 24(10):1795–1801.

Wu, H., Sun, Y. E. Epigenetic Regulation of Stem Cell Differentiation. Pediatric Research. 2006. 59: 21–25

Wu, X., Johansen, J. V., Helin, K. Fbxl10/Kdm2b recruits polycomb repressive complex 1 to CpG Islands and regulates H2Aubiquitylation. Mol Cell. 2014. 49(6):1134–46.

Xin, B., Rohs, R. Relationship between histone modifications and transcription factor binding is protein family specific. Genome Res. 2018; 28(3):321–333.

Xu, Q. and W. Xie. Epigenome in Early Mammalian Development: Inheritance, Reprogramming and Establishment. Trends Cell Biol, 2017. 28(3): 237-253,

Xu, W. H., Liang, D. Y., Wang, Q., Shen, J., Liu, Q. H., Peng, Y. B. Knockdown of KDM2A inhibits proliferation associated with TGF-β expression in HEK293T cell. Mol Cell Biochem. 2019; 456(1-2):95-104.

Xu, Y., Zhao, W., Olson, S. D., Prabhakara, K. S., Zhou, X. Alternative splicing links histone modifications to stem cell fate decision. Genome Biology. 2018. 19. 133.

Yan, X., Wu, J., Jiang, Q., Cheng, H., Han, J. J., Chen, Y. G. CXXC5 suppresses hepatocellular carcinoma by promoting TGF-beta-induced cell cycle arrest and apoptosis. J Mol Cell Biol. 2018; 10(1):48–59.

Yu, G., Wang, J., Lin, X., Diao, S., Cao, Y., Dong, R., Wang, L., Wang, S., Fan, Z. Demethylation of SFRP2 by histone demethylase KDM2A regulated osteo/dentinogenic differentiation of stem cells of the apical papilla. Cell Prolif, 2016. 49(3): 330-40.

Zhao, J., Wei, J., Mialki, R. K., et al. F-box protein FBXL19-mediated ubiquitination and degradation of the receptor for IL-33 limits pulmonary inflammation. Nat Immunol. 2012; 13(7):651–658.

Zhu, L. Y., Zhu, Y. R., Dai, D. J., Wang, X., Jin, H. C. Epigenetic regulation of alternative splicing. Am J Cancer Res. 2018; 8(12):2346–2358.

Zhu, X., Zhang, Y., Bjornsdottir, G., et al. Histone modifications influence mediator interactions with chromatin. Nucleic Acids Res. 2011; 39(19):8342–8354.

Seznam publikací autora

Publikace s IF, které se zabývaji problematikou dizertační práce

1) **Lađinović, D**., Novotná, J., Jakšová, S., Raška, I. and Vacík, T. A demethylation deficient isoform of the lysine demethylase KDM2A interacts with pericentromeric heterochromatin in an HP1a-dependent manner. Nucleus. 2017. 8(5):563-572. IF=2.2
2) Vacík, T., **Lađinović, D.** and Raška, I. KDM2A/B lysine demethylases and their alternative isoforms in development and disease. Nucleus. 2018. 9(1):431–441. IF=2.2
3) **Lađinović, D**., Pinkas, D., Liška F., Raška, I. and Vacík, T. The lysine demethylases KDM2A and KDM2B repress canonical Wnt signaling independently of the JmjC-demethylase domain. (in preparation)

Univerzita Karlova v Praze, 1. lékařská fakulta

Kateřinská 32, Praha 2

Prohlášení zájemce o nahlédnutí
do závěrečné práce absolventa studijního programu
uskutečňovaného na 1. lékařské fakultě Univerzity Karlovy v Praze

Jsem si vědom/a, že závěrečná práce je autorským dílem a že informace získané nahlédnutím do zpřístupněné závěrečné práce nemohou být použity k výdělečným účelům, ani nemohou být vydávány za studijní, vědeckou nebo jinou tvůrčí činnost jiné osoby než autora.

Byl/a jsem seznámen/a se skutečností, že si mohu pořizovat výpisy, opisy nebo kopie závěrečné práce, jsem však povinen/a s nimi nakládat jako s autorským dílem a zachovávat pravidla uvedená v předchozím odstavci.

Příjmení, jméno (hůlkovým písmem)	Číslo dokladu totožnosti vypůjčitele (např. OP, cestovní pas)	Signatura závěrečné práce	Datum	Podpis